Journal of Engineering Design and Technology

Vol. 23 No. 2, July 2023

POLITEKNIK NEGERI BALI

logic

p-ISSN. 1412-114X

e-ISSN. 2580-5649

LOGIC

Jurnal Rancang Bangun dan Teknologi

LOGIC

Jurnal Rancang Bangun dan Teknologi

Journal of Engineering Design and Technology

Gedung P3M, lt.1 Politeknik Negeri Bali, Bukit Jimbaran
PO BOX 1064 Kuta Selatan, Badung, Bali - Indonesia
Telp. (+62)361 701981 Fax. (+62)361 701128
Email: logic@pnb.ac.id

LOGIC JOURNAL TEAM

PREFACE

Logic: Jurnal Rancang Bangun dan Teknologi (Journal of Engineering Design and Technology) is a peer-reviewed research journal aiming at promoting and publishing original high quality research in all disciplines of engineering and applied technology. All research articles submitted to Logic should be original in nature, never previously published in any journal or presented in a conference or undergoing such process across the world. All the submissions will be peer-reviewed by the panel of experts associated with particular field. Submitted papers should meet the internationally accepted criteria and manuscripts should follow the style of the journal for the purpose of both reviewing and editing.

Logic is a journal covering articles in the field of civil and mechanical engineering, design, and technology published 3 times a year in March, July, and November. Language used in this journal is English.

LOGIC. P-ISSN 1412-114X
LOGIC. E-ISSN 2580-5649
Indexing : GOOGLE SCHOLAR, DOAJ, EBSCO OPEN SCIENCE DIRECTORY, SINTA, GARUDA

Best Regard,

LOGIC Editorial Team

TABLE OF CONTENTS

LOGIC
Journal of Engineering Design and Technology
Vol. 23 No.2 July 2023 ; p. 68 - 76

p-ISSN : 1412-114X
e-ISSN : 2580-5649
http://ojs2.pnb.ac.id/index.php/LOGIC

THE EFFECT OF IMPLEMENTATION OF CONSTRUCTION SAFETY MANAGEMENT SYSTEM ON THE LEVEL OF WORK ACCIDENTS

1) Department of Civil Engineering, State Polytechnic of Jakarta, Depok, Indonesia 16424

Corresponding email [1,2,3] : sdefila@gmail.com

Sri Defila [1)], Kusumo Drajad S. [1)], Kartika Hapsari S. [1)]

Abstract. The high number of construction accidents in infrastructure development projects in Indonesia is caused by the risk of danger that exists at every stage of construction. The implementation of Construction Safety Management System (SMKK) is a manifestation of the labor protection system and for construction work, SMKK can minimize and avoid the risk of fatal work accidents. This study aims to determine the effect of the application of SMKK elements on the level of work accidents and find out the elements that greatly affect the level of work accidents in the Jakarta-Bekasi Toll Road Construction Project. Data collection methods are distribution of questionnaires and interviews. Data analysis was performed using statistical analysis, namely multiple linear regression analysis. From the results of the study, based on the partial hypothesis test, it was obtained that the application of SMKK elements that partially affect the level of work accidents is the 3rd element, namely Construction Safety Support, while the other 4 elements do not have a significant influence on the level of work accidents and based on simultaneous hypothesis tests, it is obtained that the simultaneous application of SMKK elements has a significant influence on the level of work accidents. The results of the multiple regression equation show that the construction safety support element with a negative value means that it has the greatest influence that gives the possibility of work accidents occurring low compared to other SMKK elements.

Keywords : SMKK, Accident, Regression Analysis.

1. INTRODUCTION

High number of construction accidents in infrastructure development projects in Indonesia is caused by the risk of danger that exists at every stage of construction. This is a big challenge for construction service business actors in Indonesia. [1]

Based on data from BPJS Ketenagakerjaan, in 2021 there have been 234.270 workplace accidents and this number is an increase of 5,65% from the previous year, namely 2020 of 221.740 cases. [2] Based on the Ministry of PUPR (2018), the construction sector is the highest contributor to work accidents, accounting for 3,9% of the total work accidents that occur. These types of cases include falling from a height of 26%, hitting 12%, and being hit by a tool 9%. [3] One of the main causes of accidents is the lack of awareness from workers and companies about the importance of implementing K3 in work. [4] Therefore, all construction construction projects must increase their supervision, so that the number of work accidents in the construction field can be minimized. [5]

The Construction Safety Management System or commonly called SMKK is an inseparable part of the labor protection system. For construction service work, SMKK can minimize and avoid the risk of moral, material losses, loss of working hours, as well as the safety of humans and the surrounding environment which can later support the improvement of effective and efficient performance in the development process. [6]

The Jakarta-Bekasi Toll Road Project stretches for 34 km and has a very large area of work coverage. This project uses the construction of the Slab on Pile whose structure consists of a slab, pile head, and spun pile foundation whose work is at an altitude of approximately 10 m, and has about 400 workers.

Based on the Peraturan Menteri PUPR No. 10 of 2021 concerning Guidelines for Sistem Manajemen Keselamatn Konstruksi (SMKK) in Article 34, it is explained that what is included in the criteria for major construction safety risks is high hazard, workers number more than 100 people, use heavy equipment in the form of transport lift aircraft, and use high technology. [7] As a project with great construction safety risks, the Jakarta-Bekasi Toll Road Project is obliged to implement SMKK and requires good K3 implementation so that zero accidents can be achieved.

Based on the background and problems above, the researcher is interested in conducting research on the application of the construction safety management system implemented by the company to the project with the title: "The Effect of Implementation of Construction Safety Management System on the Level of Work Accidents."

2. METHODS

The overall research was following the flowchart shown in Fig.1. In this study, it starts by establishing a title that is backgrounded by the problem which is then determined to identify the problem and a problem formulation is made supported by a literature study. Then data collection is carried out which is divided into 2, namely primary data (construction safety management system on the project) and secondary data (construction safety plan documents).

Primary data collection is carried out in the first way, namely the distribution of questionnaires aimed at determining the effect of implementing the five elements of SMKK which is a basic part of the construction safety management system and is a reference in implementing a construction safety management system on the level of work accidents. Questionnaires were given to workers in offices and fields at the Jakarta-Bekasi Toll Road Project with a total of 35 people divided into several divisions, namely Health Safety Environment (HSE), engineering, quality & logistics, and workers / supervisors who were in the field. Then the second way is that the interview is conducted to obtain supporting information from the questionnaire. The interview resource person was conducted to the Head of The Health Safety Environment of the Jakarta-Bekasi Toll Road Project. Then for the collection of secondary data, namely the Construction Safety Plan Documents (RHSE) obtained through a data application to the Jakarta-Bekasi Toll Road Project.

After collecting data, data analysis can be carried out using statistical analysis, namely multiple linear regression analysis. The series of statistical analysis carried out are validity tests, reliability tests, classical assumption tests consisting of normality tests, linearity tests, multicollinearity tests, and heteroscedasticity tests, then multiple linear regression tests that produce regression equations, and finally simultaneous hypothesis tests and partial hypothesis tests are carried out. After data analysis and getting results and discussions, conclusions and suggestions can be drawn.

Research Variables

The research variables in this study are as follows (see Table 1.):

Table 1. Research Variables

Variable	Description
X1	Leadership and Labor Participation in Construction Safety
X2	Construction Safety Planning
X3	Construction Safety Support
X4	Construction Safety Operation
X5	Construction Safety Performance Evaluation
Y	Level of Work Accidents

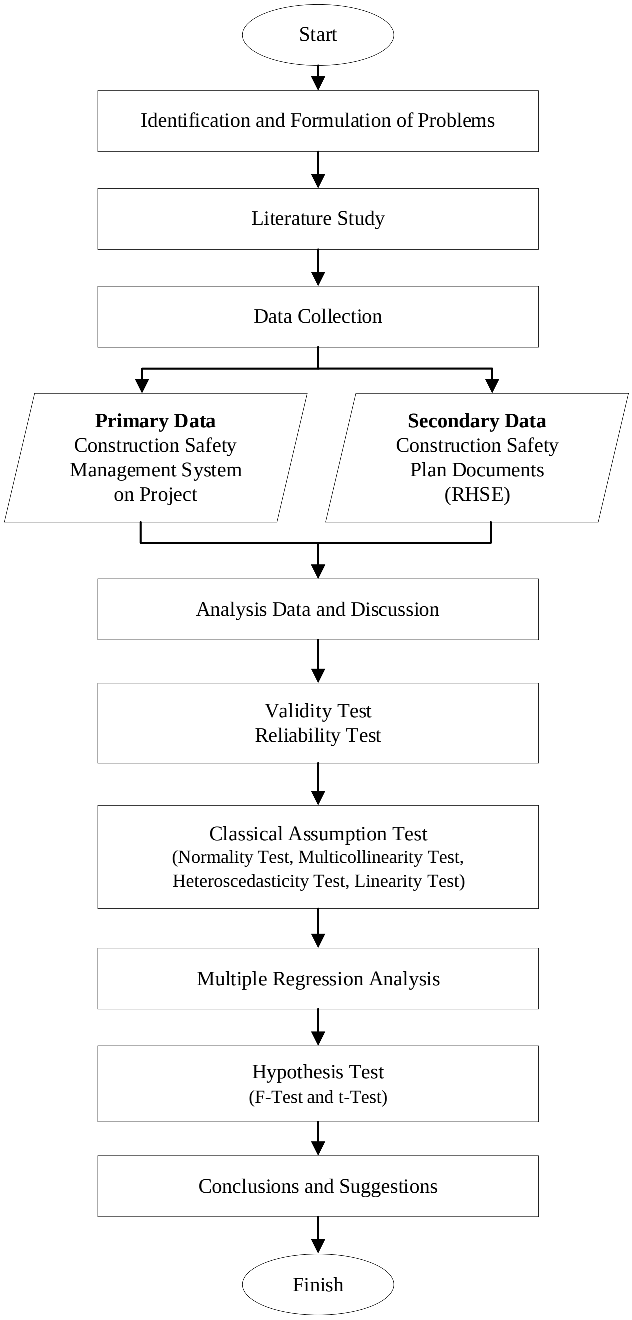

Figure 1. Flowchart

3. RESULTS AND DISCUSSION

3.1 Validity and Reliability Test

Validity tests using the SPSS application are performed by comparing the r_{count} value with the r_{table}. Obtained the value of Pearson Correlation with r_{table} for n = 35 is 0,334. The statement item is declared valid if the value of r_{count} is greater than r_{table}. The validity test results (Table 2.) state that all statements items are valid. Then the research instrument can proceed to the next stage.

Reliability test (Table 3.) using Cronbach's Alpha value requirements (value > 0.90 is Very High; 0.70 > value > 0.90 is High; 0.50 > value > 0.70 is Medium; value > 0.50 is Low). The results were obtained that the entire variable has a High level of reliability. Thus the research instrument is declared reliable and can proceed to the next stage.

Table 2. r_{count} Validity Test

Statement Code	r_{count}	Statement Code	r_{count}	Statement Code	r_{count}	Statement Code	r_{count}	Statement Code	r_{count}
1.1	0.747	2.5	0.740	3.10	0.492	4.10	0.823	6.5	0.689
1.2	0.582	**3.1**	0.678	**4.1**	0.582	**5.1**	0.736	6.6	0.499
1.3	0.585	3.2	0.664	4.2	0.730	5.2	0.762	6.7	0.377
1.4	0.807	3.3	0.815	4.3	0.781	5.3	0.843	6.8	0.467
1.5	0.705	3.4	0.872	4.4	0.814	5.4	0.788	6.9	0.396
1.6	0.700	3.5	0.614	4.5	0.524	5.5	0.841	6.10	0.673
2.1	0.781	3.6	0.710	4.6	0.747	**6.1**	0.435	6.11	0.440
2.2	0.771	3.7	0.703	4.7	0.802	6.2	0.424	6.12	0.656
2.3	0.782	3.8	0.735	4.8	0.744	6.3	0.631	6.13	0.731
2.4	0.779	3.9	0.650	4.9	0.665	6.4	0.635	6.14	0.699

Table 3. Reliability Test Results

Variable		Cronbach's Alpha Value	Reliability Level
X1	Leadership and Labor Participation in Construction Safety	0.722	High
X2	Construction Safety Planning	0.825	High
X3	Construction Safety Support	0.882	High
X4	Construction Safety Operation	0.898	High
X5	Construction Safety Performance Evaluation	0.854	High
Y	Level of Work Accidents	0.814	High

3.2 Linearity Test

Based on the results of the SPSS, the significance value obtained on all free variables (X), indicates that the Significance Value is more than 0,05. Then it can be concluded that free and bound variables have a linear relationship. This result shows that the free variable, namely the 5 elements of SMKK, has a straight line relationship with a bound variable, namely the level of work accidents.

Table 4. Significance Value Deviation from Linearity

Variable		Sig. Value
X1	Leadership and Labor Participation in Construction Safety	0.768
X2	Construction Safety Planning	0.128
X3	Construction Safety Support	0.442
X4	Construction Safety Operation	0.494
X5	Construction Safety Performance Evaluation	0.180

3.3 Normality Test

Based on the results of the SPSS, the Asymp. Sig. (2-tailed) value was obtained by 0,200. Then it can be concluded that the data is distributed normally because the value obtained is greater than 0,05.

Table 5. Asymp. Sig. (2-tailed) Value

Asymp. Sig. (2-tailed)	0.200

3.4 Multicollinearity Test
Based on the results of SPSS, the tolerance and VIF values obtained on all free variables (X), indicate that the Tolerance Value is more than (> 0,100) and the VIF is less than (< 10,00). Then it can be concluded that there are no symptoms of multicollinearity in the free variable.

This result shows that the free variable, namely 5 SMKK elements, does not have a relationship/correlation between one element and another element which can result in the coefficient of multiple regression results becoming erratic and the error being infinite.

Table 6. Tolerance and VIF Values

	Variable	Tolerance Value	VIF
X1	Leadership and Labor Participation in Construction Safety	0.252	3.971
X2	Construction Safety Planning	0.214	4.668
X3	Construction Safety Support	0.209	4.785
X4	Construction Safety Operation	0.250	3.999
X5	Construction Safety Performance Evaluation	0.273	3.664

3.5 Heteroscedasticity Test
Based on the results of the SPSS, the significance value obtained on all free variables (X), indicates that the Significance Value is more than 0,05. Then it can be concluded that there are no symptoms of heteroscedasticity. This result shows that the independent variable, namely the 5 elements of SMKK, is homogeneous, which means that the data measured are based on the same population.

Table 7. Value Significance of Heteroskedasticity

	Variable	Sig. Value
X1	Leadership and Labor Participation in Construction Safety	0.119
X2	Construction Safety Planning	0.496
X3	Construction Safety Support	0.962
X4	Construction Safety Operation	0.853
X5	Construction Safety Performance Evaluation	0.839

3.6 Multiple Regression Analysis
Based on the results of the SPSS, a multiple linear regression equation is obtained as follows.

$$\mathbf{Y = 56,911 + 0,334\, X_1 - 0,325\, X_2 - 0,606\, X_3 + 0,070\, X_4 - 0,560\, X_5}$$

The constant value obtained is 56,911, so if the SMKK element variable has a coefficient value of 0 (zero), then the level of work accident value is 56.911. However, if there is an increase every 1 unit of all free variables simultaneously, then the value of the level of work accidents will decrease by 55,284.

Table 8. Value for Multiple Regression

	Variable	β
	Constanta	56.911
X1	Leadership and Labor Participation in Construction Safety	0.334
X2	Construction Safety Planning	- 0.325
X3	Construction Safety Support	- 0.606
X4	Construction Safety Operation	0.070
X5	Construction Safety Performance Evaluation	- 0.560

3.7 Coefficient of Determination (R-Squared Test)

It is known that the result of SPSS, the Adjusted R Square value is 0,563. Thus, the free variable, namely the 5 elements of SMKK, has a simultaneous influence of 56,3% on the bound variable, namely the Level of Work Accident (Y). Then the difference of 43,7% was influenced by other factors outside of this study.

Table 9. Adjusted R Square Value

Model Summary[b]				
Model	**R**	**R Square**	**Adjusted R Square**	**Std. Error of the Estimate**
1	0.792[a]	0.627	0.563	3.284

3.8 Simultaneous Hypothesis Test

Based on the results of SPSS in the ANOVA table, the Significance Value obtained is 0,000. Then it can be concluded that the alternative hypothesis (H1) is accepted. This result shows that the free variables, namely the 5 elements of SMKK consisting of Leadership and Labor Participation in Construction Safety (X1), Construction Safety Planning (X2), Construction Safety Support (X3), Construction Safety Operations (X4), and Construction Safety Performance Evaluation (X5) simultaneously have a significant influence on the variable level of work accidents.

Table 10. Simultaneous Hypothesis Significance Value

ANOVA[a]						
Model		**Sum of Squares**	**df**	**Mean Square**	**F**	**Sig.**
1	**Regression**	525.933	5	105.187	9.753	0.000
	Residual	312.752	29	10.785		
	Total	838.686	34			

3.9 Partial Hypothesis Test

Obtained the Significance Value of < α (0,05) in the 3rd element, namely Construction Safety Support, and which obtained the significance value of > α (0,05) on the 4 elements, namely Leadership and Labor Participation in Construction Safety, Construction Safety Planning, Construction Safety Operations, and Construction Safety Performance Evaluation. So it can be concluded that only the application of the 3rd SMKK element partially exerts a significant influence on the level of work accidents. Meanwhile, other elements do not have a significant influence on the level of work accidents.

Table 11. Partial Hypothesis Significance Value

	Variable	Sig. Value
X1	Leadership and Labor Participation in Construction Safety	0.476
X2	Construction Safety Planning	0.510
X3	Construction Safety Support	0.033
X4	Construction Safety Operation	0.773
X5	Construction Safety Performance Evaluation	0.159

3.9 Effect of SMKK Elements Application on the Level of Work Accidents

From the Multiple Linear Regression Test, the following equation is generated :

$$\mathbf{Y = 56,911 + 0,334\ X_1 - 0,325\ X_2 - 0,606\ X_3 + 0,070\ X_4 - 0,560\ X_5}$$

With a coefficient of determination of 0,563. These results mean that 56,3% of SMKK elements affect the level of work accidents while the other 43,7% are influenced by other factors outside this study.

Based on the t-test, it was concluded that only the application of the Construction Safety Support element partially exerted a significant influence on the level of work accidents. While the other 4 elements do not have a significant influence on the level of work accidents.

However, based on the F-test, the simultaneous application of SMKK elements has a significant influence on the level of work accidents, it can be seen in the graph as follows.

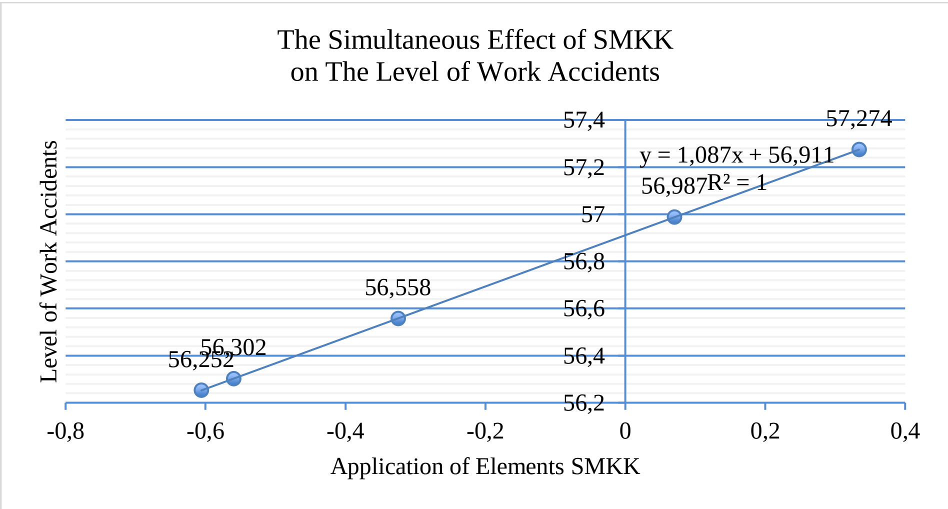

Figure 2. Simultaneous Influence

In the figure, it can be seen that the greater the value of the level of application of the SMKK element in the negative sign, the lower the Y value or the value of the level of work accidents.

If the value of the linear regression equation is assumed to have no influence (unit increment = 0) on each variable, then the value of the Level of Work Accidents (Y) obtained is 56,911. Meanwhile, if the value of the linear regression equation is assumed to have an influence of 1 unit on each variable, then the value of the Level of Work Accidents (Y) is 55,284.

To see the value of the application of each SMKK (X) element to the level of work accidents (Y) in the Jakarta-Bekasi Toll Road Project, a depiction was carried out in the graphic model as follows.

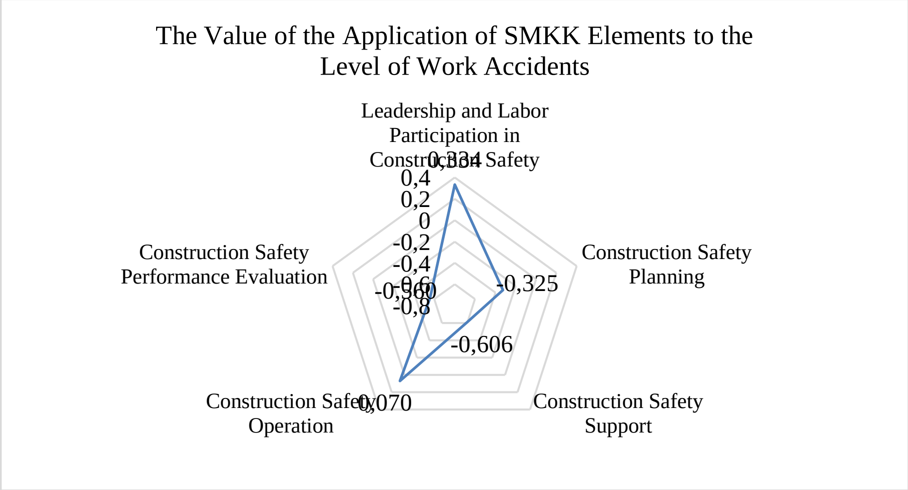

Figure 3. Graph of Application of SMKK Elements to the Level of Work Accidents

From the graph, it is interpreted that the Construction Safety Support element with a negative value means that it has the greatest influence which gives the possibility of work accidents occurring low while the leadership and labor participation element in Construction Safety with a positive value means that it has the most influence as well which can provide a high probability of accidents occurring.

3.10 Elements that Greatly Affect the Level of Work Accidents

For elements that are very influential, it is obtained from multiple regression tests by comparing the coefficient values of each SMKK element variable. The order of SMKK elements from those that are very influential to those that have a small influence on the level of work accidents are Construction Safety Support (3); Construction Safety Performance Evaluation (5); Construction Safety Planning (2); Construction Safety Operations (4); and Leadership and Labor Participation In Construction Safety (1). It is stated that the SMKK element that greatly affects the level of work accidents is the 3rd element, namely Construction Safety Support.

This is also supported based on the results of a partial hypothesis test which states that only elements of Construction Safety Support have a significant influence on the level of work accidents.

In general, the results of this study are similar to the results of research conducted by Anang Noorrahman (2014) explained that the effect of the application of SMK3 on the level of work accident was 55,7% which was measured by factors of the work environment, materials, tools and workers. The factor that affects the level of work accidents is the work environment. In this study, there were similar results, namely the effect of the application of SMKK on the level of work accident was 56.3% which was explained by elements of construction safety planning, construction safety support, and evaluation of construction safety performance. [14]

The results of this study are also in line with those conducted by Hafiza Marbun (2021) that the test results can be concluded for the variable level of work accidents can be measured by variable factors of the work environment, materials, tools, and workers and in this study, it can be concluded that the variable level of work accidents can be measured by variable 5 elements of SMKK. [15].

4. CONCLUSION

Based on the partial hypothesis test (t-test) it was obtained that only the 3rd element of Construction Safety Support partially exerted a significant influence on the level of work accidents, while the other elements did not have a significant influence on the level of work accidents. Based on the results of the simultaneous hypothesis test (F-test) it was concluded that the simultaneous application of SMKK elements has a significant influence on the level of work accidents. Then it can be concluded that if the value of the SMKK element has a negative effect and the number is higher, the value of the level of work accidents will be lower.

For a very influential element, it was found that the 3rd element, namely Construction Safety Support, greatly affects the level of work accidents, based on the results of multiple regression tests by comparing the coefficient values of each SMKK element variable. This is also supported based on the results of a partial hypothesis test which states that only elements of Construction Safety Support have a significant influence on the level of work accidents.

5. REFERENCES

[1] W. Hartono & Y. Purwandari, "Analisis Sistem Manajemen Dan Keselamatan Kerja (SMK3) Terhadap Tingkat Kecelakaan Kerja Pada Proyek Pembangunan Gedung di Tangerang Dan Sekitarnya," 2016.

[2] I. Mahdi, "Kasus Kecelakaan Kerja di Indonesia Alami Tren Meningkat," dataindonesia.id, 2022. https://dataindonesia.id/sektor-riil/detail/kasus-kecelakaan-kerja-di-indonesia-alami-tren-meningkat

[3] PARAMPARA, "Safety Construction: Komitmen dan Konsistensi Terapkan SMK3," Media Komunikasi BPSDM Kementrian PUPR, Jakarta, 2018.

[4] H. Sitohang & K. Magdalena, "Penerapan Sistem Keselamatan Kesehatan Kerja dan Lingkungan (K3L) pada Proyek Konstruksi (Studi Kasus Pembangunan Jalan Tol Cibitung-Cilincing)," 2020.

[5] D. Eko Wahyuono, "Penerapan Sistem Manajemen Keselamatan Konstruksi pada Proyek Klasifikasi Kecil Pasca diterbitkannya Peraturan Menteri Pekerjaan Umum dan Perumahan Rakyat Nomor 21/Prt/M/2019." 2021.

[6] F. Pangkey, G. Y. Malingkas, & D. Walangitan, "Penerapan Sistem Manajemen Keselamatan dan Kesehatan Kerja (SMK3) pada Proyek Konstruksi di Indonesia (Studi Kasus: Pembangunan Jembatan Dr. Ir. Soekarno-Manado)," 2012.

[7] "Peraturan Menteri PUPR Nomor 10 Tahun 2021 tentang Pedoman Sistem Manajemen Keselamatan Konstruksi".

[8] K. Drajad & L. Nurdin, "Peraturan Perundangan dan Pengetahuan Dasar Keselamatan Konstruksi." 2020.

[9] R. Soehatman, "Sistem Manajemen Keselamatan dan Kesehatan Kerja. OHSAS 18001." Jakarta: Dian Rakyat, 2010.

[10] R. Soehatman, "Smart Safety, Panduan Penerapan SMK3 Yang Efektif." Jakarta: Dian Rakyat, 2013.

[11] "Peraturan Pemerintah Nomor 14 Tahun 2021 tentang Perubahan Atas Peraturan Pemerintah Nomor 22 Tahun 2020 tentang Peraturan Pelaksanaan Undang-Undang Nomor 2 Tahun 2017 tentang Jasa Konstruksi".

[12] BPSDM. Kementrian PUPR, "Modul Sistem Manajemen Keselamatan Konstruksi (SMKK)," 2019.

[13] T. Kartika Noviastuti, "Analisis Upaya Penerapan Manajemen K3 dalam Mencegah Kecelakaan Kerja di Proyek Pembangunan Fasilitas Penunjang Bandara oleh Pt.X (Studi Kasus di Proyek Pembangunan Bandara di Jawa Tengah)," 2018.

[14] A. Noorrahman, "Analisis Sistem Manajemen Keselamatan dan Kesehatan kerja (SMK3) terhadap Tingkat Kecelakaan Kerja PT. Adhi Karya (Persero) Tbk. Divisi Konstruksi IV," 2014.

[15] A. Maddeppungeng, S. Asyiah, & H. Marbun, "Analisis Sistem Manajemen Keselamatan dan Kesehatan Kerja (SMK3) Terhadap Tingkat Kecelakaan Kerja (Studi Kasus: Proyek Pembangunan Nines Plaza & Residence, Tangerang Selatan)," 2021.

LOGIC
Journal of Engineering Design and Technology
Vol. 23 No.2 July 2023 ; p. 77 - 84

p-ISSN : 1412-114X
e-ISSN : 2580-5649
http://ojs2.pnb.ac.id/index.php/LOGIC

STUDY OF CHARACTERISTICS AND MANAGEMENT OF DRAINAGE PROBLEMS IN UBUD DISTRICT

1) Department of Civil Engineering, Faculty of Engineering and Informatics, Universitas Pendidikan Nasional, Denpasar, Bali

Corresponding email [1] :
irmasuryanti@undiknas.ac.id

Irma Suryanti[1], Putu Indah Dianti Putri[1]

Abstract. Ubud District is one of the tourism areas in Bali which is growing very rapidly. Ubud District has problems related to inundation and flooding which often occur during the rainy season. The drainage canals cannot accommodate the peak flood discharge. Because the capacity of the channel is insufficient, besides the influence of sediment and garbage, water overflows through the freeboard of the channel. This study aims to determine the characteristics of inundation and drainage in Ubud District. Primary and secondary data are used in this study which will then be used in data analysis. The analytical method used are field survey, identification of inundation and flood locations, inventory of existing drainage system, hydrology and hydraulics analysis, and drainage network planning. The result is 27 inundation locations were found in Ubud District. The inundation locations included 5 points in Lodtunduh Village, 3 points in Mas Village, 2 points in Peliatan Village, 5 points in Petulu Village, 2 points in Sayan Village, and 10 points in Ubud Village. The duration of the inundation that occurs is a minimum of 15 minutes and a maximum of 360 minutes. The height of the inundation that occurs is 12 – 50 cm with an inundation area of 0.032 – 4.67 ha and an inundation length of 12 – 2.309 m. The frequency of inundation is 3 to 10 times per year. Parameters for determining priority for drainage management based on priority scale are determined based on the characteristic parameters of inundation, economic losses, social disturbances and government facilities, transportation disturbances, and losses in residential areas. The recommendations given include normalizing the existing canal with river stone pairs of the required size that are more adequate to accommodate water discharge, especially during rains; making diversion channel with precast box culvert with the required size; and construction of new channels equipped with inlet drains per segment as entry points for inundation on the roads into the drainage channels.

Keywords : Drainage, Inundation, Flood, Characteristic, Management, Ubud

1. INTRODUCTION

According to Indonesia's Law No. 26 of 2007 concerning spatial planning, urban areas are areas that have non-agricultural main activities with the function of the area as a place for urban settlements, centralization, and distribution of government services, social services, and also economic activities [1]. In urban areas, there are many people living, and there are many public facilities, transportation, communication, and so on [2]. One of the urban areas that function as a Regional Service Center in Gianyar Regency, Bali Province is the Ubud Urban Area. Ubud District is one of the tourism areas in Bali which is growing very rapidly. The total area of Ubud District is 42.38 ha, which is 11.52% of the total area of Gianyar Regency [3]. Ubud District consists of 7 villages and 1 sub-district including Kedewatan Village, Lodtunduh Village, Mas Village, Peliatan Village, Petulu Village, Sayan Village, Singakerta Village, and Ubud Village.

One of the urban infrastructure network systems is the drainage network system. The drainage network system in question is a primary drainage channel system that is established in order to reduce waterlogging and support flood control, especially in residential, commercial, office, and tourism areas [4]. The drainage system is an important infrastructure for an urban area that is closely related to the physical environmental conditions and the socio-cultural environment that exists in the urban area [5],[6].

Flood disaster is a problem that must be faced by residents who even in certain locations must be faced them routinely. The problem of flooding is inseparable from the poor drainage caused by the development of business and housing areas which often results in the conversion of land functions from safety areas and catchment areas such as river riparian areas, and temporary water storage ponds to turning into residential areas and trading centers [7],[8],[9],[10]. This is what happened in the Ubud District, where there are stagnant water and flooding, especially during the rainy season and for a long time.

The drainage canals cannot accommodate the peak flood discharge, especially during the heavy and consecutive rainy season. Because the capacity of the channel is insufficient, besides the influence of sediment and garbage, water overflows through the freeboard of the channel. Due to minimal maintenance, there is the accumulation of waste which has become a mound of earth, thus blocking the drainage flow to the main river (estuary). The system of developing settlements from paddy fields has resulted in a change in the direction of channel use from irrigation canals to drainage canals.

On the other hand, drainage problems are also caused by significant changes in land use which have contributed greatly to increasing surface runoff. The development of tourism in Ubud District is inseparable from land use where land is needed in tourism development related to the construction of supporting facilities and infrastructure or transportation infrastructure [3]. The increase in existing water runoff is not matched by an adequate increase in drainage capacity.

Based on these problems, this study aims to determine the characteristics of inundation and drainage in Ubud District. This is done so that the flood points in several places in Ubud District can be described so that they can create a healthy and inundation-free urban environment, and can play a role in increasing water conservation, utilization, and control.

2. METHODS

2.1 Data

In researching the drainage system of an urban area, the description of the physical environment is very important information. The placement of canals, buildings, and the densities of these facilities will be greatly influenced by the condition of the planned area. In this regard, sensitivity from researchers is needed in interpreting available data both in the form of primary data and secondary data in the form of basic data and flood phenomena that have occurred, as well as existing flow patterns. Information about natural flow patterns can also be obtained from direct observations in the field during rain or flood conditions.

The data needed in this study includes primary data and secondary data. Primary data is data obtained from the field by direct measurement, and observations in the field or at the study location. While secondary data is data that can be obtained directly without having to go to the location. Secondary data is generally obtained from agencies such as the Meteorology and Geophysics Agency, the Center for Geological Research and Development, the National Coordinating Agency for Surveys and Mapping (Bakosurtanal), Bakosurtanal and other related agencies as well as previous studies. Secondary data collection includes an inventory of the existing drainage system, Gianyar District Spatial Data and its surroundings, hydrological data, regional geological maps, and topographical maps.

2.2 Analysis Methods

2.2.1 Field Survey

A tracing survey is carried out by seeking information about inundation points and the direction of flow on the main road sections, starting from the source of the arrival of water to its final disposal in the form of a river. This survey was also carried out in addition to knowing the direction of drainage flow, knowing the existing conditions, as well as knowing the causes of flooding or inundation.
Regarding people's behavior towards the existence of an existing drainage network, it is necessary to study matters relating to the management of the surrounding drainage network, whether it is following the actual drainage function, whether the community has routinely maintained the cleanliness of the canals or vice versa, even drainage channels that are not clean. there is used to accommodate household waste so it does not function optimally.

2.2.2 Identification of Inundation and Flood Locations

This activity was carried out to collect data related to the history of inundation at the study site and its surroundings which had been carried out by the Regional Government or related agencies before. Inundation and flood data identified include the location of the inundation, the length of the inundation, and the height of the inundation. It is also necessary to study the possibility of flooding from upstream which can be taken into account in planning. Accurate locations of inundation and flooding points will also provide information about the hydraulic regime of the area.

2.2.3 Inventory of Existing Drainage System

An inventory of the existing drainage system is carried out thoroughly and identification and classification are carried out based on regional zones, shape and construction model, length of the drainage channel, level of damage, a function of the dam system, and the type of drainage water carried. Also pay attention to the shape and slope of the land, the area or area to be drained to determine the drainage discharge, the types of waste water, the existence of natural settlements, the type of soil, and its characteristics. All of that will affect the condition of the existing drainage system.

2.2.4 Hydrology and Hydraulics Analysis

Hydrological analysis was carried out on the estimated design rainfall, rainfall frequency analysis, design flood discharge analysis, runoff coefficient analysis, time concentration analysis, and rain intensity analysis. The entire analysis is carried out using the applicable technical provisions. The flood calculation takes into account land cover in the study location and takes into account future development plans for the area concerning existing spatial planning conditions, and when effective rain occurs, the runoff coefficient takes into account land cover in detail [11],[12],[13].

Hydraulics analysis is carried out to determine the properties or characteristics of the flow of water in a flowing medium, which is mainly influenced by the topographical conditions of the media being traversed. This analysis is carried out to determine the condition of water flow in drainage channels, and rivers and the capacity or ability of drainage channels to carry discharge according to the topographical conditions of the drainage and to analyze hydraulic details. In this analysis, a numerical model analysis of the planned drainage system was also carried out [14], [15],[15].

2.2.5 Drainage Network Planning

In planning drainage channels, the basics of erosion-resistant channel planning will be used, namely, channels that can withstand erosion satisfactorily, which is the same by adjusting the speed of the flow or by using the walls and bottom of the channel which are given a layer that is useful both for resisting erosion. and control the loss of water seepage. The hydrological, topographical, and soil mechanical characteristics mentioned above are also very necessary when creating a new drainage network.

It can also be proposed to make horizontal drainage to eliminate the stagnation of water on the main road. Horizontal drainage above the road directly drains water into the road drainage canal, and this system can overcome flow congestion in the holes in the concrete locking the sidewalk when the road level is raised later.

3. RESULTS AND DISCUSSION

3.1 Inundation and Flood Inventory

From the results of field surveys and interviews with residents and related agencies, 27 inundation points were found in Ubud District, the locations shown in Figure 1. The inundation locations included 5 points in Lodtunduh Village, 3 points in Mas Village, 2 points in Peliatan Village, 5 points in Petulu Village, 2 points in Sayan Village, and 10 points in Ubud Village. The duration of the inundation that occurs is a minimum of 15 minutes and a maximum of 360 minutes. The height of the inundation that occurs is 12 – 50 cm with an inundation area of 0.032 – 4.67 ha and an inundation length of 12 – 2.309 m. The frequency of inundation is 3 to 10 times per year.

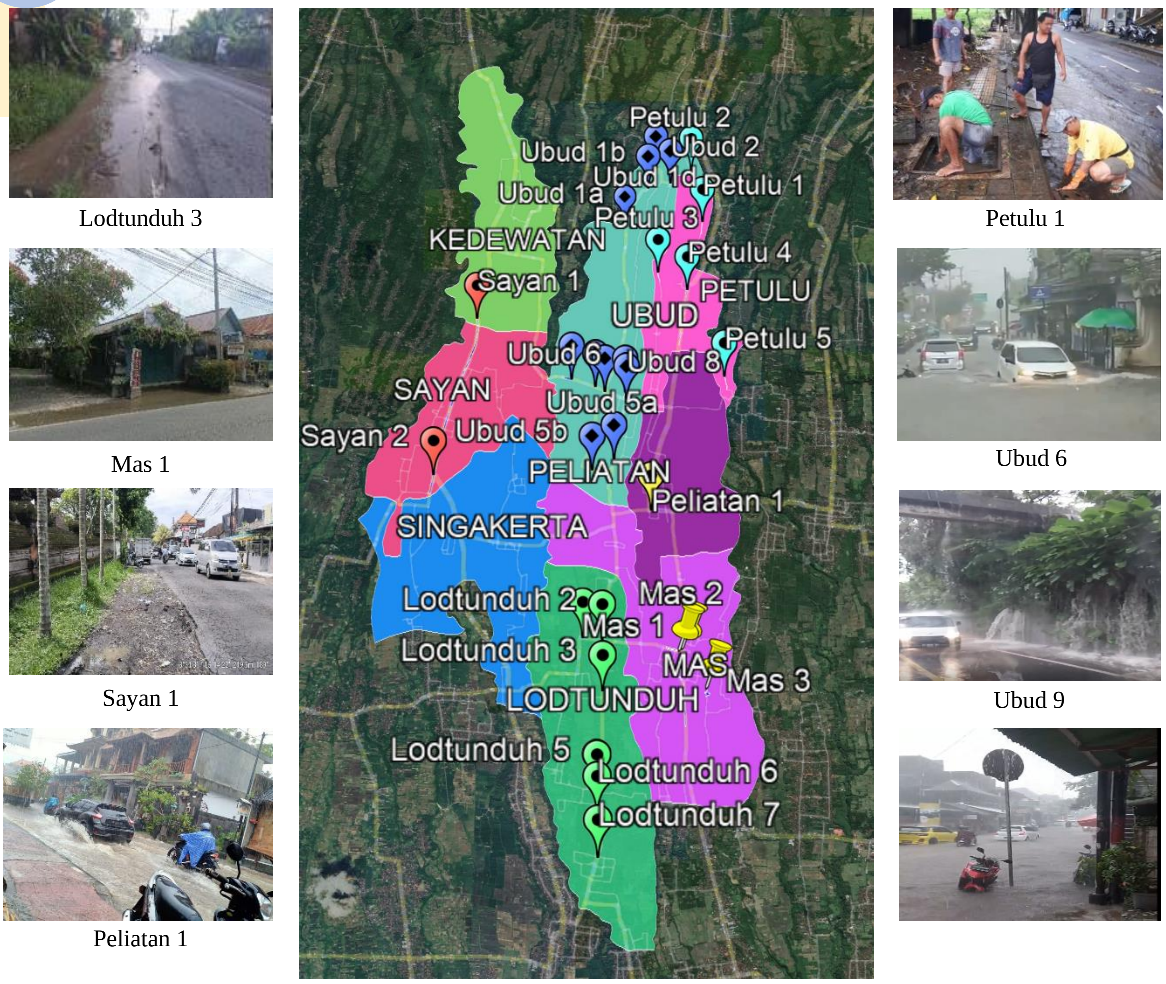

Figure 1. Location of inundation and flooding in Ubud district

The following is a list of inundations that occurred in Ubud District which is shown in Table 1.

Table 1. List of inundation and flooding in Ubud District in 2022

Location	Time (minute)	Height (cm)	Area (ha)	Length (m)	Frequency (per year)	Indication
Lodtunduh 1	60	50	0,35	549	6	The water overflows because the canals and culverts are shrinking
Lodtunduh 2	60	50	0,2	50	6	Water overflows due to small channels and is disturbed by sedimentation
Lodtunduh 3	180	40	0,43	678,3	6	The water is overflowing because the channel is getting smaller
Lodtunduh 4	240	50	0,02	53	6	The water is overflowing because the channel is getting smaller
Lodtunduh 5	240	50	0,03	93	6	There is a inundation due to the absence of road drainage channels
Mas 1	30	20	1,17	1,078	10	Water overflows because drainage channels mix with irrigation channels
Mas 2	25	25	0,33	169	6	Water overflows because drainage channels mix with irrigation channels
Mas 3	60	30	0,31	103	6	Water overflows because drainage channels mix with irrigation channels
Peliatan 1	60	20	0,85	1072	6	The water in the drainage ditch overflows onto the road
Peliatan 2	60	20	0,84	1277	6	The water in the drainage ditch overflows onto the road
Petulu 1	45	15	0,1051	220	6	The water is overflowing because the channel is getting smaller
Petulu 2	30	12	0,00972	23,2	3	Overflow of irrigation water mixed with rainwater due to small channels

Petulu 3	30	20	0,064	115	6	Overflow of irrigation water mixed with rainwater due to small channels
Petulu 4	60	30	0,9855	966	10	The water in the drainage ditch overflows onto the road
Petulu 5	15	15	0,086	229	3	The water overflowed and pooled onto the road
Sayan 1	20	20	4,67	2.309	7	The water overflowed and pooled onto the road
Sayan 2	20	20	0,57	307	4	The water overflowed and pooled onto the road
Ubud 1	180	25	0,02675	20	5	There is a inundation due to the absence of road drainage channels
Ubud 2	360	20	0,01325	17	5	There is a inundation because the drainage position is higher than the road body
Ubud 3	360	20	0,004817	8	4	There are inundation due to the large number of wild plants that prevent water from flowing into the drainage canals
Ubud 4	30	20	0,0151	20	5	There are inundation due to the large number of wild plants that prevent water from flowing into the drainage canals
Ubud 5	180	20	0,0032	12	6	There is a inundation because the drainage channel is clogged
Ubud 6	120	40	0,0537	32	5	There are inundation because the road body is broken and the channel is clogged
Ubud 7	120	25	0,0301	100	5	There are inundation because the road body is broken and the channel is clogged
Ubud 8	180	15	0,0397	52	6	There is a inundation due to clogged drainage channels
Ubud 9	60	15	0,0779	195	4	There are inundation due to the overflow of water in the gutters and the road above them
Ubud 10	60	25	0,19	230	3	There is a inundation due to clogged drainage channels

3.2 Identification of Existing Drainage Problems

Drainage in the Ubud District area has several problems related to the inundation and flooding that often befalls this area. Some of the identification of the causes of inundation and flooding are also related to drainage, including the following:

1. Drainage channels cannot accommodate peak flood discharges, especially during the heavy and consecutive rainy season. Because the capacity of the channel is insufficient, besides the influence of sediment and garbage, water overflows through the freeboard of the channel.
2. Significant changes in land use change have contributed greatly to increasing surface runoff. The increase in existing water runoff is not matched by an adequate increase in drainage capacity.
3. The settlement development system using the Land Consolidation (LC) system from paddy fields has resulted in a change in the direction of canal usage from irrigation canals to drainage canals.
4. The topography of a flat area makes it difficult for the water to drain into the sewer.
5. There is a narrowing of the river channel, especially in the middle and downstream, so that it often causes flooding
6. There is a building that crosses the river which affects the river flow system downstream. This condition can be seen in several permanent weirs, other former irrigation buildings, bridges, and other buildings.
7. High sedimentation rates in river channels have the effect of reducing river capacity. This condition can be seen in almost all river sections.
8. Disposal of garbage into the river/canal bodies. This condition occurs as a result of low public awareness to participate in maintaining the function of existing drainage channels and rivers. The existence of garbage that enters the body of the canal or river occurs in almost all existing sections.
9. Effect of tides. This condition greatly affects the discharge of water towards the estuary, especially downstream. Conditions of seawater tides will function as backwater which can hold the rate of drainage flow to the main system (river).

3.3 Management of Drainage with Priority Scale

3.3.1 Parameters for Determining Handling Priorities

Parameters for determining the priority of drainage treatment based on the priority scale determined from the following parameters:

1. The inundation parameters are height, area, duration, and frequency of inundation per year

2. Economic loss parameters include: estimated losses on existing economic facilities such as industrial areas, public facilities, social facilities, offices, housing, agricultural areas, and landscaping
3. Parameters of social disturbance and government facilities include public health, social unrest, environmental damage, and damage to government facilities
4. Parameters of transportation losses and disruptions such as obstruction of transportation access due to inundation that overflows over the road body and transportation that is economically strategic does not run smoothly
5. Parameters of losses in residential areas, especially in densely populated areas

3.3.2 Ranking of Drainage Handling Priorities

The determination of the priority scale for handling is carried out based on the five parameters of prioritization above. The value of each parameter ranges from 0-100. Scores are totaled for five parameters, where the maximum score is 500. The highest score will receive handling priority. Based on the calculation of the drainage parameter score, the priority scale ranking for each location village is obtained as follows:

Table 2. Ranking of drainage handling in each village

Location	Score	Ranking in Each Village	Location	Score	Ranking in Each Village
Lodtunduh 1	336	4	Petulu 5	209	4
Lodtunduh 2	336	5	Sayan 1	268	1
Lodtunduh 3	346	1	Sayan 2	244	2
Lodtunduh 4	346	2	Ubud 1	328	8
Lodtunduh 5	346	3	Ubud 2	319	9
Mas 1	435	1	Ubud 3	319	10
Mas 2	389	2	Ubud 4	349	6
Mas 3	223	3	Ubud 5	424	3
Peliatan 1	459	1	Ubud 6	433	2
Peliatan 2	433	2	Ubud 7	328	7
Petulu 1	179	5	Ubud 8	394	5
Petulu 2	244	3	Ubud 9	394	4
Petulu 3	384	2	Ubud 10	463	1
Petulu 4	481	1			

3.3.3 Drainage Handling Recommendations

The recommendations for handling drainage that can be given based on the ranking of treatment priorities are shown in the Table 3.

Table 3. Drainage handling recommendations

Location		Drainage Handling Recommendations
Lodtunduh	1	Channel planning with more adequate cross-sectional dimensions to catch water, especially when it rains with dimensions of 0.50 m x 0.70 m, 0.80 m x 0.40 m, 0.80 m x 1.20 m and 0.80 m x 1.00 m
	2	Making diversion channel with a precast box culvert measuring 0.80 m x 0.80 m
	3	New channel equipped with an inlet drain per segment as the entry point for stagnant water on the road into the drainage channel
Mas	1	Normalization of the existing canal with stone masonry with dimensions of 0.50 m x 0.50 m and 0.80 m x 0.80 m on the right and left sides
	2	Making diversion channel with a precast box culvert measuring 0.50 m x 0.50 m and 0.80 m x 0.80 m
	3	The new channel is equipped with an inlet drain per segment as a path for stagnant water on the road to enter the drainage channel
Peliatan	1	Channel planning with more adequate cross-sectional dimensions to catch water, especially when it rains with dimensions of 0.60 m x 1.00 m and 0.80 m x 1.00 m
	2	New channel equipped with an inlet drain per segment as the entry point for stagnant water on the road into the drainage channel
Petulu	1	Normalization of the existing channel with stone masonry with a size of 0.80 m x 0.60 m and 1.00 m x 0.60 m along the inundation path on both the right and left sides
Sayan	1	Normalization of the existing canal with stone masonry with a size of 0.80 m x 0.80 m on both the right and left sides
	2	New channel equipped with an inlet drain per segment as the entry point for stagnant water on the road into the drainage channel
Ubud	1	Normalization of the existing canal with stone masonry with dimensions of 0.40 m x 0.40 m, 0.50 m x 0.80 m, and 0.80 m x 0.80 m on both the right and left sides

2	The existing canal design will be enlarged to a size of 0.40 m x 0.60 m, 0.50 m x 1.00 m, 0.70 m x 1.00 m, and 1.00 m x 1.00 m with river stone masonry
3	Paving around the shoulder of the road is carried out so that water can flow directly into the drainage canal
4	The new channel is equipped with an inlet drain per segment as a path for stagnant water on the road to enter the drainage channel

4. CONCLUSION

Based on the discussion that has been carried out, it can be concluded that 27 inundation points were found in Ubud District. The inundation locations include 5 points in Lodtunduh Village, 3 points in Mas Village, 2 points in Peliatan Village, 5 points in Petulu Village, 2 points in Sayan Village, and 10 points in Ubud Village. The duration of the inundation that occurs is a minimum of 15 minutes and a maximum of 360 minutes. The height of the inundation that occurs is 12 – 50 cm with an inundation area of 0.032 – 4.67 ha and an inundation length of 12 – 2,309 m. The frequency of inundation is 3 to 10 times per year.

Drainage in the Ubud District area has several problems related to the inundation and flooding that often afflicts this area, the majority of which are caused by the capacity of the drainage channels not being able to accommodate rainwater discharge, and drainage blockages caused by garbage, wild plants, and sedimentation. Parameters for determining priority for drainage management based on priority scale are determined based on the characteristic parameters of inundation, economic losses, social disturbances and government facilities, transportation disturbances, and losses in residential areas.

The treatment recommendations given include normalizing the existing canal with river stone pairs of the required size that are more adequate to accommodate water discharge, especially during rains; making diversion channel with precast box culvert with the required size; and construction of new channels equipped with inlet drains per segment as entry points for inundation on the roads into the drainage channels.

5. ACKNOWLEDGEMENT

The author would like to thank the Bali - Penida Water Resources Operation and Maintenance Work Unit, Ministry of Public Works and Public Housing who have contributed to the implementation of this research.

6. REFERENCES

[1] D. P. P. Misa, I. L. Moniaga, and V. Lahamendu, “Urban Land Use Based on Area Function (Case Study: Urban Area of Airmadidi District),” *Jurnal Spasial*, vol. 5, no. 2, pp. 171-178, 2018.

[2] F. H. Mardiansjah and P. Rahayu, “Small Urban Area Development in Surrounding City of Pekalongan,” *Jurnal Geografi Gea*, vol. 20, no. 2, pp. 151-168, Oct 2020.

[3] P. C. Lindari, N. N. Subadiyasa, and I. M. Mega, “Monitoring Changes of Paddy Fields and Land Ownership in Ubud District Using Remote Sensing and GIS,” *E-Jurnal Agroekoteknologi Tropika*, vol. 7, no. 2, April 2018.

[4] N. K. S. Kartika, I. W. Muliawan, and A. A. S. D. Rahadiani, “Evaluation of the Function of the Drainage Channel on the Conditions of the Mount Rinjani Road in the West Denpasar District Area,” *Wicaksana, Journal of Environment & Development*, vol. 2, no. 1, pp. 17-24, March 2018.

[5] O. Akhir, and B. Sulistiono, “Evaluation of Urban Drainage Channel System in Yogyakarta's Laksda Adisucipto Road Area,” Thesis, Civil Engineering Program Study, Universitas Islam Indonesia, 2019.

[6] C. T. Saputra, U. Andawayanti, and M. J. Ismoyo, “Study of Urban Drainage Network in Nganjuk Regency, East Java Province,” *Journal of Water Resources Technology and Engineering*, vol. 2, no. 1, pp. 328-340, 2022.

[7] C. Fraiture, R. H. Susanto, F. X. Suryadi, and H. M. H. Wahyu, “Urban Drainage Management and Flood Control Improvement Using the Duflow Case Study: Aur Sub Catchment, Palembang, South Sumatra, Indonesia,” *Makara Journal of Technology*, vol. 21, no. 2, pp. 83-92, Aug. 2017.

[8] W. Sohn, S. D. Brody, J. H. Kim, and M. H. Li, “How Effective are Drainage Systems in Mitigating Flood Losses?,” *Cities Journal*, vol. 107, Dec. 2020.

[9] E. Meilianda, D. Alfian, etc, “Technical Review of Flood Problems and Management on the Krueng Teunom Hilir River in Aceh Province Towards Integrated Flood Disaster Mitigation,” *Journal of Civil Engineering*, vol. 28, no. 1, pp. 51-62, April 2021.

[10] A. S. Pambudi, “Problemsof Local Floods and Their Relation to Bogor City Drainage Infrastructure System,” *Indonesian Journal of Applied Research (IJAR)*, vol. 3, no. 1, pp. 10–22, Apr. 2022.

[11] L. M. D. A. Sutantri and I. N. S. Wijaya, “The Influence of Tourism Development on Changes in Agricultural Land Use in Ubud District,” *Planning for Urban Region and Environment Journal*, vol. 10, no. 1, pp. 113-124, Jan 2021.

[12] H. Aksoy, V. S. O. Kirca, H. I. Burgan, and D. Kellecioglu, "Hydrological and Hydraulic Models for Determination of Flood-Prone and Flood Inundation Areas," 7th International Water Resources Management Conference of ICWRS, Germany, 18–20 May 2016.

[13] K. Poudel, K. Basnet, and B. Sherchan, "Hydrological and Hydraulic Modeling for Flood Analysis: A Case Study for Modi Catchment," *International Journal of Engineering Research & Technology (IJERT)*, vol. 10, no. 8, pp. 534-544, August 2021.

[14] S. M. A. Omar, W. N. H. W. Ariffin, L. M. Sidek, H. Basri, M. H. M. Khambali, and A. N. Ahmed, "Hydrological Analysis of Batu Dam, Malaysia in the Urban Area: Flood and Failure Analysis Preparing for Climate Change," *International Journal Environmental Research Public Health*, vol. 19, no. 24, Dec 2022.

[15] A. Paquier, E. Mignot, and P. H. Bazin, "From Hydraulic Modelling to Urban Flood Risk," *Procedia Engineering*, vol. 115, pp. 37–44, 2015.

[16] M. Kiwanuka, S. Yuna, J. W. Mbujje, and J. B. Niyomukiza, "Flood Analysis and Hydraulic Competence of Drainage Structures Along Addis Ababa Light Rail Transit," *Journal of Environmental Science and Sustainable Development*, vol. 4, no. 2, pp. 248-272, Dec 2021.

LOGIC
Journal of Engineering Design and Technology
Vol. 23 No.2 July 2023 ; p. 85 - 95

p-ISSN : 1412-114X
e-ISSN : 2580-5649
http://ojs.pnb.ac.id/index.php/LOGIC

BEHAVIOR AND PERFORMANCE OF STEEL FRAME STRUCTURES WITH X-TYPE CONCENTRIC BRACING SYSTEM DUE TO VARIATIONS IN COMPARISON OF SPAN WIDTH TO STORY HEIGHT (L/H)

1) Department of Civil Engineering, Faculty of Engineering and Informatics, Universitas Pendidikan Nasional, Denpasar, Bali
2) Mechanical Engineering Department, Politeknik Negeri Bali, Bukit jimbaran, Badung Bali
Corresponding email [1)] :
indrakumara@undiknas.ac.id

I Nyoman Indra Kumara[1)], I Gede Fery Surya Tapa[1)], I Nengah Darma Susila[2)]

Abstract. X-type bracing is the strongest bracing. The bigger ratio of the width of the span to the high level (L/H), the slope of the angle on the bracing will be more declivous. The analysis of the structure with the L/H ratio to determine the behavior of the structure using linear analysis of response spectrum and structural performance using the static nonlinear pushover analysis (ETABS 2016) to determine the displacement target that occurred in the structure. Structural modeling is done on 3D portals with levels of 3, 5, 8 and 10 floors with different L/H variations, including L/H=1; L/H=1.25; L/H=1.5; L/H=1.75; and L/H=2. Structural modeling is planned to be in the Surabaya area with moderate soil conditions. This study obtains data such as: (1) The largest maximum drift and floor drift are at type L/H=2, (2) The largest base shear force in the nonlinear pushover analysis at each story occurs at L/H=1, (3) In the yield condition type L/H=1 has the smallest percentage of structural stiffness, but in the ultimate condition type L/H=1 has the largest percentage of structural stiffness, and (4) The highest ductility value at each story occurs in type L/H=2 . Based on these results, it shows that the greater the type of L/H in the bracing structure, the greater the displacement target produced. If the angle of bracing becomes more sloping, then the displacement and target displacement that occurs increases.

Keywords : Bracing, L/H, Response Spectrum, Pushover.

1. INTRODUCTION

The area of Indonesia is very vulnerable to earthquakes [1]. Indonesia's location is based on its geographical location in the Pacific Ring of Fire region, namely the confluence of three world tectonic plates, the Indo-Australian Plate, the Eurasian Plate, and the Pacific Plate. This makes Indonesia vulnerable to disasters such as earthquakes. Therefore, buildings in Indonesia must take into account the impact that an earthquake will have on building structures [2]. The impact of a building structure that gets an earthquake force is to experience a lateral deviation [3]. Precise calculations are needed so that the building can withstand earthquake forces. If the calculation is not correct and the structure gets too large a lateral deviation, then the structure will collapse [4]. Structural systems in buildings must be designed to resist earthquake forces (lateral forces) [5]. In terms of materials also need to be considered in designing a building. The use of steel material is most often used in the construction of high-rise buildings [6]. This is because steel has very high elasticity and strength compared to concrete [7]. So steel is the most suitable material used in bracing frame systems.

One of the systems that can withstand earthquake forces is the bracing frame system [8]. There are several parts in the bracing system, including the eccentric bracing system and the concentric bracing system [9]. Furthermore, there are two types of concentric bracing systems, namely Ordinary Concentric Bracing Systems and Special Concentric Bracing Systems. The Special Concentric Bracing System has higher stiffness when subjected to earthquake forces compared to the Ordinary Concentric Bracing System [9]. Buildings that use a bracing system will minimize the value of deformation that occurs in the building structure because bracing will increase the value of the stiffness of the structure [10]. Bracing has several types and X-type bracing is the type of bracing that has the highest structural strength value compared to other bracing types [11]. This study aims to determine the ability of a steel frame structure using concentric bracing with the X-type as a result of the variation in the ratio between span width and story height (L/H). Thus, due to the L/H ratio, different bracing angle ratios will be formed. This will cause a difference in angle, so the ability of each X-type concentric bracing of each L/H type will be known.

2. METHODS

This research will conduct research on behavior and performance in each structure. The research aims to determine the behavior of the structure using a linear response spectrum analysis. Meanwhile, to determine the performance of the structure will use a non-linear static pushover analysis using the help of the 2016 ETABS application.

The steps taken for this research began with determining the cross-sectional dimensions used in each structure. Structural data worked on in this research were typical steel structures with 3, 5, 8, and 10 stories which the dimensions for each story are 4 m. The election for those total of the stories is mostly classification that we can find at the site consisting of a special concentric bracing system model made with five different types of L/H, namely L/H=1, L/H= 1.25, L/H=1.5, L/H=1.75, and L/H=2. So that the total models to be made are 20 models, of which 1 type of L/H consists of 4 models. The modeling was carried out using the 2016 ETABS application. The structure to be modeled is assumed to be in the Surabaya area with moderate soil conditions. The function of the building that will be used in each building is an office. Here are the materials and load used in each structure:

a) Steel profile material
   The steel material used in all steel profiles is ASTM A992, with the following data:
   - Yield Stress (Fy) = 344,74 MPa
   - Ultimate stress (Fu) = 448,16 MPa
   - Modulus of elasticity of steel (E) = 200.000 MPa

b) Corrugated steel deck material
   - Melting stress (Fy) = 550 MPa
   - Steel deck thickness (td) = 0,70 mm
   - Steel deck weight = 7,35 kg/m^2
   - Sliding link (@90 mm) = 19 mm

c) Concrete materials
   - Compressive strength (f'c) = 25 MPa
   - Modulus of elasticity of concrete (Ec) = 23.500 MPa
   - Concrete slab thickness = 120 mm

d) Dead Load
   The dead load has been calculated by the 2016 ETABS application, the additional dead load on the floor slab is 166 kg/m^2, and the additional dead load on the roof plate is 142 kg/m^2.

e) Live Load
   The structure is assumed to be used as an office building, so the live load on the floor used according to SNI 1727:2013 [12] is 2.4 kN/m^2 and the live load used on the roof is 0,96 kN/m^2.

f) Earthquake Load
   The earthquake load used on the structure is class D in the Surabaya area. The place choices in Surabaya are because Surabaya is an industrial city also the classification of class D is the current primary situation at the site.

After the structural data is determined, then the criteria are checked for each structure with a stress ratio. Next, calculate the deviation between floors based on the classification from SNI 1726:2012. The structure studied is in risk category II (office). Then a nonlinear pushover static analysis is carried out which will produce a curve due to the base shear force and displacement which is called the capacity curve. After obtaining the capacity curve for each type of L/H, the value of the stiffness of the structure can be determined. Stiffness of the structure can be seen from the slope of the capacity curve in yielding and ultimate conditions. If the displacement values at the time of melting and ultimate conditions are known, then the value of the ductility of each structure can be known. Next determine the displacement target by determining the assumption that there is a maximum displacement that may occur as a result of the earthquake load. The displacement target in this study used the ASCE 41-13 NSP (Nonlinear Static Procedure) method which is available in the ETABS 2016 software application. Determination of the displacement target based on the nonlinear static procedure is carried out by constructing an idealization curve from the capacity curve resulting from the static nonlinear pushover analysis. With the idealization curve, it will be known the target displacement that occurs from the structural model. After knowing the target displacement of the structure, it can also be known the level of performance of each structure.

3. RESULTS AND DISCUSSION

Cross Section Dimensions

Determining the cross-sectional dimensions used in each structure is carried out by checking the criteria for each structure with a stress ratio of less than 0.95. The dimensions used in the structure are the dimensions obtained for the largest L/H type (L/H=2). Dimensions and stress ratios in the 3-floor, 5-floor, 8-floor and 10-floor models can be seen in Table 1 to Table 4.

Table 1. Dimensions and Stress Ratio on the 3 Floor Model

Structure Model for 3 Floors							
Structure Elements	Structural Element Dimensions	Stress Ratio					
		L/H= 1	L/H= 1,25	L/H=1.5	L/H= 1.75	L/H= 2	Status
BA floors 1-3	W310 × 310 × 179	0,043	0,083	0,108	0,203	0,889	OK
BI floors 1-3	W360 × 370 × 196	0,059	0,109	0,182	0,273	0,895	OK
K floors 1-3	W360 × 410 × 216	0,100	0,220	0,273	0,345	0,846	OK
BR floors 1-3	HSS177,8 × 177,8 × 9,5	0,094	0,226	0,371	0,487	0,943	OK

Table 2. Dimensions and Stress Ratio on the 5 Floor Model

Structure Model for 5 Floors							
Structure Elements	Structural Element Dimensions	Stress Ratio					
		L/H= 1	L/H= 1,25	L/H=1.5	L/H= 1.75	L/H= 2	Status
BA floors 1-5	W310 × 310 × 179	0,043	0,083	0,116	0,223	0,899	OK
BI floors 1-5	W360 × 370 × 196	0,071	0,121	0,198	0,286	0,939	OK
K floors 1-3	W360 × 410 × 314	0,223	0,270	0,327	0,377	0,901	OK
K floors 4-5	W360 × 370 × 196	0,092	0,125	0,198	0,290	0,870	OK
BR floors 1-5	HSS177,8 × 177,8 × 9,5	0,097	0,230	0,311	0,656	0,923	OK

Table 3. Dimensions and Stress Ratio on the 8 Floor Model

Structure Model for 8 Floors							
Structure Elements	Structural Element Dimensions	Stress Ratio					
		L/H= 1	L/H= 1,25	L/H=1.5	L/H= 1.75	L/H= 2	Status
BA floors 1-8	W310 × 310 ×179	0,043	0,083	0,107	0,204	0,899	OK
BI floors 1-5	W360 × 370 ×196	0,086	0,121	0,200	0,270	0,905	OK
BI floors 6-8	W310 × 310 × 202	0,089	0,129	0,198	0,296	0,936	OK
K floors 1-3	W360 × 410 × 463	0,217	0,273	0,331	0,400	0,945	OK
K floors 4-5	W360 × 410 × 287	0,115	0,219	0,290	0,318	0,939	OK
K floors 6-8	W310 × 310 × 342	0,087	0,109	0,151	0,231	0,701	OK
BR floors 1-8	HSS177,8 × 177,8 × 9,5	0,097	0,239	0,330	0,459	0,940	OK

Table 4. Dimensions and Stress Ratio on the 10 Floor Model

Structure Model for 10 Floors							
Structure Elements	Structural Element Dimensions	Stress Ratio					
		L/H= 1	L/H= 1,25	L/H=1.5	L/H= 1.75	L/H= 2	Status
BA floors 1-8	W310 × 310 × 179	0,043	0,083	0,107	0,204	0,899	OK
BA Lt 9-10	W310 × 310 × 179	0,043	0,083	0,107	0,223	0,899	OK
BI floors 1-5	W360 × 370 × 196	0,087	0,127	0,184	0,261	0,819	OK
BI floors 6-8	W310 × 310 × 202	0,092	0,137	0,200	0,282	0,890	OK
BI floors 9-10	W310 × 310 × 202	0,083	0,127	0,188	0,273	0,878	OK
K floors 1-3	W360 × 410 × 592	0,100	0,235	0,281	0,355	0,913	OK
K floors 4-5	W360 × 410 × 463	0,092	0,120	0,243	0,306	0,801	OK
K floors 6-8	W310 × 310 × 314	0,110	0,142	0,269	0,336	0,870	OK
K floors 9-10	W310 × 310 × 216	0,095	0,134	0,182	0,265	0,892	OK
BR floors 1-8	HSS203,2 × 203,2 × 4,8	0,216	0,284	0,356	0,437	0,847	OK

Deviation between floor levels

Determination of the deviation between floors based on the classification of SNI 1726: 2012 [13] the structure studied is in risk category II (office). So that the requirements of the deviation between floors of the design level should not be more than 0,020 hsx. The level height of each structure is 4000 mm, then the allowable deviation of each structural model is 80 mm. The results of the deviations between storey levels on floors 3, 5, 8 and 10 along with the X and Y directions can be seen in Figure 1−4.

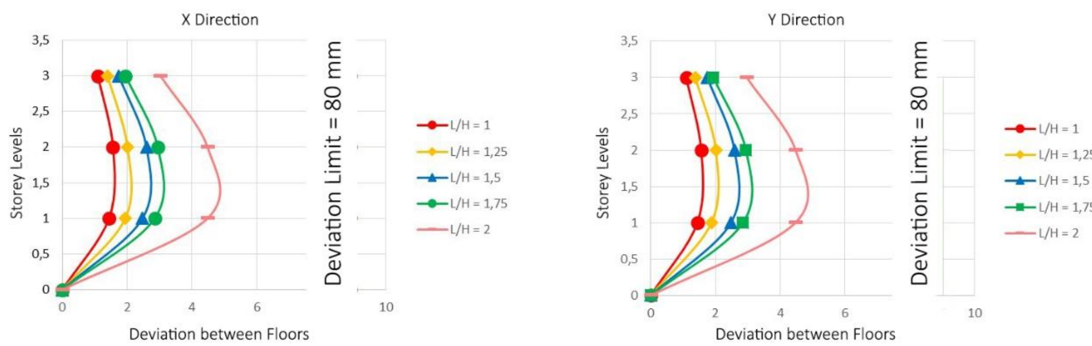

Figure 1. Deviation between Floors at Level 3 Floor X and Y Direction.

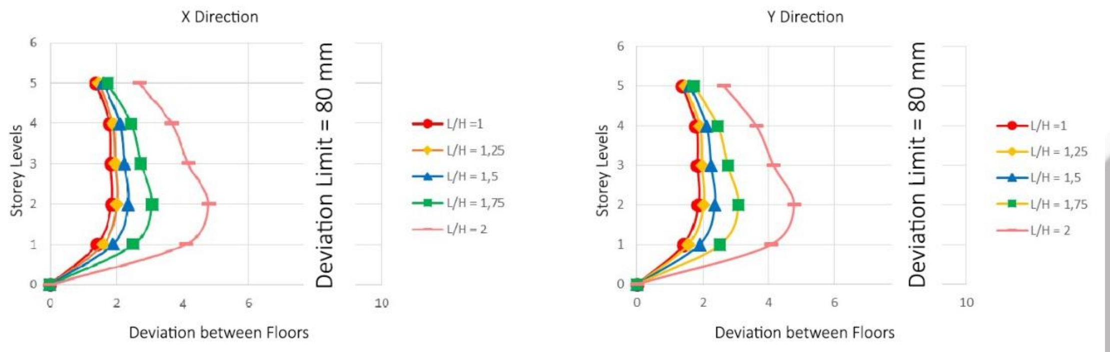

Figure 2. Deviation between Floors at Level 5 Floor Y Direction

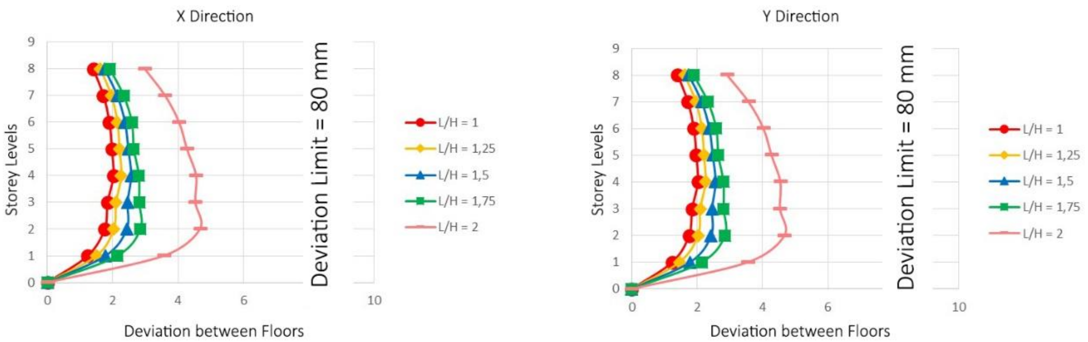

Figure 3. Deviation between Floors at Level 8 Floor Y Direction

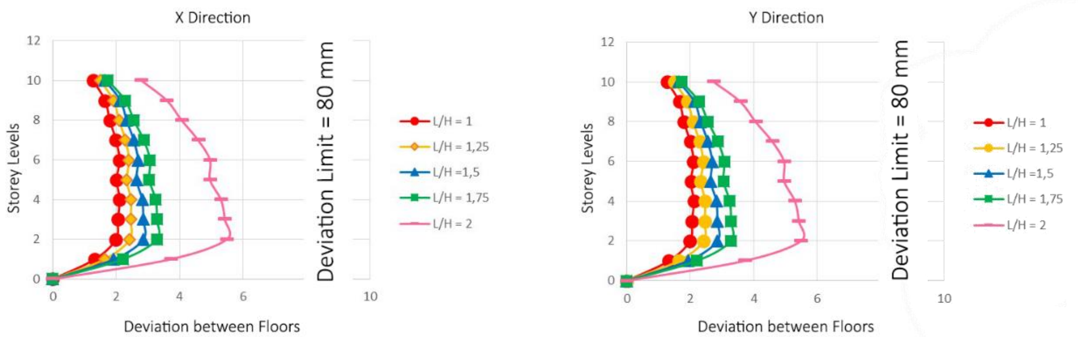

Figure 4. Deviation between Floors at Level 10 Floor Y Direction

Based on the results from Figure 1−4, the deviation between storey floors at each level in the X direction and Y direction occurs at type L/H=2. This is due to the smaller the resulting bracing angle, the less resistance of the bracing in resisting the deformation received by the structure.

Pushover Nonlinear Static Analysis

In this pushover analysis it will produce a curve due to the base shear force and displacement which is called the capacity curve. With the existence of a capacity curve it will also be known the capacity of the structure including the stiffness of the structure and the ductility of the structure. The results of the day's pushover analysis can be seen in Figure 5−8.

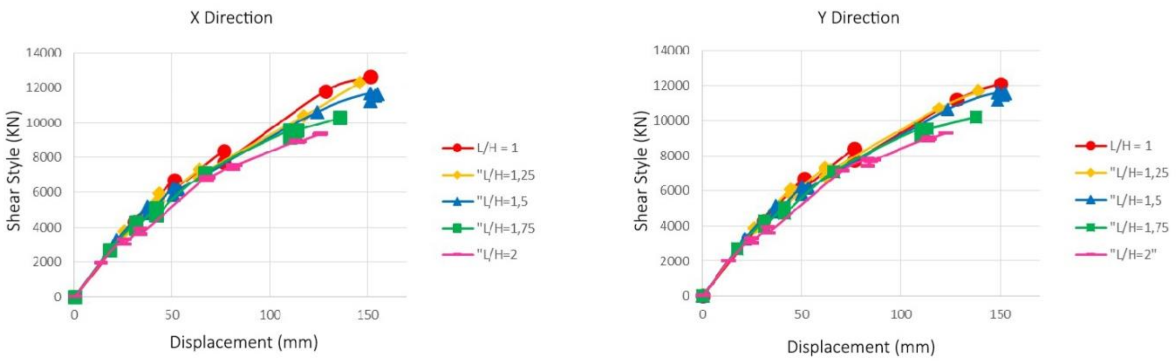

Figure 5. Comparison of Capacity Curves in X and Y Directional 3 Storey Structures.

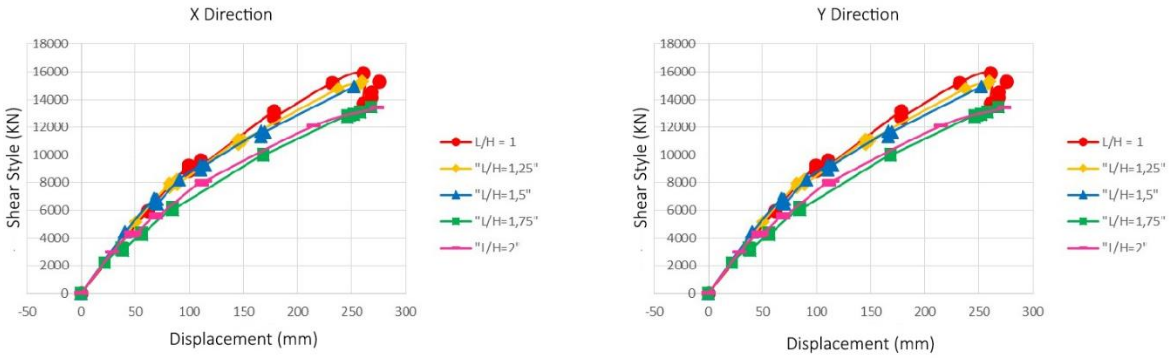

Figure 6. Comparison of Capacity Curves in X and Y Directional 5 Storey Structures.

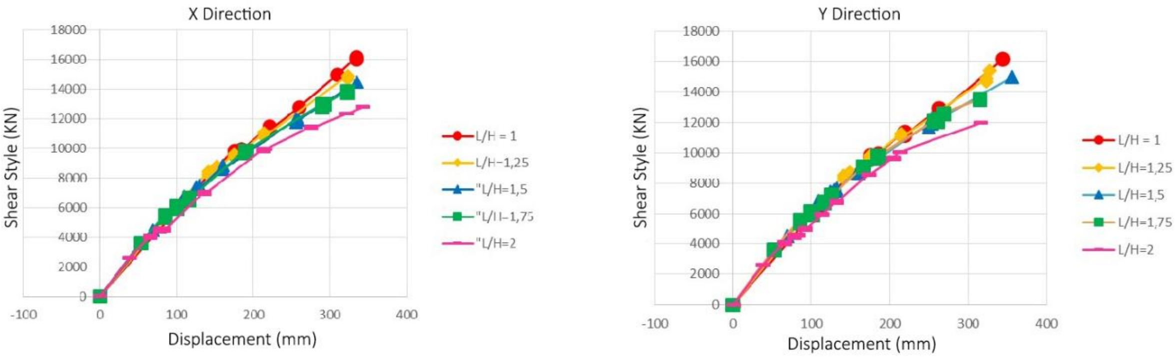

Figure 7. Comparison of Capacity Curves in X and Y Directional 8 Storey Structures.

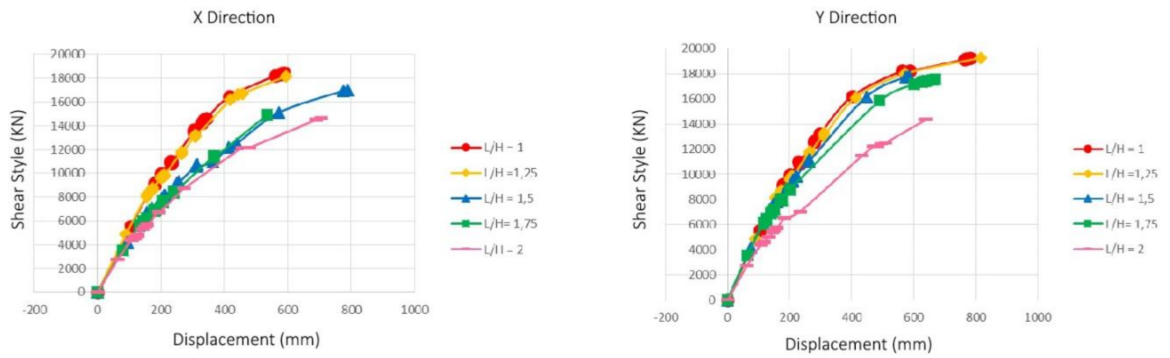

Figure 8. Comparison of Capacity Curves in X and Y Directional 10 Storey Structures.

Based on the results obtained, for a 3-storey building the largest base shear force occurs in the L/H=1 type in the X direction of 12,263 KN with a displacement of 151 mm, while the Y direction is 12,124 KN with a displacement of 150 mm. Furthermore, in a 5-storey building the largest base shear force occurs in type L/H=1 in the X direction of 15,316 KN with a displacement of 275 mm, while in the Y direction of 15,937 KN with a displacement of 262 mm. Then, in the 8-storey building the largest base shear force occurs in the L/H=1 type in the X direction of 16,173 KN with a displacement of 334 mm, while the Y direction is 16,168 KN with a displacement of 343 mm. In the 10-storey building the largest base shear force occurs in the L/H=1 type in the X direction of 18,221 KN with a displacement of 561 mm, while the Y direction is 18,236 KN with a displacement of 563 mm.

Structure Stiffness

After obtaining the capacity curve for each type of L/H, the value of the stiffness of the structure can be determined. The magnitude of the structural stiffness value is the result of the comparison between the base shear force (V) to the displacement (δ), both in yield (y) and ultimate (u) conditions. The results of structural stiffness can be seen from the slope of the capacity curve in yielding and ultimate conditions. Based on the data in Table 5 to Table 12, it can be seen that in the melting condition, the L/H=1 type is the L/H type which has the smallest percentage of stiffness at each level. Meanwhile, in the ultimate condition the greatest structural stiffness at each level occurs in the L/H=1 type. So that it can be said that in the ultimate condition, the greater the L/H type, the smaller the stiffness value of the structure. The relation between the structural stiffness and the shear force is the bigger of the structure stiffness in the building, it will resist with the bigger shear force.

Table 5. Structural Stiffness with 3 Storey Levels in Melting Conditions

Parameter	L/H=1		L/H=1.25		L/H=1.5		L/H=1.75		L/H=2	
	X	Y	X	Y	X	Y	X	Y	X	Y
Vy (kN)	4.293	4.294	3.770	3.879	3.286	3.289	2.706	2.709	1.957	1.976
δy (m)	0,03	0,03	0,025	0,026	0,022	0,022	0,018	0,028	0,013	0,013
K (kN/m)	143.100	138.516	150.800	149.192	149.364	149.500	150.333	150.500	150.538	152.000
%	100	100	105	108	104	108	106	109	105	110

Table 6. Structural Stiffness with 3 Floor Levels in Ultimate Condition

Parameter	L/H=1		L/H=1.25		L/H=1.5		L/H=1.75		L/H=2	
	X	Y	X	Y	X	Y	X	Y	X	Y
Vy (kN)	12.676	12.124	12.277	11.704	11.645	11.596	10.295	10.228	9.343	9.315
δy (m)	0,151	0,15	0,147	0,145	0,154	0,153	0,135	0,138	0,125	0,123
K (kN/m)	83.616	80.827	83.517	80.717	75.617	75.791	76.259	74.116	74.744	75.732
%	100	100	99	99	91	94	91	92	89	93

Table 7. Structural Stiffness with 5 Storey Levels in Melting Conditions

Parameter	L/H=1		L/H=1.25		L/H=1.5		L/H=1.75		L/H=2	
	X	Y	X	Y	X	Y	X	Y	X	Y
Vy (kN)	5.968	5.970	5.145	5.280	4.427	4.432	2.211	2.215	2.943	2.962
δy (m)	0,061	0,061	0,05	0,051	0,041	0,041	0,022	0,022	0,028	0,026
K (kN/m)	97,836	97.869	102.900	103.529	107.976	108.098	100.500	100.682	105.107	113.923
%	100	100	105	106	110	111	103	103	107	116

Table 8. Structural Stiffness with 5 Floor Levels in Ultimate Condition

Parameter	L/H=1		L/H=1.25		L/H=1.5		L/H=1.75		L/H=2	
	X	Y	X	Y	X	Y	X	Y	X	Y
Vy (kN)	15.912	15937	15.804	15.453	14.946	15.828	13.432	13.784	13.401	13.269
δy (m)	0,26	0,262	0,26	0,258	0,253	0,294	0,268	0,262	0,273	0,264
K (kN/m)	61.200	60.828	60.785	59.895	59.075	53.837	50.119	52.611	49.088	50.261
%	100	100	99,3	98,5	96,5	88,5	81,9	86,5	80,2	82,6

Table 9. Structural Stiffness with 8 Storey Levels in Melting Conditions

Parameter	L/H=1		L/H=1.25		L/H=1.5		L/H=1.75		L/H=2	
	X	Y	X	Y	X	Y	X	Y	X	Y
Vy (kN)	6.484	6.489	5.521	5.533	4.460	4.470	3.614	3.616	2.590	2.539
δy (m)	0,111	0,111	0,089	0,089	0,069	0,069	0,053	0,053	0,039	0,038
K (kN/m)	58.414	58.459	62.034	62.169	64.638	64.783	68.189	68.226	66.410	66.816
%	100	100	106	106	111	111	117	117	114	114

Table 10. Structural Stiffness with 8 Floor Levels in Ultimate Condition

Parameter	L/H=1		L/H=1.25		L/H=1.5		L/H=1.75		L/H=2	
	X	Y	X	Y	X	Y	X	Y	X	Y
Vy (kN)	16.172	16.180	14.910	15.414	14.486	15.055	13.886	13.533	12.788	11.975
δy (m)	0,333	0,343	0,322	0,327	0,334	0,355	0,322	0,314	0,342	0,316
K (kN/m)	48.565	47.172	46.304	47.138	43.371	42.268	43.124	43.099	37.392	37.896
%	100	100	95	99	89	90	88	91	77	80

Table 11. Structural Stiffness with 10 Storey Levels in Melting Conditions

Parameter	L/H=1		L/H=1.25		L/H=1.5		L/H=1.75		L/H=2	
	X	Y	X	Y	X	Y	X	Y	X	Y
Vy (kN)	5.522	5.525	4.834	4.837	4.175	4.280	3.532	3.533	2.708	2.710
δy (m)	0,128	0,129	0,110	0,110	0,094	0,094	0,079	0,079	0,062	0,062
K (kN/m)	43.141	42.829	43.945	43.973	44.415	45.532	44.709	44.722	43.677	43.710
%	100	100	102	103	103	106	104	104	101	102

Table 12. Structural Stiffness with 10 Floor Levels in Ultimate Condition

Parameter	L/H=1		L/H=1.25		L/H=1.5		L/H=1.75		L/H=2	
	X	Y	X	Y	X	Y	X	Y	X	Y
Vy (kN)	18.468	18.221	18.161	17.999	15.125	17.817	15.962	17.548	14.488	14.323
δy (m)	0,586	0,567	0,594	0,572	0,572	0,575	0,608	0,670	0,687	0,637
K (kN/m)	31.515	32.136	30.574	31.467	26.442	30.986	26.253	26.191	21.089	22.485
%	100	100	97	98	84	96	83	82	67	70

Structural Ductility

After knowing the value of the displacement during the melting condition and the ultimate condition, it can be known the value of the ductility of each structure. The ductility value of the structure is the result of a comparison between the displacements in the melting state (δy) and the ultimate condition (δu). Based on data from Tables 13 to 16, the type L/=1 is used as a comparison for the structural ductility of each type of L/H. The greatest structural ductility at the 3 story level in the X direction and Y direction occurs in the L/H=2 type with a value of 9.3. The greatest structural ductility at the 5 storey level in the X and Y directions occurs in type L/H=2 with values of 9.7 and 9.4 respectively. The greatest structural ductility at the 8 storey level in the X direction and Y direction occurs in the L/H=2 type with values of 8.9 and 8.2 respectively. The greatest structural ductility at the 10 story level in the X and Y directions occurs in type L/H=2 with values of 11 and 10.6 respectively. So at each level, the greatest ductility occurs at type L/H=2.

Table 13. Structure Ductility with Level 3 Floors

Parameter	L/H=1		L/H=1.25		L/H=1.5		L/H=1.75		L/H=2	
	X	Y	X	Y	X	Y	X	Y	X	Y
δu (m)	0,151	0,15	0,146	0,145	0,155	0,152	0,136	0,138	0,125	0,123
δy (m)	0,031	0,031	0,025	0,026	0,022	0,021	0,018	0,018	0,013	0,013
Daktailitas	4,9	4,9	5,7	5,6	7,1	7,1	7,6	7,8	9,3	9,3
%	100	100	116	114	145	145	153	159	188	191

Table 14. Structure Ductility with Level 5 Floors

Parameter	L/H=1		L/H=1.25		L/H=1.5		L/H=1.75		L/H=2	
	X	Y	X	Y	X	Y	X	Y	X	Y
δu (m)	0,275	0,262	0,260	0,259	0,252	0,253	0,268	0,263	0,273	0,265
δy (m)	0,061	0,061	0,050	0,051	0,041	0,040	0,037	0,037	0,028	0,028
Daktailitas	4,5	4,3	5,2	5,1	6,2	6,3	7,3	7,2	9,7	9,4
%	100	100	116	118	138	146	162	167	215	219

Table 15. Structure Ductility with Level 8 Floors

Parameter	L/H=1		L/H=1.25		L/H=1.5		L/H=1.75		L/H=2	
	X	Y	X	Y	X	Y	X	Y	X	Y
δu (m)	0,334	0,344	0,323	0,328	0,335	0,355	0,322	0,315	0,342	0,316
δy (m)	0,111	0,111	0,089	0,089	0,069	0,069	0,053	0,053	0,039	0,038
Daktailitas	3,0	3,1	3,6	3,7	4,9	5,2	6,1	6,0	8,9	8,2
%	100	100	120	119	162	168	202	194	295	266

Table 16. Structure Ductility with Level 10 Floors

Parameter	L/H=1		L/H=1.25		L/H=1.5		L/H=1.75		L/H=2	
	X	Y	X	Y	X	Y	X	Y	X	Y
δu (m)	0,588	0,587	0,594	0,573	0,573	0,573	0,608	0,661	0,688	0,657
δy (m)	0,128	0,129	0,111	0,111	0,095	0,085	0,079	0,071	0,063	0,062
Daktailitas	4,6	4,5	5,4	5,2	6,0	6,7	7,7	9,3	11,0	10,6
%	100	100	117	114	131	149	167	205	239	234

Displacement Target

Then determine the displacement target, namely the assumption that there is a maximum displacement that may occur as a result of the earthquake load. The displacement target in this study used the ASCE 41-13 NSP (Nonlinear Static Procedure) method which is available in the ETABS 2016 software application. Determination of the displacement target based on this nonlinear static procedure is carried out by making an idealization curve of the capacity curve resulting from a static nonlinear pushover analysis. So, with the idealization curve, it will be known the displacement target that occurs from the structural model [14]. Based on data from Table 17 to Table 20, it is known that the largest displacement target for each type occurs at type L/H=2. So that the greater the type L/H in the bracing structure, the greater the displacement target produced.

Table 17. Target Displacement and Basic Shear Force of 3 Floor Structure Model

Type	Displacement Target (mm)		Basic Shear Force (KN)	
	X	Y	X	Y
L/H = 1.00	0,052	0,052	6.270	6.271
L/H = 1,25	0,070	0,070	7.434	7.505
L/H = 1,50	0,098	0,098	8.982	8.993
L/H = 1,75	0,129	0,129	10.297	10.326
L/H = 2.00	0,195	0,194	9.343	9.315

Table 18. Target Displacement and Basic Shear Force of 5 Floor Structure Model

Type	Displacement Target (mm)		Basic Shear Force (KN)	
	X	Y	X	Y
L/H = 1.00	0,114	0,114	9.425	9.431
L/H = 1,25	0,137	0,137	10.602	10.737
L/H = 1,50	0,152	0,152	11.069	11.082
L/H = 1,75	0,192	0,190	10.809	10.842
L/H = 2.00	0,264	0,262	13.533	13.494

Table 19. Target Displacement and Basic Shear Force of 8 Floor Structure Model

Type	Displacement Target (mm)		Basic Shear Force (KN)	
	X	Y	X	Y
L/H = 1.00	0,192	0,193	10.244	10.258
L/H = 1,25	0,211	0,211	10.912	10.987
L/H = 1,50	0,233	0,233	11.169	11.164
L/H = 1,75	0,259	0,258	12.050	12.006
L/H = 2.00	0,408	0,401	12.788	12.788

Table 20. Target Displacement and Basic Shear Force of 10 Floor Structure Model

Type	Displacement Target (mm)		Basic Shear Force (KN)	
	X	Y	X	Y
L/H = 1.00	0,246	0,246	9.696	9.699
L/H = 1,25	0,278	0,278	10.262	10.251
L/H = 1,50	0,315	0,314	10.630	10.626
L/H = 1,75	0,356	0,357	11.185	10.891
L/H = 2.00	0,565	0,571	13.128	13.388

Structure Performance Level

After knowing the target displacement of the structure, it can be known the level of performance of each structure. Based on FEMA 273, the determination of the performance level of the structure is based on the calculation between the target displacement and the total height of the building. The structure performance level grouping is divided into 3, namely: Immediate Occupancy (IO), Life Safety (LS), and Collapse Prevention (CP) [15]. The performance level of each structure can be seen in table 21 to table 24.

Tabel 21. Structural Performance Level In 3 Floor Model

Parameter	L/H=1		L/H=1.25		L/H=1.5		L/H=1.75		L/H=2	
	X	Y	X	Y	X	Y	X	Y	X	Y
Displacement Target (m)	0,052	0,052	0,07	0,07	0,098	0,098	0,129	0,129	0,195	0,194
Height (m)	12	12	12	12	12	12	12	12	12	12
Drift Ratio (%)	0,43	0,43	0,58	0,58	0,82	0,82	1,08	1,08	1,63	1,62
Performance Levels	IO	IO	LS	LS	LS	LS	LS	LS	CP	CP

Tabel 22. Structural Performance Level In 5 Floor Model

Parameter	L/H=1		L/H=1.25		L/H=1.5		L/H=1.75		L/H=2	
	X	Y	X	Y	X	Y	X	Y	X	Y
Displacement Target (m)	0,114	0,114	0,137	0,137	0,152	0,152	0,19	0,19	0,264	0,262
Height (m)	12	12	12	12	12	12	12	12	12	12
Drift Ratio (%)	0,57	0,57	0,69	0,69	0,76	0,76	0,95	0,95	1,32	1,31
Performance Levels	LS	LS	LS	LS	LS	LS	LS	LS	LS	LS

Tabel 23. Structural Performance Level In 8 Floor Model

Parameter	L/H=1		L/H=1.25		L/H=1.5		L/H=1.75		L/H=2	
	X	Y	X	Y	X	Y	X	Y	X	Y
Displacement Target (m)	0,192	0,192	0,211	0,211	0,233	0,233	0,259	0,258	0,408	0,401
Height (m)	12	12	12	12	12	12	12	12	12	12
Drift Ratio (%)	0,6	0,6	0,66	0,66	0,73	0,73	0,81	0,81	1,28	1,25
Performance Levels	LS	LS	LS	LS	LS	LS	LS	LS	LS	LS

Tabel 24. Structural Performance Level In 10 Floor Model

Parameter	L/H=1		L/H=1.25		L/H=1.5		L/H=1.75		L/H=2	
	X	Y	X	Y	X	Y	X	Y	X	Y
Displacement Target (m)	0,246	0,246	0,278	0,278	0,315	0,314	0,356	0,357	0,565	0,571
Height (m)	12	12	12	12	12	12	12	12	12	12
Drift Ratio (%)	0,62	0,62	0,7	0,7	0,79	0,79	0,89	0,89	1,41	1,43
Performance Levels	LS	LS	LS	LS	LS	LS	LS	LS	LS	LS

So, based on data from Tables 21 to Table 24, it shows that the highest level of performance is in the 3-story structure model in the X direction and Y direction with type L/H=2, which is at the Collapse Prevention (CP). The level of Collapse Prevention (CP) occurs when 0% -0.5% = IO ; 0.5%-1.5% = LS ; > 1.5% = CP level which if 0%-0,5% = IO ; 0,5%-1,5% = LS ; > 1,5% = CP.

4. CONCLUSION

The conclusions that can be drawn from this research are: (1) The greater the increase in the type of L/H, the greater the deviation generated by the structural model, (2) After performing a nonlinear pushover analysis, the largest shear and displacement forces on each story occur in the type L/H=1, (3) In the melting condition, type L/H=1 is the type L/H which has the smallest percentage of stiffness at each level. However, in the ultimate condition, the greatest structural stiffness at each story occurs in the L/H=1 type. So that it can be said that in the ultimate condition, the greater the L/H type, the smaller the stiffness value of the structure, (4) The greatest value of structural ductility at each story occurs in the L/H=2 type in both the X and Y directions, (5) Based on ASCE 41-13 NSP model displacement targets L/H=2, all level models experience the largest displacement targets in the X and Y directions when compared to the other 4 types of L/H, (6) The highest level of structural performance occurs in the 3-floor structure model with type L/H=2, namely at the Collapse Prevention (CP) level, while for other structural models all are at the Life Safety (LS) level.

5. REFERENCES

[1] Amirsardari, A., Sofi, M., Lumantarna, E., Imran, I., & Duffield, C. (2019). Impact of earthquakes on the transportation infrastructure of indonesia: A preliminary study. Civil Engineering Dimension. 21(1), 19-28.
[2] Rajindra, R., Suardi, I., Sabara, Z., Pushpalal, D., Samad, M. A., Yani, A., & Umam, R. (2019). Diversity, resilience, and tragedy: Three disasters in Palu of Indonesia. International Journal of Innovation, Creativity and Change. 5(2), 1592-1607
[3] Doğangün, A., Yön, B., Onat, O., Emin Öncü, M., & Sağıroğlu, S. (2021). Seismicity of East Anatolian of Turkey and failures of infill walls induced by major earthquakes. Journal of Earthquake and Tsunami. 15(04), 2150017.
[4] Eren, N., Brunesi, E., & Nascimbene, R. (2019). Influence of masonry infills on the progressive collapse resistance of reinforced concrete framed buildings. Engineering Structures. 178, 375-394.
[5] Terán-Gilmore, A., Roeslin, S., Tapia-Hernández, E., & Cuadros-Hipólito, E. (2021). Displacement-based design of tall earthquake-resistant diagrid systems. Journal of Building Engineering. 35, 102022.
[6] Liew, J. Y. R., Chua, Y. S., & Dai, Z. (2019). Steel Concrete Composite Systems for Modular Construction of High-Rise Buildings. In Structures Elsevier. 21, 135-149.
[7] Shi, X., Park, P., Rew, Y., Huang, K., & Sim, C. (2020). Constitutive Behaviors of Steel Fiber Reinforced Concrete Under Uniaxial Compression and Tension. Construction and Building Materials. 233, 117316.
[8] Hashemi, A., Clifton, G. C., Bagheri, H., Zarnani, P., & Quenneville, P. (2020). Proposed Design Procedure for Steel Self-Centring Tension-Only Braces with Resilient Connections. In Structures Elsevier. 25, 147-156.
[9] Hemmati, A., Kheyroddin, A., & Farzad, M. (2020). Experimental Study of Reinforced Concrete Frame Rehabilitated by Concentric and Eccentric Bracing. Journal of Rehabilitation in Civil Engineering. 8(1), 97-108.
[10] Zhang, G., Xu, L. H., & Li, Z. X. (2021). Development and Seismic Retrofit of An Innovative Modular Steel Structure Connection Using Symmetrical Self-Centering Haunch Braces. Engineering Structures. 229, 111671.
[11] Seker, O. (2022). Seismic Response of Dual Concentrically Braced Steel Frames with Various Bracing Configurations. Journal of Constructional Steel Research. 188, 107057.
[12] National Standardization Agency. (2013). Minimum Load for the Design of Buildings and Other Structures: SNI 1727-2013.
[13] National Standardization Agency. (2012). Earthquake Resistance Planning Procedures for Building and Non-Building Structures: SNI 1726-2012.
[14] Speicher, M. S., & Harris III, J. L. (2018). Collapse Prevention Seismic Performance Assessment of New Buckling-Restrained Braced Frames Using ASCE 41. Engineering Structures. 164, 274-289.
[15] Chopra, A. K., & Goel, R. K. (2002). A Modal Pushover Analysis Procedure for Estimating Seismic Demands for Buildings. Earthquake Engineering & Structural Dynamics. 31(3), 561-582.

LOGIC
Journal of Engineering Design and Technology
Vol. 23 No.2 July 2023 ; p. 96-103

p-ISSN : 1412-114X
e-ISSN : 2580-5649
http://ojs2.pnb.ac.id/index.php/LOGIC

THE EFFECT OF NON-EXCUSABLE DELAY FACTORS ON THE COMPLETION OF BUILDING CONSTRUCTION PROJECTS

1) Department of Civil Engineering, State Polytechnic of Jakarta, Prof. DR. G.A. Siwabessy Street, UI New Campus, Kukusan, Depok City, Indonesia

Corresponding email [1] :
alvindunaufal10@gmail.com

Alvin Dunaufal [1], I Ketut Sucita [1], Jonathan Saputra [1]

Abstract. A problem that often occurs in construction projects is the delay in the implementation process. Various factors cause the delay, but in developing countries such as Indonesia, the dominant delay occurs because the implementing contractor causes it for unforgivable reasons (non-excusable delay). This study aims to determine the influence of the non-excusable delay parameter and the relationship between these factors. The research is quantitative with data collection techniques in the form of unstructured interviews, field observations, and surveys using research questionnaires with the number of respondents obtained as many as 33 people consisting of the owner, construction management consultant, quantity surveyor consultant, and ends with confirmation of the results. Research on the implementing contractor. Data analysis was performed using multiple linear regression analysis. The test results of multiple linear regression analysis show that the non-excusable delay factor can significantly affect the completion of construction projects. The influence of each element is 0.434 units for the lack of contractor competence, 0.067 units for inappropriate implementation planning, and -0.097 for inefficient field management units. And simultaneously, these three factors can significantly increase the project delay value index.

Keywords : Delay; Non-Excusable Delay; Contractor; Construction Project

1. INTRODUCTION

A construction project is an activity or work that involves many parties, including owners, consultants, and contractors, to achieve specific goals with certain costs, quality, and time constraints. It starts with the planning stage and continues through the implementation and maintenance stages [1].

In construction, a delay is a problem that occurs most often [2]. Project delays are a source of problems that often occur in every construction project development. Construction project delays based on the nature and compensation provided can be classified into three parts such as Compensable Delay (CD), Excusable Delay (ED), and Non-Excusable Delay (NED) [3]. The problem of work implementation that often occurs in almost all sectors of the construction work implementation is dominated by work time delays [4]. In Indonesia, delays in construction projects that are dominant are unforgivable delays and are included in the Non-Excusable Delay (NED) category, which are predominantly caused by the implementing contractor as a result of the same delay factor [5]. It can be interpreted that the implementing contractor has no right to demand compensation for any form of delay that occurs.

Non-Excusable Delay (NED) is a delay in which the implementing contractor is fully responsible to the project owner [5]. Of the many factors and indicators of delays in construction projects in Indonesia, three leading indicators often hinder the implementation of construction projects according to the implementing contractor, including the lack of competent engineers in carrying out the work, the lack of required human resources planning, and the lack of monitoring activities for the result of the work implementation [6]. Construction project delays are also dominantly caused by the low level of work productivity, which is also influenced by the scope of the work environment [7].

It is planned that by the end of 2022, one of the projects in the South Jakarta area, precisely in the Tanjung Barat station area, will complete an apartment by carrying the concept of Transit Oriented Development (TOD) housing. In its implementation until the end of January 2022, there have been projected delays with a deviation value of -10.2327%. A large number with indications of delay factors that have been confirmed from various parties that the delays that occur are caused by the implementing contractor and are classified as work default activities, where work default activities are characterized by deviations in the execution of work from the initial contract [8]. With an indication of the delay, a Show Cause Meeting (SCM) was held in April 2022. The three dominant problems that cause delays are Lack of Contractor Competence, Improper Implementation Planning, and Inefficient Field Management, as shown in Figure 1 [9].

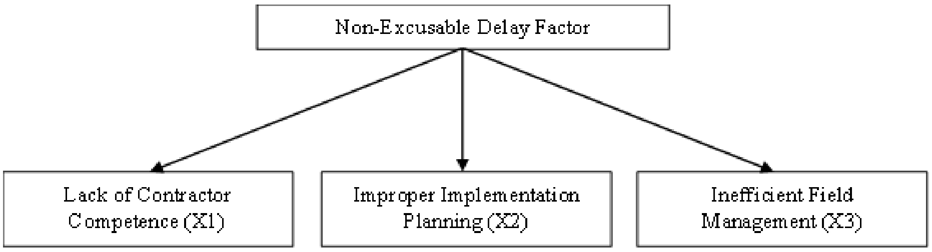

Figure 1. Non-Excusable Delay Factor

Lack of Contractor Competence is affected by the effectiveness of management, and contractor staff is affected by problems such as poor planning and scheduling, lack of supervision during implementation, lack of coordination and communication between related parties, and lack of skilled workers [10]. The impact that may also be caused by the lack of competence of existing contractors is the increase in the number of work accidents due to a lack of knowledge in work supervision [11]. Incompatibility of planning with implementation in the field can result in delays in construction projects [12]. One of the impacts of poor planning is the swelling overhead costs [13]. In preparing good field management, you must make the best possible planning so that the project objectives in terms of price, quality, and time can be completed according to the plan and create a clean and healthy field site by involving all aspects and parties [14].

This research data management will use data analysis methods by using statistical analysis using multiple linear regression analysis models to test every existing problem, such as the influence of the delay factor partially to answer the impact of each delay factor and determine the relationship between delays simultaneously from each delay factor, which exists.

From each of the existing problems, the initial hypotheses that arise are explained in Figure 2.

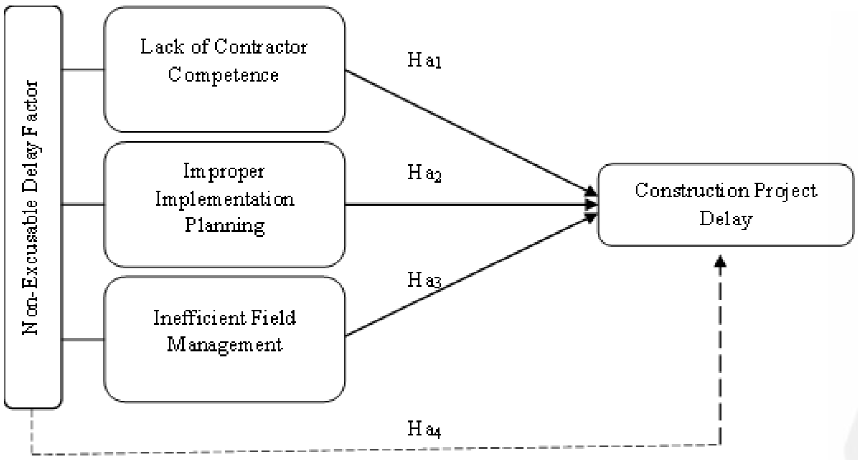

Figure 2. Research Framework

The description of Figure 2 is as follow:

→ The effect of each independent variable on the dependent variable
⇢ The influence of the relationship of independent variables simultaneously on the dependent variable

H_{01} = No significant influence of the lack of Contractor Competence on the Construction Project Delay
Ha_1 = A significant influence of the lack of Contractor Competence on the Construction Project Delay

H_{02} = No significant influence of the Improper Implementation Planning on the Construction Project Delay
Ha_2 = A significant influence of the Improper Implementation Planning on the Construction Project Delay

H_{03} = No significant influence of the Inefficient Field Management on the Construction Project Delay
Ha_3 = A significant influence of the Inefficient Field Management on the Construction Project Delay

H_{04} = No significant simultaneous effect of the lack of Contractor Competence, Improper Implementation Planning and Inefficient Field Management on Construction Project Delays
Ha_4 = A significant simultaneous effect of the lack of Contractor Competence, Improper Implementation Planning and Inefficient Field Management on Construction Project Delays

2. METHODS

The stages of research activities carried out in this study, among others:

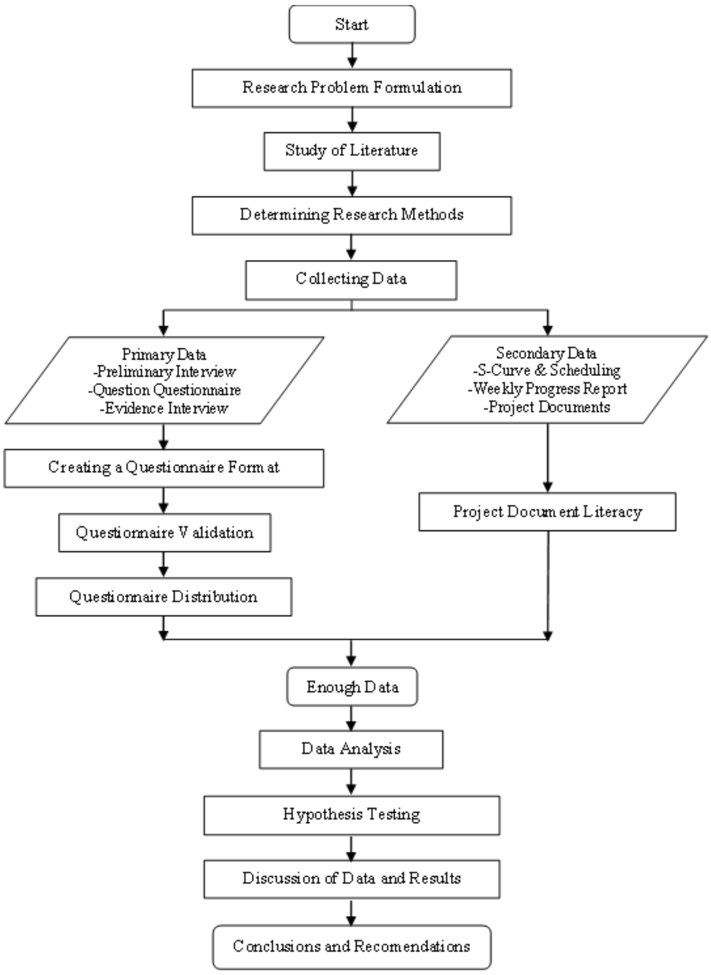

Figure 3. Research Schematic Flow

Two types of data needed for this investigation are primary and secondary data. Then the data collection method used for writing this thesis, namely:

1. Primary Data
   The primary data in this study came from unstructured interviews, preliminary interview results from sheets, and questionnaires from respondents using indicators of factors causing Non-Excusable Delay (NED) delays

and construction project completion.
   a. Interview Method
   b. Questionnaire Method
2. Secondary Data
   Secondary data is information collected from various existing sources [15]. In this study, secondary data were in the form of documents related to the work assessment of contractors, weekly progress of achieving physical implementation in the field, initial contract documents, and the S-curve on the TOD Design Project of Mahata Tanjung Barat.

The population is a generalization area consisting of objects or people selected to be studied because they have specific attributes and characteristics from which conclusions can be made [16]. The population in this study which are incorporated into the research respondents came from the owner, the Constitutional Court consultant, and the QS consultant.

To ensure that the sample represents the size and composition of the population [16], this study is planned to collect as many as 33 research respondents from employees focused on the Rusunami TOD construction project of Mahata Tanjung Barat, which can be seen in the following table.

Table 1. Research Respondents

Position	**Quantity**
Project Leader	1 Person
Head of Construction Department	1 Person
Head of Planning and Licensing Department	1 Person
Owner Staff	4 Person
Team Leader (Consultant)	1 Person
Architectural Expert (Consultant)	2 Person
Structural Expert (Consultant)	1 Person
MEP Expert (Consultant)	2 Person
HSE Expert (Consultant)	2 Person
Architecture Supervisor (Consultant)	2 Person
MEP Supervisor (Consultant)	2 Person
Administration (Consultant)	1 Person
Owner Staff On Job Training (OJT)	8 Person
Architectural Consultant (QS)	1 Person
Structural Consultant (QS)	1 Person
Total Respondents	**30 Person**

3. RESULTS AND DISCUSSION

Data on the characteristics of research respondents can be seen in the following tables:

Table 2. Characteristics by Gender

No	Gender	Number of Respondents	Percentage (%)
1	Male	24	80%
2	Female	6	20%
	Total	30	100%

It can be seen that as many as 80% of research respondents are male.

Table 3. Characteristics by Age Range

No	Age (Years)	Number of Respondents	Percentage (%)
1	20 – 30	12	40%
2	31 – 40	9	13%
3	41 – 50	5	17%
4	> 50	4	30%
	Total	30	100%

It can be seen that 40% of the research respondents are 20-30 years old.

Table 4. Characteristics Based on Experience

No	Work experience	Number of Respondents	Percentage (%)
1	Housing	6	20%
2	Building < 4 Floor	3	10%
3	Building 4 - 8 Floor	4	13%
4	Building > 8 Floor	17	57%
	Total	30	100%

It can be seen that the experience of respondents in working is dominated by 57% having handled a building project > 8 floors.

Table 5. Characteristics Based on Length of Work

No	Length of work	Number of Respondents	Percentage (%)
1	< 3 years	9	30%
2	3 - 6 years	6	20%
3	7 - 10 years	7	23%
4	> 11 years	8	27%
	Total	30	100%

It can be seen that the dominant research respondents are respondents with more than 11 years of experience in the same position by 27%.

The test results from multiple linear regression analysis to find the existing relationship forms can be seen in the following table:

Table 6. Linear Regression Test Results

		B	Sig.
1	(Constant)	13.466	0
	Lack of Contractor Competence (X1)	0.434	0.087
	Improper Implementation Planning (X2)	0.067	0.802
		-0.097	0.673

Inefficient Field Management (X3)	

It can be seen that the results of the linear regression that has been carried out can be notated into an equation as follows:

$$\hat{Y} = 13.466 + 0.434x_1 + 0.067x_2 - 0.097x_3 \quad (1)$$

Refer to Eq. (1), the evaluation of the results of linear regression analysis

It can also be interpreted that every time there is no influence of the Non-Excusable Delay factor, the delay in the construction project itself has a constant of 13.466 units. If each independent variable affects one unit, it will have an effect of 0.434 units for each X1, 0.067 units for the X2 variable, and -0.097 units for the X3 variable.

And based on the results in the regression test table (Table 6.) above, it can also be seen that each independent variable factor that exists partially does not have a significant effect, characterized by all significance values greater than 0.05.

As for testing the Non-Excusable Delay factor simultaneously, the test results can be seen in the following table:

Table 7. F Test Results (ANOVA)

Model		F	Sig.
1	Regression	3.633	0.026
	Residual		
	Total	3.633	0.026

It can be seen that if the three factors of unforgivable delay occur simultaneously or simultaneously, it will significantly impact the increase in delays that occur. The resulting significance value can prove it is smaller than 0.05.

And to see the dominant factor in each of the existing delay indicators can be seen in the following table:

Table 8. Recapitulation of Descriptive Analysis Results

No	Indicator	Variable	%
1	X1	Lack of contractor's financial capacity (X1.1)	90.0%
2	X2	Inaccuracy of workforce planning (X2.4)	96.0%
3	X3	Lack of work control and monitoring (X3.1)	94.0%
4	Y	Percentage of Plan Completed (PPC) (Y)	97.4%

Based on the tests that have been carried out with 30 research respondents and the confirmation of the results with the implementing contractor, temporary conclusions can be made as follows:

1. Respondents agree with a relatively high average rating above 90% for each variable indicator, each of which is found to be a dominant factor causing delays. And it has been confirmed that the biggest obstacle in the construction of this project is the financial condition still affected by the Covid-19 pandemic.
2. The regression test analysis results obtained a regression equation with the constant value of project delays without the Non-Excusable Delay factor of 13.466 units. Meanwhile, if the three indicators affect the existing variable factors, it will increase by 0.434 for X1, 0.067 for X2, and -0.097 for X3.
3. Unlike the T-Test results, when viewed partially in each of the existing independent variable indicators, there is no significant effect on each Non-Excusable Delay factor.

4. However, if viewed from the results of the F-Test, which was carried out to find the value of the relationship between Non-Excusable Delay factors, it was found that there was a significant influence on the delay that occurred.
5. And the meaning is based on the hypothesis that has been made. When viewed partially for each indicator of the delay factor, the answers H01, H02, and H03 are accepted in the three initial hypotheses, which means that there is no significant partial effect of the Non-Excusable Delay factor indicator that can affect the delay that occurs. In contrast to the simultaneous hypothesis, it can be concluded that Ha4 is accepted, which means that the Non-Excusable Delay factor significantly influences delays in building construction projects.
6. And the confirmation of the research results has been done to the contractor. Indeed, the delay occurred purely because of the existing financial problems. This causes an impact on all elements of the current work units, such as the inability to engineer the addition of overtime hours and the addition of human resources.
7. This means that this study also agrees that the three factors of Non-Excusable Delay, including Lack of Contractor Competence, Improper Implementation Planning, and Inefficient Field Management, affect any increase in the number of construction project delays. As in line with previous research.

4. CONCLUSION

From the results of the discussion of the research that has been done, it can be concluded several things as follows:

1. When viewed partially, Non-Excusable Delay not significantly impact Construction Project Delays (Y). Non-Excusable Delay factors include Lack of Contractor Competence (X1), Improper Implementation Planning (X2), and Inefficient Field Management (X3). Positive X1 and X2 values impact delays, and negative X3 values resulting on the decrase of delays. This means that efforts to suppress the number of uncertainties can be stopped by reducing each indicator between X1 and X2 and increasing X3 indicators, such as improving the coordination of communication relations of each party involved.
2. If viewed partially, the three indicators of the Non-Excusable Delay factor will significantly affect any delays. This means there is a need to develop problem-solving solutions for each of the same detrimental delay factors.

5. REFERENCES

[1] H. Hassan, “Faktor-Faktor Penyebab Keterlambatan Pada Proyek Konstruksi dan Alternatif Penyelesaiannya, Studi Kasus: di Manado Town Square III),” *J. Sipil Statik*, vol. 4, pp. 657–664, 2016.

[2] I. Mahamid, A. Bruland, and N. Dmaidi, “Causes of Delay in Road Construction Projects,” *J. Proj. Manag. Eng.*, vol. 28, no. 3, pp. 300–310, 2012.

[3] Y. unit. Messah, T. Widodo, and M. Adoe, “Kajian Penyebab Keterlambatan Pelaksanaan,” *Univ. Nusa Cendana*, vol. II, no. 2, pp. 157–168, 2013.

[4] T. P. Dewanata, “Analisis Faktor Dominan Keterlambatan Waktu Mulai Proyek Konstruksi dari Sudut Pandang Pengguna Jasa,” *Skripsi Thesis, Univ. Tarumanagara*, 2016.

[5] R. C. Islami, J. Yang, and A. Wibowo, “Identifying Non-Excusable Delay Causes for Developing Countries : An Empirical Study from Indonesia,” *19th Symp. Constr. Eng. Manag. 2015*, no. April 2017, 2015.

[6] S. Andrean, “Excusable Delay Pada Proyek Konstruksi,” 2018.

[7] G. A. Wijaya, I. K. Sucita, and J. Saputra, “Analisis Tingkat dan Faktor Produktivitas Tenaga Kerja pada Pekerjaan Struktur Atas di Proyek X,” vol. 13, no. 2, 2021.

[8] B. G. Hwang and S. Yang, “Rework and Schedule Performance: A Profile of Incidence, Impact, Causes, and Solution,” *Eng. Constr. Archit. Manag.*, vol. 21, no. 2, pp. 190–205, 2014.

[9] A. Adam, P. E. B. Josephson, and G. Lindahl, “Aggregation of factors causing cost overruns and time delays in large public construction projects: Trends and implications,” *Eng. Constr. Archit. Manag.*, vol. 24, no. 3, pp. 393–406, 2017, doi: 10.1108/ECAM-09-2015-0135.

[10] G. S. . Elawi, M. Algahtany, and D. Kashiwagi, “Owner’s Perpective of Factors Contributing to Project Delays: Case Studies of Road and Bridge Projects in Saudi Arabia,” *Procedia Eng.*, no. 145, pp. 1402–1409, 2016.

[11] H. Doloi, A. Sawhney, K. C. Iyer, and S. Rentala, “Analysing factors affecting delays in Indian construction projects,” *Int. J. Proj. Manag.*, vol. 30, no. 4, pp. 479–489, 2012, doi: 10.1016/j.ijproman.2011.10.004.

[12] M. M. Marzouk and T. I. El-Rasas, “Analyzing delay causes in egyptian construction projects,” *J. Adv. Res.*, vol. 5, no. 1, pp. 49–55, 2014, doi: 10.1016/j.jare.2012.11.005.

[13] C. . Amoatey, A. . Ameyaw, E. Adaku, and S. Famiyeh, “Analysing Delay Causes and Effects in Ghanaian State Housing Construction Projects,” *Int. J. Manag. Proj. Bus.*, vol. 8, no. 1, pp. 198–214, 2015.

[14] M. Gündüz, Y. Nielsen, and M. Özdemir, “Quantification of Delay Factors Using the Relative Importance Index Method for Construction Projects in Turkey,” *J. Manag. Eng.*, vol. 29, no. 2, pp. 133–139, 2013, doi: 10.1061/(asce)me.1943-5479.0000129.

[15] D. . Siyoto and M. . Sodik, *Dasar Metodologi Penelitian*, (Ayup (ed. Literasi Media Publishing, 2015.
[16] Sugiyono, *Metode Penelitian Kuantitatif, Kualitatif, dan R&D*. Bandung: Alfabeta, 2018.

LOGIC
Journal of Engineering Design and Technology
Vol. 23 No.2 July 2023; p. 104 - 110

p-ISSN : 1412-114X
e-ISSN : 2580-5649
http://ojs2.pnb.ac.id/index.php/LOGIC

AN ANALYSIS OF EMISSIONS EXHAUST GAS ON 4-STROKE ENGINE BASED ON IOT GAS ANALYZER

1) Department of Mechanical Engineering, State Polytechnic of Malang, Indonesia

Correponding email 3): asrori@polinema.ac.id

Mokhammad Khatami1), Agus Sujatmiko1), Asrori Asrori1)

Abstract. According to the Air Quality Live Index (AQLI), Indonesia's air quality has continued to deteriorate in the last two decades, so Indonesia is officially ranked 17th as the country with the worst air quality in the world. This is due to the population explosion in Indonesia causing industrial activity to also increase. The high levels of exhaust emissions in vehicles, of course, requires the need for technology to measure vehicle exhaust gases to reduce the impact of air pollution. However, the procurement of exhaust emission test equipment is still expensive, so only certain class workshops have this tool. In addition, the reading results of the vehicle's OBD (On Board Diagnostic) system are only able to display the condition or reading value of the Lambda sensor because other gas sensor readings such as CO_2, HC, and CO cannot be displayed on the OBD reading results. The purpose of this study is to describe the design of the tool and the results of measuring CO and HC levels through the Blynk application. Research methods that use several gas sensors, such as MQ-7 and TGS-2602 (CO gas) and MQ-2 and TGS-2611 (HC gas), are then compared with the measurement results of a standard gas analyzer. The results showed that the MQ-7 value is close to the accuracy at 1000 rpm and 5000 rpm, namely 99.68% and 99.49%, while the level of accuracy at 3000 rpm is 99.37%. The TGS-2602 sensor at 1000 rpm only has the best accuracy and accuracy, namely 99.67% and 99.77%. The level of accuracy of the MQ-2 sensor has the best value at 1000 rpm rotation, which is 95.71% and the level of accuracy has the highest value at 7000 rpm rotation, which is 100%. For the level of accuracy of the TGS-2611 sensor, it has an accuracy level of 1000 rpm rotation of 94.65% and the level of accuracy of the sensor obtains very good values at 1000 rpm, 7000 rpm, and 9000 rpm rotation of 100%.

Keywords: CO gas, ESP32, Gas Analyzer, HC gas, sensors gas.

1. INTRODUCTION

According to the Air Quality Live Index (AQLI), Indonesia's air quality has continued to deteriorate in the last two decades, so Indonesia is officially ranked 17th as the country with the worst air quality in the world [1]. This is due to the population explosion in Indonesia, causing industrial activities to also increase. The main factor that causes the air quality in Indonesia to decline is vehicle exhaust emissions [2][3].

The high levels of exhaust gas emissions in vehicles, of course, requires the need for technology to measure vehicle exhaust gases to reduce the impact of air pollution [4][5]. However, the procurement of exhaust emission test equipment is still expensive, so only certain class workshops have this tool and the cost of testing exhaust emissions is also expensive. In addition, the results of the vehicle's OBD (On Board Diagnostic) system readings are only able to display the condition or value of the Lambda sensor readings because other gas sensor readings such as CO_2, HC, and CO cannot be displayed on the OBD reading results. Exhaust gas emission test equipment or Exhaust Gas Analyzer can measure vehicle exhaust emission levels in the form of CO, HC, CO_2, O_2, NO_x, and Lambda [6].

Based on the description above, in this study, the author does a test for exhaust emission devices on vehicles with the Internet of Things (IoT) concept [7]. The purpose of this study is to describe the design to compare the results of measuring CO and HC levels through the Blynk application. This device consists of a set of gas sensors and a microcontroller named NodeMCU ESP32 which is equipped with displaying exhaust emission measurement data on Android via the Blynk application.

2. METHODS

The research design used the following model:

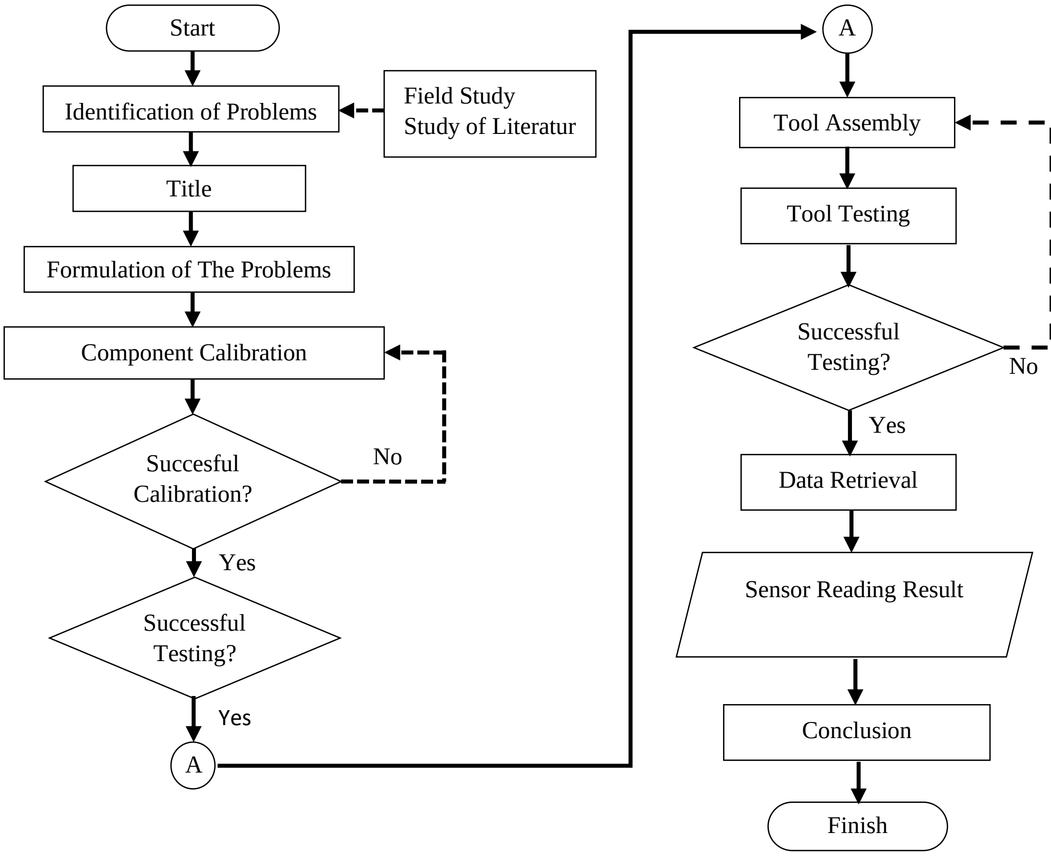

Figure 1. Implementation Flow Chart

The research used was an experimental study comparing CO gas sensors, namely MQ-7 with TGS-2442, and HC gas sensors, namely MQ-2 with TGS-2611, on variations in motorcycle RPM rotation on exhaust gas emissions. Experimental research is research conducted on data variables through the manipulation process stage by giving certain treatments to research subjects [8].

The first step that will be carried out is to perform the first calibration on the sensor through pre-heating and determining the ordinate and abscissa on the sensor datasheet graph. After obtaining the ppm value, the sensor will be compared with the ppm value of the Gas Analyzer on the same independent variable (the amount of RPM) to obtain the second calibration result. Data collection begins with preparing a test motorcycle that has been warmed up so that it is in an idle condition. The gas analyzer probe and all sensors are placed on the motorcycle exhaust and covered with cloth. This is so that the gas emissions that come out can be caught by all sensors and gas analyzers with the same gas. The ppm range for each sensor is different, such as for detecting CO gas, namely MQ7 at 20-2.000 ppm [9][10] and TGS2602 having 1-30 ppm [11][12], while for detecting HC gas, MQ2 has a range of 300-10.000 ppm [13][14] and TGS2611 at 500-10.000 ppm [15][16]. The final result of all data retrieval can be seen through a gadget with IoT Remote software that has been installed and programmed with sensors.

Data was collected by calibrating each sensor by determining the ordinate and abscissa values from the sensitivity graph based on the MQ2, MQ7, TGS2606, and TGS2611 sensor datasheets. This experiment begins by determining the value of room air (Ro) through programming in the Arduino IDE. ESP32 has a 12-bit analog pin so it can convert analog data to 4095, meaning that the value 0 indicates a voltage of 0 volts and the value 4095 represents a voltage of 5 volts. The purpose of this is to do this as a pre-heating stage on the sensor for 1 hour with the following formula:

$$VRL = \frac{V_{in}}{ADC} \dots\dots\dots\dots\dots\dots\dots (1)$$

$$R_s = \left(\frac{V_{in}}{VRL} - 1\right) RL \dots\dots\dots (2)$$

$$R_o = \frac{R_s}{9.6} \dots\dots\dots\dots\dots\dots\dots\dots (3)$$

Where:
VRL = Output voltage
V_{in} = Input voltage
ADC = Analog value
RL = Load resistance
R_o = Resistance of sensor
R_s = Resistance in different gases

Furthermore, the sensor will get the ppm value through the intersection of the sensor datasheet graph with the following formula [17]:

$$m = \frac{log(y_2) - log(y_1)}{log(x_2) - log(x_1)} \dots\dots\dots\dots (4)$$

$$b = log(y) - m\,log\,(x) \dots\dots\dots\dots (5)$$

$$ppm = \frac{log_{10}(ratio) - b}{m} \dots\dots\dots\dots (6)$$

3. RESULTS AND DISCUSSION

In detail, the hardware design consists of ESP32 components, Sensors MQ2, MQ7, TGS2602, TGS2611, I2C, LCD, DHT11, and other indicators, namely LEDs. The source used is sourced from DC voltage. Prior to compile coding, all sensors will be pre-heated first in order to obtain air conditions (Ro) as a condition for carrying out the first calibration with the sensor datasheet.

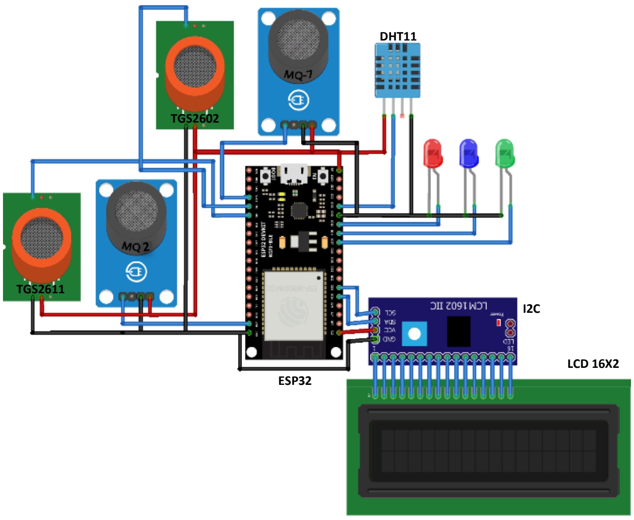

Figure 2. Software Design

Software design for ESP32 aims to embed system work algorithms with the C++ sketch language to program ESP32. The software used for coding is the Arduino IDE. When the coding process has been compiled and then uploaded to ESP32 using a micro USB connection, it will be embedded directly and stored in ESP32. In general, the performance of the program works by reading the parameters on the gas sensor (Pin D22, Pin D15, Pin D2, and Pin 4). If the sensor detects CO and HC gases, the system will display sensor values on the LCD and the gadget. Changes in these values will be monitored continuously when all sensors are active.

Before the sensor will be tested, the first calibration is carried out with a graph of the sensitivity of the sensor datasheet. The goal is to get an accurate ppm value according to the sensor datasheet. The reading results are then calculated and the ppm value is obtained from the sensitivity graph of the sensor datasheet in the Arduino IDE program. The gas analyzer used is QRO-401.

Table 1. First Calibration Results

RPM Rotation	Standard Gas Analyzer		IoT-Based Gas Analyzer			
			MQ Sensor Type		TGS Sensor Type	
	CO(%)	HC(ppm)	CO(%)	HC(ppm)	CO(%)	HC(ppm)
1000	4.3	599.5	5.91	633	6.35	593
3000	4.75	445	5.5	510.5	5.515	455.5
5000	5.44	162	6.41	336	6.265	199
7000	5.225	143.5	5.75	301	6.065	141.5
9000	5.97	128	6	280	6.98	129

After the output results are obtained in the form of ppm on all sensors and gas analyzers, then a linear regression comparison is performed for the next calibration so that the output value is obtained with accurate results. The results of this comparison will later be in the form of a formula which will later be combined with the previous coding and compiled coding to the Arduino IDE.

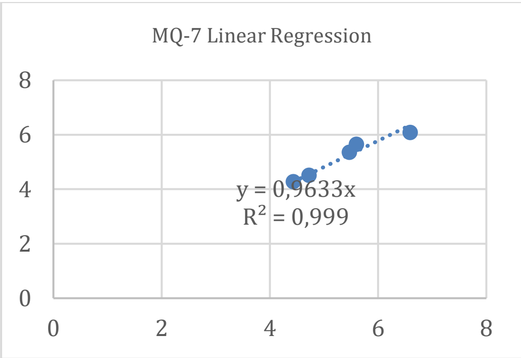

(a)

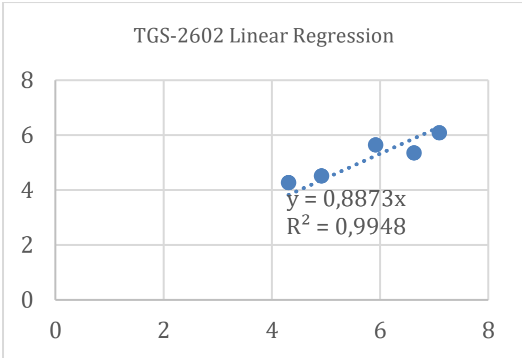

(b)

Figure 3. Linear Regression of CO Gas

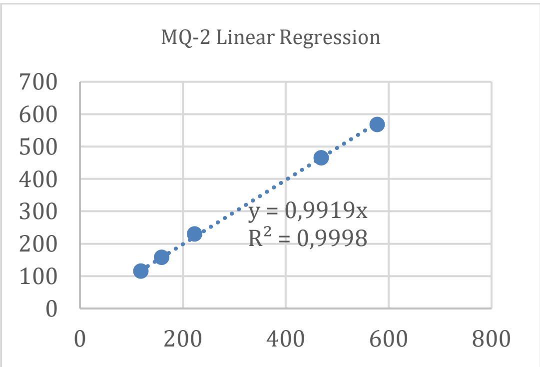

(a)

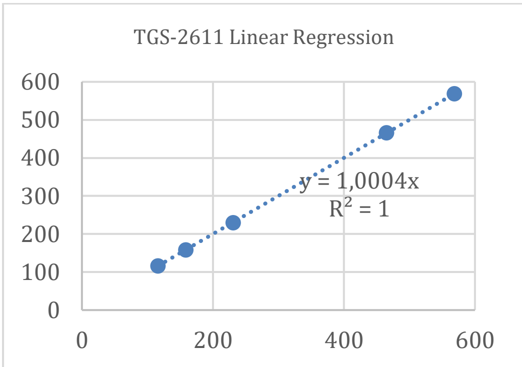

(b)

Figure 4. Linear Regression of HC Gas

The gas sensor calibrations in Fig. 3 (a,b) and Fig. 4 (a,b) show the CO and HC gas sensor readings with a standard gas analyzer whose values are known. Based on the data obtained for linear regression sensor MQ-7 equation Y = 09633x with a value of R2 = 0.999, linear regression sensor TGS-2602 equation Y = 0.8873x with a value of R2 = 0.9948, linear regression sensor MQ-2 equation Y = 0.9919x with a value of R2 = 0.9998, linear regression sensor TGS-2611 equation Y = 1.0004x with a value of R2 = 1 which is then used as a gas sensor function (calibration).

Based on the results of the regression analysis related to the relationship between the difference in CO and HC readings from the sensor and the gas analyzer. This shows that the curve forms a pattern so that the regression model of the curve is normal and normally distributed. This is because the plots of the data are spread out and follow a normal distribution pattern.

Table 2. Second Calibration Results

RPM Rotation	Standard Gas Analyzer		IoT-Based Gas Analyzer			
			MQ Sensor Type		TGS Sensor Type	
	CO(%)	HC(ppm)	CO(%)	CO(%)	HC(ppm)	HC(ppm)
1000	4.275	568.5	4.43	577.5	4.31	568.5
3000	4.51	466	4.72	469	4.92	465
5000	5.645	230	5.6	222.5	5.915	231
7000	5.355	158.5	5.47	158.5	6.63	158.5
9000	6.085	116	6.59	118	7.095	116

In the graph above (Fig. 4) the results of the TGS-2611 sensor readings compared to a standard gas analyzer are close to perfect accuracy for HC gas. The 2000-3000 rpm rotation has a difference of only 1 ppm. When compared to the MQ-2, it has a difference with a range that is quite far as the validity of the measuring instrument. Referring to the Regulation of the Minister of Environment the CO value limit does not exceed 4.5% and HC 1200 ppm [18][19]. This shows that the linear regression equation as a calibration function can improve the performance of each sensor to be good. The validation results from the linear regression analysis on the sensor can give good results with an accuracy level of 99.51% and an accuracy of 98.89% [20].

In testing the performance of a gas sensor measuring instrument obtained from the results of the 2nd reading. Then the level of accuracy of the entire test gas sensor is obtained.

Table 3. CO and HC Value from Gas Analyzer

CO Value on Gas Analyzer	4.3	4.75	5.44	5.225	6.1
HC Value on Gas Analyzer	568.5	466	230	158.5	116

Table 4. The Accuracy and Precision of the MQ-7 Sensor

Rotation (RPM)	1000	3000	5000	7000	9000
Experiment 1	4.42	4.8	5.58	5.4	6.66
Experiment 2	4.44	4.64	5.62	5.54	6.52
Average	4.43	4.72	5.6	5.47	6.59
St. Deviation	0.01	0.11	0.03	0.10	0.10
Accuracy (%)	99.68	97.60	99.49	98.19	98.50
Precision (%)	96.98	99.37	97.06	95.31	91.97

Table 5. The Accuracy and Precision of the TGS-2602 Sensor

Rotation (RPM)	1000	3000	5000	7000	9000
Experiment 1	4.3	4.86	5.55	6.72	6.97
Experiment 2	4.32	4.98	6.28	6.54	7.22
Average	4.31	4.92	5.915	6.63	7.095
St. Deviation	0.01	0.08	0.52	0.13	0.18
Accuracy (%)	99.67	98.28	91.27	98.08	97.51
Precision (%)	99.77	96.42	91.27	73.11	83.69

Table 6. The Accuracy and Precision of the MQ-2 Sensor

Rotation (RPM)	1000	3000	5000	7000	9000
Experiment 1	560	512	260	129	114
Experiment 2	595	426	185	188	122
Average	577.5	469	222.5	158.5	118
St. Deviation	24.75	60.81	53.03	41.72	5.66
Accuracy (%)	95.71	87.03	76.16	73.68	95.21
Precision (%)	98.42	99.36	96.74	100.00	98.28

Table 7. The Accuracy and Precision of the TGS-2611 Sensor

Rotation (RPM)	1000	3000	5000	7000	9000
Experiment 1	547	510	280	129	112
Experiment 2	590	420	182	188	120
Average	568.5	465	231	158.5	116
St. Deviation	30.41	63.64	69.30	41.72	5.66
Accuracy (%)	94.65	86.31	70.00	73.68	95.12
Precision (%)	100.00	99.79	99.57	100.00	100.00

In this test, the value obtained from the precision and accuracy of measuring instruments for several gas sensors (X) with a standard gas analyzer (Y). The MQ-7 and TGS-2602 sensors have a level of accuracy and accuracy that is still not accurate enough for each rotation (rpm). In MQ-7, the values that are close to the accuracy at 1000 rpm and 5000 rpm are 99.68% and 99.49%, while the level of accuracy at 3000 rpm rotation is close to the accuracy of 99.37%. This is influenced by the sensor material which has low conductivity so that the heater component as sensitivity to the sensor becomes less precise. For the TGS-2602 sensor, only at 1000 rpm has the accuracy and accuracy of 99.67% and 99.77%. Referring to the TGS-2606 sensor datasheet, this type of sensor has a low sensitivity range of 1-30 rpm so that in the first round it can work properly according to gas analyzer standards.

In the HC gas test, the level of accuracy and accuracy of the MQ-2 sensor has a significant difference. The level of accuracy of the MQ-2 sensor has the best value at 1000 rpm, which is 95.71% and the lowest value is 73.68%. And for the level of accuracy, it has a high accuracy value that is even the same as the standard gas analyzer value, at 7000 rpm rotation which is 100%, and followed by 3000 rpm rotation of 99.36%. For the level of accuracy, the TGS-2602 sensor has a low level of accuracy, with the highest value at 1000 rpm of 94.65%. However, at the level of accuracy, the sensor obtained a very good value compared to other sensors, namely at 1000 rpm, 7000 rpm, and 9000 rpm at 100%, followed by 3000 rpm rotation, 5000 rpm at 99.79%, and 99.57%.

The standard gas analyzer value calculation is the average of 2 tests. When compared to the average sensor with a standard gas analyzer, it is actually not much different. So, the accuracy level deviates far from the standard gas analyzer value. However, the accuracy of the designed measuring instrument can be a reference in determining the standard measuring instrument by knowing the ability of the measuring instrument to read measurements that can be close to the actual size value.

4. CONCLUSION

In the first calibration, it was found that the TGS-2602 sensor value could not approach the CO value with a standard gas analyzer. This is influenced by the sensitivity of the TGS-2602 sensor which has a low range of 1-30 ppm. The MQ-2 sensor in detecting HC gas is still far from the standard gas analyzer value. Compared to the TGS-2611 sensor, the HC value is almost as accurate as that of a standard gas analyzer. This is because the MQ-2 sensor datasheet has a sensitivity range of 300-10,000 ppm, while the TGS-2611 has a range of 10,000-250,000 ppm. Even though the CO value on MQ-2 is obtained according to the range, this is also influenced by the material factors of each sensor. Based on the data obtained for linear regression sensor MQ-7 equation Y = 09633x with a value of R2 = 0.999, linear regression sensor TGS-2602 equation Y = 0.8873x with a value of R2 = 0.9948, linear regression sensor MQ-2 equation Y = 0.9919x with a value of R2 = 0.9998, linear regression sensor TGS-2611 equation Y = 1.0004x with a value of R2 = 1 which is then used as a gas sensor function (calibration). HC gas testing, the level of accuracy and accuracy of the MQ-2 sensor has a significant difference. The level of accuracy of the MQ-2 sensor has the best value at 1000 rpm, which is 95.71% and the lowest value is 73.68%. And for the level of accuracy, it has a high accuracy value that is even the same as the standard gas analyzer value, at 7000 rpm rotation which is 100% and followed by 3000 rpm rotation of 99.36%. For the level of accuracy the TGS-2602 sensor has a low level of accuracy, with the highest value at 1000 rpm of 94.65%. However, at the level of accuracy the sensor obtained a very good value compared to other sensors, namely at 1000 rpm, 7000 rpm and 9000 rpm at 100%, and followed by 3000 rpm rotation, 5000 rpm at 99.79% and 99.57%. This IoT gas analyzer has several weaknesses that can be developed in further research, such as sensor sensitivity reassembled with material changes and heater sensors so that when the preheating time is faster and needs to be done regarding repeatability for consistency the sensor when used regularly.

5. ACKNOWLEDGEMENT

We express our deepest gratitude to the Department of Mechanical Engineering, State Polytechnic of Malang, so that articles from this undergraduate thesis can be completed.

6. REFERENCES

[1] Anjani, A. (2022, Mar.22). *Negara dengan Polusi Udara di Dunia, Indonesia Peringkat 1 di Asia Tenggara* [online]. Available: https://www.detik.com/edu/detikpedia/d-5995671/negara-dengan-polusi-udara-di-dunia-indonesia-peringkat-1-asia-tenggara.

[2] Huboyo, H. S., Handayani, W., & Samadikun, B. P., "Potential air pollutant emission from private vehicles based on vehicle route", *IOP conference series: Earth and Environmental Science*, vol. 70, no. 1, p. 012013, June. 2017.

[3] Padoan, E., & Amato, F., In Non-exhaust emissions. Vehicle non-exhaust emissions: impact on air quality, pp. 21-65, Academic Press, 2018.

[4] Purwadi, A., Suhandi, S., & Enggarsasi, U., "Urban air pollution control caused by exhaust gas emissions in developing country cities in public policy law perspective". *International Journal of Energy Economics and Policy*, 10(1), 31-36, 2020.

[5] Merkisz, J., Fuć, P., Lijewski, P., & Pielecha, J., "Actual emissions from urban buses powered with diesel and gas engines", *Transportation Research Procedia*, 14, 3070-3078, 2016.

[6] Martawati, M. E., & Hardiyana, H., "Pembuatan Dan Analisis Pembacaan sensor Karbon Dioksida Pada Gas Analyzer Terhadap Variasi Bahan Bakar Berbasis Aplikasi Android", *JURNAL ELTEK*, 15(2), 95-112, 2017.

[7] Jon Endri, Elizah Fitri, and Suroso, "Design and Build an Internet of Things (IoT) Automatic TV Broadcasting Antenna System", LOGIC, vol. 22, no. 3, pp. 225–233, Nov. 2022.

[8] Jaedun, A, Metodologi penelitian eksperimen. Edisi-12. Yogyakarta: Fakultas Teknik UNY, 2011.

[9] Abraham, S., & Li, X., "Design of a low-cost wireless indoor air quality sensor network system", *International Journal of Wireless Information Networks*, 23, 57-65, 2016.

[10] Babu, K. S., & Nagaraja, C., "Calibration of MQ-7 and Detection of Hazardous Carbon Mono-oxide Concentration in Test Canister", *International Journal of Advance Research, Ideas and Innovations in Technology*, 4(1), pp. 18-24, 2018.

[11] Kartika, V. S., Rivai, M., & Purwanto, D., "Spoiled meat classification using semiconductor gas sensors, image processing and neural network", *International Conference on Information and Communications Technology (ICOIACT)*, pp. 418-423, March. 2018.

[12] Rahman, S., Alwadie, A. S., Irfan, M., Nawaz, R., Raza, M., Javed, E., & Awais, M., "Wireless E-nose sensors to detect volatile organic gases through multivariate analysis", *Micromachines*, 11(6), 597, 2020.

[13] A. Manuaba, "Research and application of ergonomics in developing countries, with special reference to Indonesia", *Indones. J. Ergon.* vol. 1, no. 1, pp. 24–30, 2000.

[14] Vasuki, A., Christaline, J. A., Akila, V., & Sathiya, R., "A Low-Cost Air Quality Tracking System Design", *International Conference on Innovative Data Communication Technologies and Application (ICIDCA)*, pp. 901-904, IEEE, 2023.

[15] Martawati, M.E., Susilo, S.H., Asrori, A. & Lulut, W.," Automatic Mirror Folding Design Arduino-Based", *Logic: Jurnal Rancang Bangun Dan Teknologi*, 21(2), pp. 93–96, 2021.

[16] Yantidewi, M., Muntini, M. S., Deta, U. A., & Lestari, N. A., "The design of a PC-based real-time system for monitoring Methane and Oxygen concentration in biogas production", *Journal of Physics: Conference Series*, Vol. 997, No. 1, p. 012018, 2018.

[17] Wahyudi, B. A., Edy, D. L., "Automation of Welding Fumes based on MQ-2 Sensor in Welding Laboratory". *Jurnal Temapela*, Vol 3, no. 1, pp. 1-9, Nov. 2020.

[18] *Peraturan Menteri Lingkungan Hidup Republik Indonesia Nomor 06 Tahun 2006 Tentang Pedoman Umum Standarisasi Kompetensi Personil dan Lembaga Jasa Lingkungan*, MLH6-2006, 02 Agu 2006.

[19] Wahyu, M., & Rahmad, H., "The Effect of 10% Bioetanol and Carbon Cleaner Mixtures with Engine Gurah Technique on The Level of CO Emission in Corolla Twincam AE 92". *VANOS Journal of Mechanical Engineering Education*, 3(2), 2018.

[20] Priyonggo, B., Subrata, I. D. M., & Setiawan, R. P. A., "Rancang Bangun dan Pengujian Penetrometer Digital dengan Perekam Data Berbasis Android", *Jurnal Keteknikan Pertanian*, 7(1), pp. 83-90, 2019.

LOGIC
Journal of Engineering Design and Technology
Vol. 23 No.2 July 2023; p. 111 - 120

p-ISSN : 1412-114X
e-ISSN : 2580-5649
http://ojs2.pnb.ac.id/index.php/LOGIC

DESIGN OF PLASTIC MELTING EQUIPMENT WASTE BANK SCALE USING QUALITY FUNCTION DEPLOYMENT METHOD

1) Department of Industrial Engineering, University of Ahmad Dahlan, Yogyakarta, Indonesia

Correponding email [1] :
isana_prisa@ie.iad.ac.id

Isana Arum Primasari[1], Endah Utami[1], Gita Indah Budiarti[1], Okka Adiyanto[1]

Abstract. The COVID-19 pandemic has triggered the rise of online purchases, resulting in the accumulation of plastic packaging waste. Plastic is most widely used because it is lightweight, flexible, cheap and easy to obtain, but its waste is difficult to decompose, which has an impact on the environment. Eco-bricking is one way that waste banks often reduce the amount of plastic waste. The obstacle in making eco-bricks is sore hands and calluses because it takes a lot of energy to compact the plastic. On the other hand, there is a lot of concentrated cooking oil waste that is still untreated, causing difficulties when disposing of it. Through this research, the design of a waste bank scale plastic melting machine is carried out with the raw materials of plastic bags and concentrated cooking oil into new materials that are more useful. The Quality Function Deployment (QFD) method with an Ergonomics approach is the basis for the stages of making product design from collecting consumer voices to making detailed tool designs. The operation of the tool uses simple technology so that it is easy to use by members of the Gurami Semanu waste bank. A total of 34 respondents will be the basis for determining product design. The results of the design of a bank-scale plastic melting tool in the form of a lidded stainless-steel pot with a stirrer. The heater used for melting uses LPG gas with automatic operation using a button.

Keywords : waste bank, plastic waste, melting machine, QFD.

1. INTRODUCTION

The problem of waste has long been a topic of discussion for all circles of society, starting from the smallest community groups such as households to the ministry, but has not been able to overcome it. Plastic is one type of waste that is increasingly accumulating, especially during the COVID-19 pandemic due to the large number of purchases via online which results in almost all package packaging coated with plastic so as not to get wet in the rain. Plastic is most widely used in everyday life because it is lightweight, flexible, cheap and easy to obtain, but the waste is increasingly unstoppable and the most worrying thing about the environment is that plastic is difficult to decompose so that it will further pollute the environment. The solution to handling plastic waste that is being developed is eco-bricking, but eco-bricking requires a long time and strong labor.

The partners in this research are members of the Gurami Semanu Waste Bank consisting of 34 men and women. So far, plastic waste has been used by the Gurami Waste Bank into eco-brick products. The products produced are chairs, tables, decorative shelves, and various household equipment. Based on initial observations, there were some complaints felt by eco-brickers in the form of reddish bruises when first making eco-bricks after several times working, calluses appeared around the palms of the hands caused by the friction force of the hands with the pressing stick when inserting plastic pieces into the bottle. Other complaints include left and right hands aching and getting tired quickly because it takes extra energy to compact the plastic into the eco-brick.

Based on the results of the NBM (Nordic Body Map) questionnaire, complaints were obtained on several parts of the body felt by eco-brickers, namely very painful conditions in the neck, shoulders, upper arms, palms, waist and back. The results of initial observations that have been made show that the working position when making eco-bricks causes MSDs (Musculoskeletal disorder) as shown in Figure 1.

Figure 1. Eco-bricking Process

Eco-bricking requires that all plastic used to make eco-bricks must be clean and dry so a selection and washing process is needed if dirty before the plastic is put in a plastic bottle. On the other hand, the community also has used cooking oil waste which has been processed into soap and candles, but limited to good used cooking oil while the black and thick used cooking oil is not suitable for use because it requires a more expensive process to purify. The members of the Gurami Semanu Waste Bank hope that there are other solutions for processing plastic waste other than being used as eco-bricks so that recycling plastic waste becomes easier while utilizing the concentrated and unprocessed used cooking oil. Therefore, they hope that there are other solutions for processing plastic waste besides being utilized into eco-bricks.

Based on these problems, research was conducted to process used cooking oil and plastic, especially crackle because it is too much wasted to become a new material as a substitute for conblock in the hope that the results of waste processing can produce an easier and more useful process. Making this new material requires a melting tool that is safe, simple, and affordable. Given that the users of this tool will be the public involved in waste bank activities, it is hoped that the smelting tool can be used by all members of the Waste Bank. Through simple technology combined with the needs of waste processing tools, a simple tool design can be made but can help solve problems in the abundance of plastic waste and obstacles in making Eco bricks. This melting tool is a plastic melting tool with crackle plastic raw materials and concentrated used cooking oil to become a new material, namely conblock. The novelty of this research is the melting process between crackle plastic waste and concentrated used cooking oil but has not yet reached the test related to the strength of the new material produced.

As research related to alternative plastic waste management is for asphalt mixtures as a durability enhancer [10] where the asphalt mixture is an aggregate and asphalt binder which is derived from petroleum [9]. Some studies provide the addition of recycled polymers to be used as additives in asphalt mixtures. The results of these studies showed a similarity in the mix materials with the modified binder [11]. The addition of these additives will provide an increase in the durability of the asphalt and will also obtain high economic benefits [8].

Research on the utilization of plastic waste for road construction has also been carried out in Ghana by utilizing HDPE and PP plastic types for asphalt mixtures [13]. In this research, the type of plastic waste was melted manually with a temperature between 1600-1700C. Further research was conducted by Sevil Kofteci [22]. In this study only uses 1 type of plastic waste, namely HDPE as a mixture for making asphalt and aims to determine the effect of HDPE plastic material on the performance of asphalt mixtures.

In the field of construction materials PET can be used as a cement mixture with demolition construction waste [10]. Construction and demolition produce stone waste in urban areas, these wastes are generally diverted to landfills. To reduce the amount of waste disposed of, there is a possibility of using the waste in brick products [13]. Sustainability is currently a top priority in the construction industry. Nowadays plastic can be used as an aggregate so it will be one way to handle plastic waste [9].

2. METHODS

This research is basic research that tries to find a solution to the problem of reducing non-organic waste, especially plastic bags, packets of online delivery packages, and other plastic bags used to fill eco-brick bottles. The waste is utilized together with concentrated used cooking oil waste to be processed together.

2.1 Population, Sampling, Sampling Technique

The population of this study were the users of eco-brick printer products, namely the managers and members of the Gurami Semanu Garbage Bank, a total of 34 people consisting of 28 mothers and 6 fathers so that sampling used nonprobability sampling. Nonprobability sampling allows for any member of the population to be selected into a sample with zero chance. This technique is carried out based on certain characteristics which include circumstances, quantity, volunteerism and so on. The sampling in this study used purposive sampling where respondents were determined by the researcher because not everyone understands how to Eco brick and has done it.

2.2 Data Collection Method

Data collection is done by distributing open questionnaires to respondents to get the voice of consumers or respondents regarding the tools to be made. Respondents in the study were all managers and members of the Gurami Semanu Waste Bank totaling 34 people consisting of 26 women and 8 men. Based on the results of collecting consumer voice data, a closed questionnaire was made to select variables that are considered important by consumers in the design of the tool to be made. Consumer voice data is used to obtain keywords from consumer desires for form, function and other variables that will be attached to the tools made. All this data will be used to create a house of quality. HOQ is the initial stage of a long series of processes in product design.

2.3. Research Design

This research tries to provide a solution to the problem of processing plastic waste by presenting a tool that can melt plastic so that it can be formed into new materials. Figure 2 shows the design of the research to be conducted, starting from the abundance of plastic waste, which has recently been widely reprocessed into eco-ricks. Eco-bricks have helped reduce waste, but there are still obstacles in making them because they still use human labor, so they take a long time and require extra energy to compact.

The Waste Bank carries out the mandate in the 3R (reuse, reduce, recycle) program for organic and non-organic waste. The 3R program is very likely to be implemented if there is support from all parties including the surrounding community. The community cannot be expected to have much role in processing waste independently but can support this program if assisted with waste processing equipment that can be used together.

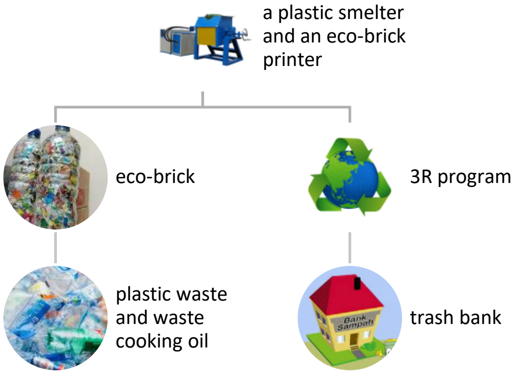

Figure 2. Flow of research

Appropriate waste processing equipment is a plastic smelter and an eco-brick printer. The stages in product design are carried out to produce tool designs that are in accordance with consumer desires. The research stage begins with the preparation of a closed questionnaire based on consumer voices from an open questionnaire as shown in Figure 2. The results of the questionnaire distribution were used to compile HOQ so that the desired product quality was obtained. Next, component requirements planning, production process planning and manufacturing planning were carried out. Based on this planning, the product design was determined through several considerations so that the resulting product design was in accordance with consumer desires.

Product design is made in the form of 3-dimensional images using solid works software to facilitate the manufacture of product prototypes. Through simple technology combined with the need for waste processing tools with crackle plastic and used cooking oil as raw materials, a waste bank scale plastic melting tool design was made to become an eco-brick that can be operated by all members of the waste bank. In the future, this tool can be used jointly with other waste banks under BumKal management.

3. RESULTS AND DISCUSSION

Data on consumer needs and desires were obtained by filling out questionnaires. The questionnaire used in data collection is an open questionnaire with the aim of getting as many needs and wants from consumers as possible-determination of the sample through consideration and specific criteria according to research needs. The considerations used in determining the respondents in this questionnaire were members of the Gurami Semanu trash can who are used to making eco-bricks and have received socialization regarding eco-bricks. This eco-brick printer will be used by partners, namely the Gurami Garbage Bank in Semanu, although it is possible that other waste banks can also use it.

Based on this, there were 34 members of the waste bank consisting of 26 women and 8 men who were respondents. Table 1 shows the results of collecting consumer voices regarding their needs and desires for the design of a waste bank scale plastic smelter.

Table 1 Attributes of consumer needs and wants

No Attribute	Attribute
1	Hands are not exposed to heat during the process
2	Ease of cleaning
3	It's not difficult to operate
4	There is a tool to remove the smelting results
5	Fuel is easy to get
6	Can be moved at any time
7	The size of the tool according to the room (not big)
8	There is an automatic stirrer
9	The tool is not heavy
10	Tools are not easy to rust
11	Cheap price
12	There is a temperature indication
13	There is a place to add ingredients
14	There is a timer

Based on the results of consumer voting, a closed questionnaire was prepared to assess the level of consumer interest using the Likert scale as shown in Table 2.

Table 2 Level of consumer interest

	Attribute													
	1	2	•3	4	5	6	7	8	9	10	11	12	13	14
Importance level	5	4.9	5	4.8	5	4.9	4.9	5	5	5	5	4.9	3.9	3.1

3.1 House of quality (HOQ)

House of quality is the first stage in the application of the Quality Function Development (QFD) methodology, used to translate customer needs or requests based on the results of consumer voice screening. The results of the HOQ preparation can be seen in Figure 3.

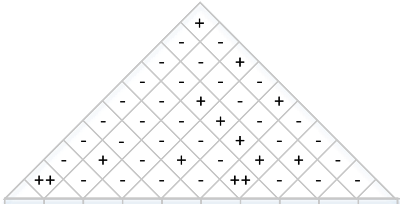

	Added heat protection	Choose quality materials	Added operation buttons	Added function for channel end	Selection of fuel type	added tool switching function	Determination of the amount of capacity	Added temperature control	Added material entry	Added timer	importance value	performance value	sales point
Safe when used	○										4.8	4.8	1.5
Easy to clean		○									4.8	4.8	1.2
Easy to operate			○			▲					4.7	4.8	1.2
Added output faucet function				○							4.8	4.7	1
Fuel is easy to get					○						4.7	4.8	1.2
Easy to move						○	▲				4.8	4.8	1
Capacity according to needs							○				4.7	4.8	1.2
There is an automatic stirrer			○								4.8	4.8	1
Light material		○									4.8	4.8	1.2
The material is not easy to rust		○									4.8	4.8	1.5
Affordable prices		▲									4.8	4.8	1.5
There is temperature control								○			4.8	4.8	1
There is a place to add materials									○		4.8	4.8	1
There is a timer										○	4.8	4.8	1.2
Degree of difficulty	3	4	3	3	4	3	3	4	3	3			
target value	3	4	4	4	4	4	2	4	4	4			
Absolute importance	42.8	135	87	42.4	43.1	48.3	48	43.1	43.2	43.2			
relative	2	10	9	1	3	8	7	4	5	6			

Figure 3 House of Quality

3.2 Part deployment

Part deployment is the process of determining the parts that will be used to arrange products according to consumer expectations as described in the HOQ. The results of the preparation of the deployment part are shown in Figure 4.

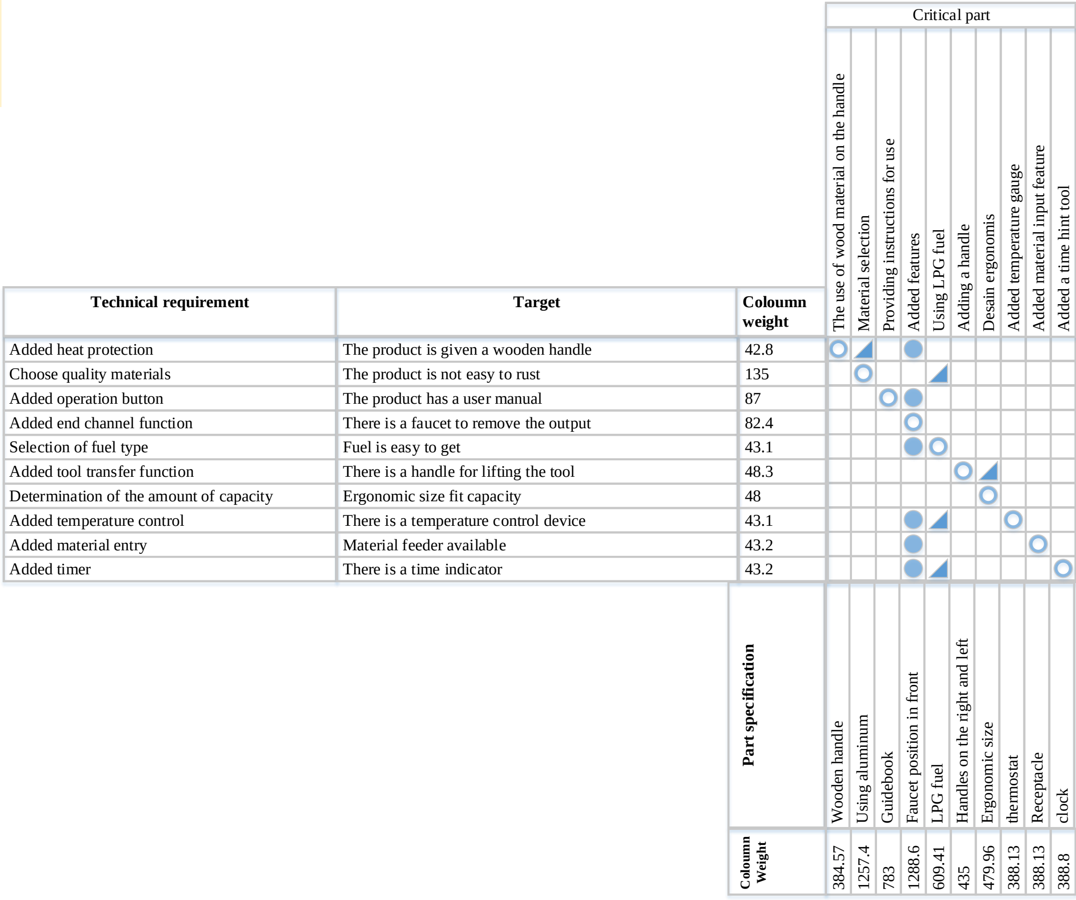

Figure 4 Part deployment

3.3 Design of a Plastic Melting Tool

Several things are considered in designing a plastic smelting tool as described below:

Anthropometric Data

Anthropometric data were taken from measurements of all 36 members of the Gurami waste bank plus several Semanu residents. The results of measuring the Anthropometric data are 36 body dimension data, then the 5th percentile, 50th percentile, and 95th percentile is calculated as the basis for determining product size. Table 3 shows the results of determining the percentiles and selecting the body dimensions used according to the product design requirements.

Table 3 Body dimension requirements for tool design

Dimensions	Percentile (cm)		
	5	50	95
Body height (D1)	117.51	152.55	187.60
Eye height (D2)	108.21	142.19	176.17
Elbow height (D4)	73.1	95.62	118.14
Fingertip height (D7)	40.53	60.36	80.18
Knee height (D15)	36.13	48.09	60.05
Shoulder width (D17)	26.32	38.72	51.13
Length of forward arm (D24)	48.33	66.15	84
Forward grip length (D25)	43.72	56.69	69.67
Length of arm span to side (D32)	111.38	152.68	194

Percentiles are used to adjust the size of the tool to fit the worker's body size so that it is comfortable to use. Following are the results of selecting percentiles for each dimension:

Body height (D1)
In the body height dimension (D1) the small percentile or 5th percentile is used. The body height dimension is used to measure the height of the tool to be designed. Selection of the 5th percentile so that users of the smallest tools have no difficulties when operating the tool. The 5th percentile size value on D1 is 117.51 rounded up to 118 cm.

Eye Height (D2)
In the eye height dimension (D2) the small percentile or 5th percentile is used. The eye height dimension is used to adjust the height of the plastic smelting tool to be designed. Selection of the 5th percentile so that users of the smallest tools have no difficulties when monitoring the plastic smelting process. The 5th percentile size value on D2 is 108.21 cm rounded up to 109 cm.

Elbow height (D4)
In the elbow height dimension (D4) the small percentile or 50th percentile is used. The elbow height dimension is used to determine the height of the mixing container for the tool to be designed. The 50th percentile is used so that all tool users can operate the stirrer comfortably. The 50th percentile size value on D4 is 95.62 cm rounded up to 96 cm.

Fingertip Height (D7)
For the fingertip height dimension (D7), the largest percentile or 95th percentile is used. The fingertip height dimension is used to adjust the height of the operational button for the tool to be designed. The 95th percentile is used to adjust the smallest size so that the tool user can reach the operational buttons comfortably. The 95th percentile size value on D7 is 80.18 cm rounded up to 81 cm.

Knee height (D15)
For the knee height dimension (D15) the largest percentile or 95th percentile is used. The knee height dimension is used to adjust the height of the final canal which is the place for channeling the smelting results into the ecobrick mold. The 95th percentile is used to adjust the largest size so that tool users can reach the end channel facilities comfortably. The 95th percentile size value on D15 is 60.05 cm rounded up to 60 cm.

Shoulder Width (D17)
For the shoulder width dimension (D17), the normal or 50th percentile is used. The shoulder width dimension is used to adjust the width of the tool to be designed. The 50th percentile is used so that all tool users can operate the tool comfortably during the production process. The 50th percentile size value on D17 is 38.72 cm rounded up to 39 cm.

Forward Arm Span Length (D24)
For the forward hand span length dimension (D24), the small percentile or 5th percentile is used. The forward hand span length dimension is used to adjust the size of the tool's distance from the front point of the tool to the back point of the tool to be designed. The 5th percentile is used to adjust the smallest size so that tool users can reach all the facilities in front of them comfortably when operating the tool. The 5th percentile size value on D24 is 48.33 cm rounded up to 49 cm.

Forward Grip Length (D25)
For the forward hand grip length dimension (D25), the small percentile or 5th percentile is used. The forward hand grip length dimension is used to adjust the size of the tool's distance from the leading point of the tool to the back point of the tool to be designed. The 5th percentile is used to adjust for the smallest size the user of the tool can hold the plastic smelter cover comfortably. The 5th percentile size value on D25 is 43.72 cm rounded up to 44 cm.

Length of Hand Span to Side (D32)
For the long dimension of the hand span to the side (D32), the small percentile or 5th percentile is used. The long dimension of the hand span to the side is used to adjust the size of the tool's distance from the right point of the tool to the left point of the tool to be designed. The 5th percentile is used to adjust the smallest size so that tool users can carry the plastic smelter comfortably when using or cleaning the tool. The 5th percentile size value on D32 is 111.38 cm rounded up to 112 cm.

A recap of all the anthropometric dimensions used according to the selected percentiles results in the dimensions of the plastic bag smelting tool. as presented in Table 4. Determination of the dimensions of the size of the tool to be designed is shown in Table 4 with details: the height of the tool is at intervals of 109 - 118cm, the height of the mixing container is 96 cm, the height of the operational button is 81 cm, the height of the final canal is 60 cm, the width of the tool is at intervals of 39 - 112cm, and the tool length is in the size interval of 44 - 49cm.

Table 4. Dimensions of the plastic smelter

Tool Dimensions	Anthropometric Dimension	Percentiles	Size (cm)
Tool + furnace height	D1, D2	5	109 - 118
Container Height	D4	50	96
Operational Button Height	D7	95	81
Final Channel Height	D15	95	60
Tool Width	D17, D32	50, 5	39 - 112
Stirrer length	D24, D25	5	44 - 49

3.4 Analysis of Materials and Products Forming Plastic Melting Equipment

The plastic smelting tool is made based on the consideration of the various constituent components with the following explanation:

There are two alternatives for selecting heating devices, namely LPG and electricity. The type of LPG heater uses LPG gas as a heating source while the electric heating type uses electrical components as a heating source.

There are two alternatives for selecting the type of stirrer, namely helical ribbon, and paddle anchor. Both types of stirrers are suitable for the process of mixing materials that have a high level of viscosity and operate at low rpm rotational speeds. Helical ribbon is used in various levels of viscosity. This type is operated with minimum clearance between the tube wall and the stirrer. This type also allows axial flow at low speeds [18]. Paddle anchors are suitable for use at a high level of viscosity. This type will be optimal if it is driven with a low stirring speed [18].

There are three alternatives for choosing the Final Channel Location, namely the position in front, below, and by casting. The positions of the front end and bottom pour lines are more suitable for use with LPG heater types. When using an electric heater, the three positions of the final channel location can be used.

There are three alternatives for choosing the type of material, namely steel, stainless steel, and aluminum. The material used is divided into two types of parts, namely the frame and the mixing bowl. The frame section uses a material suitable for the material being melted, namely steel, while the material in the mixing vessel has two alternative materials, namely stainless steel, and aluminum.

Based on the choice of morphological chart, several alternative designs were developed. The results of the selection of components are as follows: Electric heater, paddle anchor type stirrer, three layers of tube, output valve on the bottom side, steel frame material, aluminum stirrer container material.

The results of the waste bank scale plastic smelter design using Solidworks software are shown in Figure 5, while the details of the constituent components can be seen in Figure 6.

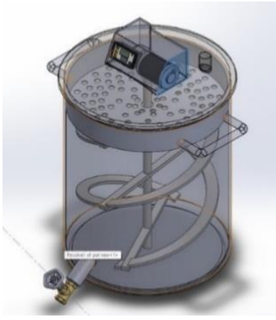

Figure 5. Design of a garbage bank scale plastic smelter

Figure 6. Design of a waste bank scale plastic smelter

3.5 Description of Tool Use

The plastic smelter is a production tool that uses electricity and heat. Electrical energy is used to rotate or stir automatically from plastic bags and used cooking oil. Meanwhile, heat energy is sourced from an LPG gas stove which is useful for heating raw materials while stirring. In use, the operator of the tool manually inserts the ingredients into the mixing container, then if you want to stir, the operator must first turn on the stirrer by pressing the operational button.

Then the stove heater is turned on by rotating the stove lever according to the desired amount of fire (temperature). The stirring process continues until all the ingredients are dissolved and mixed into a thick liquid which is ready to be poured into the ecobrik mold container. After use, to remove the production results, the operator must prepare a container for the plastic smelting results. Pouring the mixed results is done by releasing the container hook then pouring the container through the output faucet to move the produce.

This result is in line with several studies by Intan [21], and Bhushaiah [18] which have utilized plastic waste to turn into bricks or the like as building materials. Various studies have carried out mixing plastic with a mixture of other materials to be melted together, which basically has the same goal of reducing plastic waste to be melted down into new materials [21].

4. CONCLUSION

This research has resulted in a design proposal for a waste bank scale plastic smelter in accordance with the needs and desires of consumers. This tool is used to melt plastic bags mixed with used cooking oil to become a new material in the form of conblock. This melting tool is a plastic melting tool with crackled plastic raw materials and concentrated used cooking oil to become a new material, namely conblock. The novelty of this research is the melting process between crackle plastic waste and concentrated used cooking oil but has not yet reached the test related to the strength of the new material produced.

5. REFERENCES

[1]. A. Arulrajah, S. Perera, Y. C. Wong, S. Horpibulsuk, and F. Maghool, “Stiffness and flexural strength evaluation of cement stabilized PET blends with demolition wastes,” Construction and Building Materials, vol. 239, p. 117819, 2020.
[2]. A. K. Jassim, “Recycling of Polyethylene Waste to Produce Plastic Cement,” Procedia Manufacturing, vol. 8, no. October 2016, pp. 635–642, 2017.
[3]. A. Kusnayat, S. Martini, E. Shabrina, A. Rizal, Application of Reverse Engineering for Modified Anchor Impeller, diakses dari www.semanticscholar.org , 2018
[4]. A. L. Murmu and A. Patel, “Towards sustainable bricks production: An overview,” Construction and Building Materials, vol. 165, pp. 112–125, 2018
[5]. A. S. Ouda and M. Gharieb, “Development the properties of brick geopolymer pastes using concrete waste incorporating dolomite aggregate,” Journal of Building Engineering, vol. 27, no. May 2019, p. 100919, 2020.

[6]. C. Arredondo-Orozco et al., “A novel energy-efficient machine to compress inorganic residues in eco-bricks as a sustainable construction strategy for low-cost housing,” Iberian Conference on Information Systems and Technologies, CISTI, vol. 2019-June, no. June, pp. 19–22, 2019.
[7]. C. Zhou, “Production of eco-friendly permeable brick from debris,” Construction and Building Materials, vol. 188, pp. 850–859, 2018.
[8]. D. Landi, S. Gigli, M. Germani, and M. Marconi, “Investigating the feasibility of a reuse scenario for textile fibres recovered from end-of-life tyres,” Waste Management, vol. 75, pp. 187–204, 2018.
[9]. D. Lesueur, “The colloidal structure of bitumen: Consequences on the rheology and on the mechanisms of bitumen modification,” Advances in Colloid and Interface Science, vol. 145, no. 1–2, pp. 42–82, 2009.
[10]. D. Movilla-Quesada, A. C. Raposeiras, L. T. Silva-Klein, P. Lastra-González, and D. Castro-Fresno, “Use of plastic scrap in asphalt mixtures added by dry method as a partial substitute for bitumen,” Waste Management, vol. 87, pp. 751–760, 2019.
[11]. G. Polacco, S. Filippi, F. Merusi, and G. Stastna, “A review of the fundamentals of polymer-modified asphalts: Asphalt/polymer interactions and principles of compatibility,” Advances in Colloid and Interface Science, vol. 224, pp. 72–112, 2015
[12]. H. Limami, I. Manssouri, K. Cherkaoui, and A. Khaldoun, “Study of the suitability of unfired clay bricks with polymeric HDPE & PET wastes additives as a construction material,” Journal of Building Engineering, vol. 27, no. June 2019, p. 100956, 2020.
[13]. J. K. Appiah, V. N. Berko-Boateng, and T. A. Tagbor, “Use of waste plastic materials for road construction in Ghana,” Case Studies in Construction Materials, vol. 6, pp. 1–7, 2017.
[14]. M. H. Wu, C. L. Lin, W. C. Huang, and J. W. Chen, “Characteristics of pervious concrete using incineration bottom ash in place of sandstone graded material,” Construction and Building Materials, vol. 111, pp. 618–624, 2016.
[15]. M. Jayaprakash, I. Deeksha, and M. Soumya, “PET Bottles for Eco-friendly Building in Sustainable Development,” International Journal of Current Trends in Engineering & Research, vol. 2, no. 5, 2016
[16]. P. L. Paihte, A. C. Lalngaihawma, and G. Saini, “Recycled Aggregate filled waste plastic bottles as a replacement of bricks,” Materials Today: Proceedings, vol. 15, pp. 663–668, 2019.
[17]. Q. Afzal, S. Abbas, W. Abbass, A. Ahmed, R. Azam, and M. Rizwan Riaz, “Characterization of sustainable interlocking burnt clay brick wall panels: An alternative to conventional bricks,” Construction and Building Materials, vol. 231, p. 117190, 2020.

[18]. R. Bhushaiah, S. Mohammad, and D. S. Rao, “Study of Plastic Bricks Made From Waste Plastic,” International Research Journal of Engineering and Technology, p. 1122, 2008
[19]. R. S. Kognole, K. Shipkule, and K. S. | M. P. | L. P. | U. Survase, “Utilization of Plastic waste for Making Plastic Bricks,” International Journal of Trend in Scientific Research and Development, vol. Volume-3, no. Issue-4, pp. 878–880, 2019
[20]. S. A. Wahid, S. M. R. Rawi, and N. M. Desa, “Utilization of Plastic Waste in Foundry Sand Bricks,” Journal of Basic and Applied scientific Research, vol. 5, no. 1, pp. 35–44, 2015.
[21]. S. K. Intan and S. Santosa, “Utilization of PTE and LDPE plastic waste and building material waste as bricks,” Korean Journal of Materials Research, vol. 29, no. 10, pp. 603–608, 2019.
[22]. S. Köfteci, “Effect of HDPE Based Wastes on the Performance of Modified Asphalt Mixtures,” Procedia Engineering, vol. 161, pp. 1268–1274, 2016.
[23]. S. N. Amir and N. zulaikha Yusof, “Plastic in Brick Application,” Trends in Civil Engineering and its Architecture, vol. 3, no. 1, pp. 341–344, 2018.
[24]. T. Smith, S. Tighe, and R. Fung, “Concrete Pavements In Canada: A Review Their Usage And Performance,” in 2001 Annual Conference and Exibition of The Transportation Association Of Canada, 2001.

LOGIC
Journal of Engineering Design and Technology
Vol. 23 No.2 July 2023 ; p. 121 - 130

p-ISSN : 1412-114X
e-ISSN : 2580-5649
http://ojs2.pnb.ac.id/index.php/LOGIC

CUTTING SPEED ANALYSIS OF ORGANIC WASTE CHOPPING MACHINE FLYWHEEL MODEL LEVEL CONTROL

1) Mechanical Engineering Department, Politeknik Negeri Bali, Indonesia.

Correponding email [1] :
putudarmawa@pnb.ac.id

I Putu Darmawa[1], I Nengah Ludra Antara[1], I Nyoman Sutarna[1], Ida Bagus Puspa Indra[1], I Nyoman Gunung[1]

Abstract. This machine is used to chop leaves, twigs and branches into very small pieces, to avoid the bad smell due to the decay of organic waste and can be used as compost. The amount of cutting speed on the organic waste chopping machine with a chopping time of 2.5 kg of ketapang leaves is the average time obtained without flywheels 2.0 minutes and with flywheels 1.7 minutes, a time difference of 0.3 minutes. The chopping time of 2.5 kg of ketapang branches with an average time obtained without a flywheel of 2.2 minutes and with a flywheel of 2.0 minutes, a time difference of 0.2 minutes. The chopping time of teak branches is 2.5 kg with an average time obtained without a flywheel of 2.6 minutes and with a flywheel of 2.0 minutes, so the time difference is 0.6 minutes. So the cutting speed using a flywheel is better. The results of the productivity obtained on the organic waste chopping machine, for the results of leaf chopping productivity without a flywheel of 48% and those using a flywheel of 58%, and the results of leaf chopping with a flywheel are 10% more productive, for the productivity of chopping twigs without a flywheel of 44% and those using a flywheel of 49%, so the results of chopping twigs with a flywheel are 5% more productive, and the results of chopping branches without a flywheel of 37% and those using a flywheel of 49%, so the results of chopping branches with a flywheel are 12% more productive.

Keywords : analysis, machine cutting speed, organic waste and flywheel.

1. INTRODUCTION

Technology development basically aims to answer the need for equipment efficiency, both existing and still being designed. So an effective technology utilization effort must first be able to produce effective products, one of which is the application of appropriate machines for chopping organic waste, the success of this machine must be based on the usefulness of the products produced with the level of effectiveness. Waste chopping tools in general that are usually used are not equipped with flywheels. But with the development of technology, there has begun to develop appropriate tools in the form of organic waste chopping tools that can chop organic waste such as leaves, twigs and branches, various types of organic waste on the Bali State Polytechnic campus.

This chopping machine is equipped with a flywheel to increase the torque of the rotary knife rotation so that the rotary knife rotation remains stable when chopping hard enough organic waste. And this chopping machine is used to chop several types of organic waste from leaves, twigs and tree branches. With an area of approximately 12 hectares of Bali State Polytechnic campus park and the waste generated per day reaching approximately 10 m3, then based on this background the author tries to analyze the cutting speed of the flywheel model organic waste chopping machine and measure how much organic waste is chopped so that this tool can be said to be effective.

Organic waste is waste from organic materials that can be decomposed by microbes, organic waste consists of wet and dry waste that can be reprocessed into functional products, organic waste is actually classified as environmentally friendly waste because it can be decomposed naturally by microbes, but natural decomposition takes time. So when organic waste is not processed quickly and accumulates, it can cause unpleasant odors, as shown in Figure 1. For the decomposition process to be faster, human intervention is needed, by utilizing appropriate technology, namely an organic waste reading machine that can produce economic value.

Figure 1. organic waste

A combustion motor is a type of heat engine that includes an internal combustion engine. Internal Combustion Engine (I.C. Engine) is a heat engine that converts the chemical energy of fuel into mechanical work, namely in the form of shaft rotation. In gasoline engines with the Otto cycle, two types of engines are known, namely 4-stroke (four-stroke) and 2-stroke (two-stroke) engines. For a 4-stroke engine, there are 4 piston movements or 2 crankshaft rotations for each combustion cycle, while for a 2-stroke engine, there are 2 piston movements or 1 crankshaft rotation for each combustion cycle [1][2][3].

Flywheel or rila wheel or force balancing wheel is one of the round-shaped engine elements with a large mass weight and is directly connected to the crankshaft, usually located before or after the connecting device for out-put. This flywheel functions as a force balancer and regulates engine rotation so that engine rotation can run properly. The working principle of this flywheel is to keep the engine rotation running normally and not rigidly so that the resulting out-put can be controlled [4][5], the shape of the Flywheel model as shown in Figure 2.

Figure 2. Flywheel

Cutting is the process of mechanically separating a solid material along a specific line by a cutting tool. The cutting tool is described as a material blade (knife) with a sharp edge. This cutting causes a material to have 2 new shapes called pieces or flakes, which are smaller than the original. The cutting process begins with the intersection (contact) between the blade and the cutting material. as shown in Figure 3 [6][7][8].

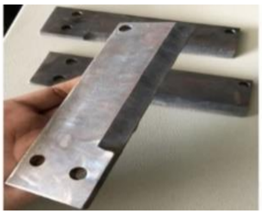

Figure 3. Cutting Blade

The shaft is one of the most important parts of the engine. Almost all machines forward the power of rotation with the intermediation of the shaft. Shafts can generally be installed gears, pulleys, and naf that rotate with the shaft. The loading on the shaft depends on the amount of power and rotation that is forwarded, as well as the effect of the force generated by the parts that are supported and rotate with the shaft [9][10][11].

Bearing is one part of the machine element that serves to support the shaft so that rotation can take place safely [12][13]. Bearings can be classified on the basis of bearing movement against the shaft, namely, glide bearings, and rolling bearings. On the basis of the direction of the load on the shaft, namely, radial bearings, and axial bearings.

The pulley serves to forward and change the rotation along with the belt from the driving source to the shaft or component to be driven. Belt pulleys are made of cast iron or steel. For lightweight construction set pulleys of aluminum alloy. There are various types of pulleys on the belt according to the belt being driven, namely pulleys for flat belts, pulleys for V belts and pulleys for rotating belts [14][15][16].
Belts or belts are made of rubber and have trapezium containers with weaves, teterons and the like used as belt cores to carry large pulls. The V-belt is wrapped around a V-shaped pulley groove. The twisted part of the belt will bend so that its inner width will increase and the friction force will also increase due to the influence of the wedge shape, which will result in large power transmission at relatively low tension [14][16].

Productivity is often identified with efficiency in the sense of a ratio between outputs and inputs. As a measure of efficiency or productivity of human labor, the ratio is generally in the form of output produced by work activities divided by the hours of work contributed as a source of input with rupiah or other units of production as the benchmark dimension [17].

The purpose of this study is to determine the cutting speed and productivity results on the flywheel model organic waste chopping machine and without flywheels. In the analysis of this flywheel model organic waste chopping machine, only analyzes the cutting speed of the knife, and analyzes the effect of using flywheels and without using flywheels on the cutting speed.

2. METHODS

The design of this research is analytical research, that is analyzing the effect of the cutting speed of the flywheel model organic waste chopping machine on the results of its chopping and conducting machine trials on chopping organic waste. The first test tested the cutting speed without using the Flywheel and the second test tested the cutting speed using the Flywheel.

The location for conducting research on analyzing the cutting speed of the flywheel model organic waste chopping machine from start to finish, at the Bali State Polytechnic Campus, part of the Maintenance and Repair Engineering Service Unit (UPT-PP), especially in the garden section. The research time was 4 months, from February 1st, 2022, to May 2nd, 2022.

Data sources are obtained through surveys in the field by studying data on productivity and the advantages and disadvantages of the machine (flywheel model organic waste chopping machine), also studying theories related to analysis, literature, journals, and other sources.

In this study, instruments or tools are needed that support the process of collecting analysis data from material preparation to obtaining test result data. The instruments needed are stopwatches, pushrods, tachometers, and digital scales.

The research procedure for analyzing the problem of productivity on the results of shredding organic waste shredding tools is as follows:
a) Weighing the materials to be tested
b) Prepare a stopwatch and tachometer
c) Starting the combustion motor
d) Measuring the RPM of the combustion motor with a tachometer
e) Putting the material that has been weighed into the chopping machine
f) Measuring the time with a stopwatch while the machine is chopping
g) Ending machine operation
h) Weighing back the material that has been chopped
i) Recording the data obtained
j) Cleaning the machine

3. RESULTS AND DISCUSSION

3.1 Results

1) The tool to be analyzed has the function to chop leaves, twigs, and branches. The working concept of this tool is that the rotation of the combustion motor is forwarded by the pulley to the shaft where on the shaft there are 4 chopping knives and 1 fixed knife.

Caption:
1. Motor fuel
2. Order
3. Enumerator room
4. Blade shaft
5. Funnel input
6. Flywheel

Figure 4. Flywheel model organic waste shredder

The initial stage before the testing process of the organic waste chopper is to prepare raw materials in the form of leaves, twigs and branches that will be tested for the efficient level of the tool. Next, measure the weight of the leaves and twigs to be tested.

2) Working Principle of Tool

The working principle of the organic waste chopping machine with flywheels is that first the rotation of the gasoline motor will be forwarded using a V-belt pulley to the shaft, this machine uses two shafts, namely the shaft for the chopping knife and the shaft for the roll pusher, in the chopping knife shaft there are four chopping blades, one fixed knife. When each raw material consisting of leaves, twigs and branches is inserted into the organic waste chopping machine with flywheels, the waste will be pulled by the roll pusher into the chopping knife. When twigs, branches and leaves are chopped, the results will be pushed to the output of the machine, so that the chopped results will move out through the drain contained in the organic waste chopping machine with the flywheel.

3) Ability of Organic Waste to Hold the Load Under the Knife

a) Leaf

Leaf hardness is data that must be known to start calculations on leaf chopping knives, in this test using ketapang leaves. The specifications of the flywheel model organic waste chopping machine knife are:

Chopping blade = 31 cm
Fixed blade = 31 cm
Thickness of chopping blade = 3 mm
Thickness of fixed blade = 10 mm
Number of chopping blades = 4 pc
Number of fixed blades = 1 pc

How to test leaf hardness:
1) Collect approximately 1 kg of leaves and tie them together, to make sure it can use scales.
2) Place the leaves on the anvil where the test piece is placed.
3) Give a load on the pressing pad. Perform pressure using a leaf chopper knife until the leaf breaks or the maximum load has occurred.

Table 1. Leaf Testing

Leaf Type	Number of Leaf (Kg)	Load
Ketapang	1	2,2 kg

b) Twig

The hardness of the twig is the data that must be known to start the calculation on the twig chopping knife. In this analysis, the author tested Ketapang twigs.
How to test the hardness of twigs:
1) Cut twigs with a diameter of 2 cm with a length of 10 cm as many as 4 pieces.
2) Place the twig on the anvil where the test piece is placed.
3) Give a load on the pressure pad. Do it until the twig is broken or the maximum load has occurred.

Table 2. Twig Testing

Number of twig (pcs)	Load
4	4,93 kg

c) Branch
1) The hardness of the branch is the data that must be known to start the calculation on the chopping blade. In this analysis the author tested teak branches as the main material. In accordance with the procedure used.
How to test the hardness of the branch:
1) Take a branch weighing 1 kg.
2) Place the branch on the anvil where the test object is placed.
3) Give a load on the pressure pad and then do it until the branch breaks or the maximum load has occurred.

Table 3. Branch testing

Branch type	Number of branch (pc)	Load
1 Teak	1	5,12 Kg

3.2 Data Testing

Based on the results of productivity testing of the flywheel model organic waste chopping machine, the following data will be used as a reference in determining the comparison between testing organic waste chopping machines using flywheels with organic waste chopping machines without flywheels. from the results of the analysis, it can be explained in the form of a table below:

Table 4. Leaf chopping test results
Leaf Testing Without Flywheel

Testing Number	Cutting Speed (Rpm)	Input (Kg)	Time (Minute)	Output (Kg)	Productivity (%)
1	2800	2.5	2.1	2.44	46 %
2	2800	2.5	2.0	2.42	48 %
3	2800	2.5	2.0	2.41	48 %
Average	2800	2.5	2.0	2.42	48 %

Table 5. Leaf chopping test results
Leaf Testing With Flywheel

Testing Number	Cutting Speed (Rpm)	Input (Kg	Time (Minute)	Output (Kg)	Productivity (%)
1	2800	2.5	1.7	2.45	58 %
2	2800	2.5	1.6	2.43	61 %
3	2800	2.5	1.8	2.46	55 %
Average	2800	2.5	1.7	2.45	58 %

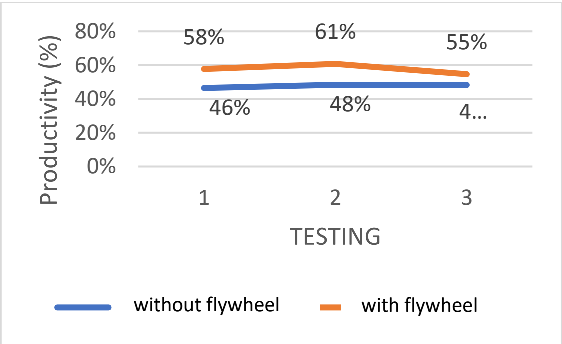

Figure 5. Graph of leaf shredding productivity results

Based on Figure 5 above, it can be concluded that leaf chopping on machines without using flywheels is 46%, 48%, 48% and with flywheels amounting to 58%, 61%, 55%. This means that by using a flywheel the results of chopped leaves are more productive by 10%.

Table 6. Twig chopping test results
Twig Testing Without Flywheel

Testing Number	Cutting Speed (Rpm)	Input (Kg)	Time (Minute)	Output (Kg)	Productivity (%)
1	2800	2.5	2.3	2.43	42%
2	2800	2.5	2.1	2.46	47%
3	2800	2.5	2.2	2.42	44%
Average	2800	2.5	2.2	2.44	44%

Table 7. Twig chopping test results
Twig Testing with Flywheel

Testing Number	Cutting Speed (Rpm)	Input (Kg)	Time (Minute)	Output (Kg)	Productivity (%)
1	2800	2.5	2.1	2.44	46 %
2	2800	2.5	1.9	2.45	52 %
3	2800	2.5	2.0	2.41	48 %
Average	2800	2.5	2.0	2.43	49 %

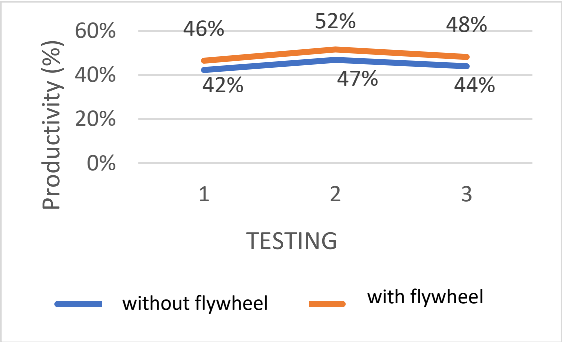

Figure 6. Graph of twig shredding productivity results

Based on Figure 3.3 above, it can be concluded that the chopping of twigs on the machine without using flywheels is 42%, 47%, 44% and with flywheels amounting to 46%, 52%, 48%. This means that by using flywheels the results of chopped twigs are more productive by 5%.

Table 8. Branch Chopping Test Results
Branch Testing Without Flywheel

Testing Number	Cutting Speed (Rpm)	Input (Kg)	Time (minute)	Output (Kg)	Productivity (%)
1	2800	2.5	2.5	2.42	39 %
2	2800	2.5	2.7	2.41	36 %
3	2800	2.5	2.6	2.42	37 %
Average	2800	2.5	2.6	2.42	37 %

Based on Figure 3.4 above, it can be concluded that the chopping of branches on the machine without using flywheels is 39%, 36%, 37% and with flywheels amounting to 46%, 49%, 46%. This means that by using a flywheel the chopped branches are more productive by 12%.

Table 9. Branch Chopping Test Results
Branch Testing with Flywheel

Testing Number	Cutting Speed (Rpm)	*Input* (Kg)	Time (minute)	*Output* (Kg)	Productivity (%)
1	2800	2,5	2,1	2,41	46 %
2	2800	2,5	2,0	2,43	49 %
3	2800	2,5	1,9	2,44	51 %
Average	2800	2,5	2,0	2,43	49 %

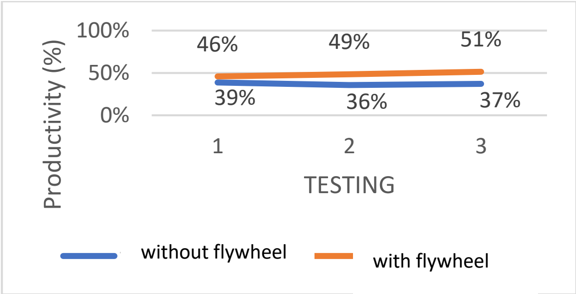

Figure 7. Graph of branch shredding productivity results

3.3 Effect of Time on Organic Waste Shredding

a) The shredding of Ketapang leaf type waste in 3 tests can be seen in Figure 8 below:

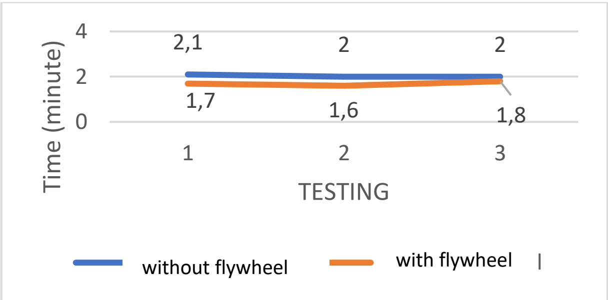

Figure 8. Comparison chart of leaf shredding time

Based on Figure 8, it can be seen that the chopping time of 2.5 kg of Ketapang leaves is the average time obtained without flywheels 2.0 minutes and with flywheels 1.7 minutes. And the time difference is 0.3 minutes.

b) Enumeration of Ketapang twig type waste in 3 tests can be seen in Figure 9 below:

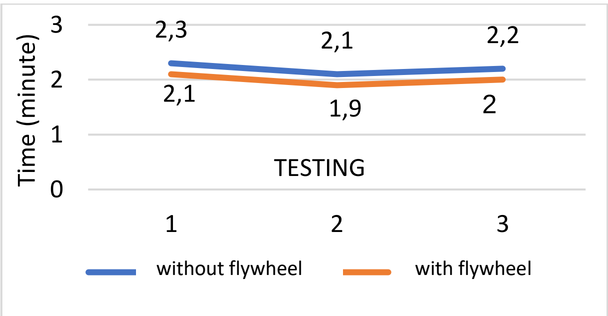

Figure 9. Comparison chart of twig shredding time

Based on Figure 9, it can be seen that the chopping time of 2.5 kg of Ketapang branches is the average time obtained without flywheels 2.2 minutes and with flywheels 2.0 minutes. And the time difference is 0.2 minutes.

c) The chopping of teak branch type waste in 3 tests can be seen in Figure 10 below:

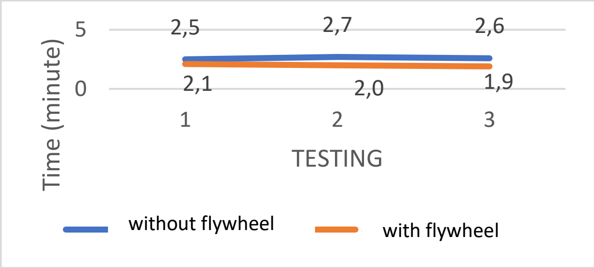

Figure 10. Comparison chart of branch shredding time

Based on Figure 10, it can be seen that the time of chopping teak branches as much as 2.5 Kg. The average time obtained without flywheels is 2.6 minutes and with flywheels is 2.0 minutes. And the time difference is 0.6 minutes.

3.4 Chopping Leaves, Twigs and Branches Without Flywheel

The criteria for good chopped leaves, twigs and branches ranges from 1 cm to 3 cm after chopping. Because the smaller the size, the easier it is to decompose with the soil.

The following are photos of the chopped leaves, twigs and branches without using a flywheel:

1) The results of chopped leaves after being chopped by an organic waste chopping machine without a flywheel turned out to be chopped in accordance with, the size of the chopped results ranged from 1 cm - 1.9 cm, as in Figure 3.8 as follows.

Figure 11. Leaf shredding results without flywheel

2) The results of chopped twigs after being chopped by an organic waste chopping machine without flywheels turned out to be chopped according to the criteria, the size of the chopped results ranged from 1.5 cm – 2.7 cm, as in Figure 3.9 as follows.

Figure 12. Twigs shredding results without flywheel

3.5 Shredding Leaves, Twigs and Branches with Flywheel

The following are photos of the chopped leaves, twigs and branches without using flywheels:

1) The results of chopped leaves after being chopped by an organic waste chopping machine with a flywheel turned out to be chopped according to the criteria, the size of the chopped results ranged from 1.3 cm - 1.5 cm, as in Figure 13 as follows.

Figure 13. Results of leaf shredding with flywheel

2) The results of chopped twigs after being chopped by an organic waste chopping machine with flywheels turned out to be chopped according to the criteria, the size of the chopped results ranged from 1.3 cm - 2.4 cm, as in Figure 3.11 as follows.

Figure 14. The result of chopping branches with a flywheel

3) The results of chopped branches after being chopped by an organic waste chopping machine with a flywheel have met the criteria, which ranges from 1.2 cm to 2.2 cm, as shown in Figure 15 as follows.

Figure 15. The result of chopping branches with a flywheel

4. CONCLUSIONS

Based on the results of the above analysis it can be concluded:

a. From the test data that has been obtained, it can be concluded that the cutting speed on the organic waste chopping machine with a chopping time of 2.5 kg of Ketapang leaves is the average time obtained without flywheel 2.0 minutes and with flywheel 1.7 minutes, so the time difference is 0.3 minutes. For the chopping time of 2.5 kg of Ketapang branches, the average time obtained without a flywheel is 2.2 minutes and with a flywheel is 2.0 minutes, so the time difference is 0.2 minutes. When chopping teak branches as much as 2.5 kg, the average time obtained without a flywheel is 2.6 minutes and with a flywheel 2.0 minutes, so the time difference is 0.6 minutes, so the cutting speed using a flywheel is better.

b. From the test data that has been obtained, it can be concluded the results of the productivity of organic waste chopping machines. The productivity results of leaf chopping without flywheels are 48% and those using flywheels are 58%, so the results of leaf chopping with flywheels are 10% more productive. The productivity results of chopping twigs without flywheels are 44% and those using flywheels are 49%. Then the results of chopping twigs with flywheels are 5% more productive. The productivity results of chopping branches without a flywheel are 37% and those using a flywheel are 49%. Then the results of chopping branches with flywheels are 12% more productive, so chopping using a flywheel is better and more productive.

From the results of the productivity analysis of the organic waste chopper, the author can suggest for users of organic waste chopping machines with flywheel models to be careful when entering organic waste into the funnel / input because there is a pusher that will pull organic waste into the chopping knife, and readers who want to develop this analysis can use various types of organic waste, and don't forget to pay attention to work safety.

5. REFFERENCES

[1] Arends, B.P.M. And. Berenschot, H. 1980. Gasoline Motors. Erlangga. Jakarta
[2] Badawi, A. 2015. Elephant Grass Chopping Machine. Muhammadiyah University of Tangerang.
[3] Irawan. A. P. 2009. Machine Elements. Diktat. Tarumanagara University
[4] Suradi. S. M. 2011. Effect of Flywheel Weight on Vehicle Acceleration. Electro Media
[5] Muzaky. 2014. Selection of Materials and Benefits. Sriwijaya State Polytechnic
[6] Person. S. 2013. Elephant Grass Chopping Knife. Jakarta. Graha Ilmu Publisher
[7] Mott R.L. 2004. Machine Elements in Mechanical Design: Integrated Machine Element Design Book II. West Sumatra: Andi Publisher.
[8] Noviyanti Nugraha, Dany Septyangga Pratama, Polite Sopian, Nicolaus Roberto. 2019. Design of a Household Organic Waste Counter Machine. Green Engineering Journal No.3 Vol. 3, November 2019.
[9] Shigley. J. E. 1983. Elephant Grass Chopper Machine. West Java: Department of Mechanical Engineering, State Polytechnic of Malang.
[10] Purwaningsih. 2009. Grass Chopper Machine. Bengkulu Agricultural University
[11] Salim. 1991. Counter Machine Theories. Jakarta. Script Earth.
[12] Sularso and Suga. K. 2002. Basic Planning and Selection of Machine Elements. Pradnya Paramita, Jakarta
[13] Suarsana, I Ketut. 2003. Knowledge of Engineering Materials. Denpasar. Department of Mechanical Engineering, Faculty of Engineering, Udayana University.
[14] Sularso and Suga. K. 2004. Basic Planning and Selection of Machine Elements. Jakarta. PT. Pradnya Paramita, Jakarta-Indonesia.
[15] Schreiter. R. J. 1991. Definition of Analysis According to Experts. In Information Technology Magazine
[16] Yamin. M, Dita Satyadarma, Pulungan Naipospos. 2008. Design of Crusher Type Garbage Counter Machine.
[17] Budianto, Dodong. 1987. Basic Techniques for Selecting Wood Industry Machinery & Equipment. Kanisius Yogyakarta

LOGIC
Journal of Engineering Design and Technology
Vol. 23 No.2 July 2023 ; p. 131 - 137

p-ISSN : 1412-114X
e-ISSN : 2580-5649
http://ojs2.pnb.ac.id/index.php/LOGIC

THE IMPACT OF PIPE Ø 0,5 HEATER LENGTH AND TEMPERATURE ON OVALITY AND THE DIFFERENCE IN PIPE THICKNESS FOR ITS BENDING

Musholli [1], Sudarmadji [2], Dianta Mustofa Kamal [3]

1) Mechanical Enggineering Department, State Polytechnic of Malang, Jl. Soekerno-Hatta 9, Malang 65141, Indonesia
2) Heavy Equipment Engineering at SMK 6 Malang, Jl Ki Ageng Gribig No 28 Malang, Malang 65141, Indonesia
3) Mechanical Engineering Department, State Polytechnic of Jakarta, Jl. Prof.DR. G.A. Siwabessy, Kampus Universitas Indonesia, Depok 16425

Email [1]): sholie.coy3@gmail.com

Abstract. Ferrous metal is of material utilized mostly for many objects or kinds of stuff to help humans and their work easier. Low-carbon steel is one of the ferrous metal natures that could be utilized when transforms into more useful objects. There be cold as well as hot working to undertake. Molting by bending pipe includes cold working due to it being bent as its recrystallization temperature is lower. When the process is undertaken, the pipe dimension would be oval which needs to be examined by enumerating a lower-recrystallization temperature and whether or not to shrink the pipe ovality percentage. In addition, as the pipe is bent there would be changes in the pipe dimension because it would drives pulls as well as puts pressure on one of the cross-sectional areas so the pipe percentage of dimension/thickness changes should also be examined. Methods to apply are a series of experiments by firstly treating heating which is up to 650^o C and bending pipe as its temperature goes lower between 410^o C – 500^o C. These two types of independent variables that differ only in their cross-sectional areas of heating also resulted in impacting on both ovality percentage and the pipe thickness of its cross-sectional area.

Keywords : Pipe Bending, Pipe Heating, Pipe 0,5 Inch, Temperature, Ovality, Induction

1. INTRODUCTION

Ferrous metal is a kind of metal to have the chemical element of iron (Fe). Ferrous metal is categorized into two main types, namely cast iron with a 2,0 – 4,5% of carbon level and steel of 0,05 – 2,0%. Based on chemical composition [1]. Low-carbon steel has 0,05 % - 0,20% C of carbon level It is malleable and easy to machine [2]. There are two methods of metal forming, namely the process of cold working conducted through a lower-recrystallization temperature, exactly at room temperature and; and the process of hot working conducted through a high temperature. Changing the pipe shape, from straight to curve, is among the process of bending. In this procedure, the outer shape of the pipe would pull out, and its inner pressure that is resulted in the pipe wrinkles [4].

The hot bending is done through a plasticity process on metal at an upper-recrystallization temperature. One of the advantages of this kind of bending is to save power during the process that is resulted in fine and identical grains at the time of recrystallization [5]. “The advantages of this kind include: (a) can reduce metal’s porosity, (b) inclusion impurity is fragmented and spread through metal, (c) rough and columned grain are softened, (d) physical trait expands, (e) need lower powers to change metal shape [36]”. While the disadvantages include having rough grain due to oxidation and the difficulty of reaching a precise measure as having sustained diminution after a hot working [5].

There are various types of the metal formation including handling, forging, punching, pulling, and bending [5]. Pipe bending is among the approaches to bending pipe into a preferred shape to do. Of course, there are many approaches for shaping metal as well as pipe. To bend a pipe is to provide pressure on it so that it causes plasticity deformation on any part to bend. There are two kinds of shaping pipe, namely shaping pipe through piercing and welding.

The ultimate bending radius may be lower than that of the radius of the element referral compensated [5]. The fact that there would be a spring-back during the bending process generally brings significant impacts in adjusting the time needed.

On this spring back, material thickness is a dominantly input parameter and is followed by the punch radius and bending angle. While on the spring-go, bending angle material plays a dominantly input parameter and is followed by the material thickness and punch radius [7].

Other materials experiencing a force out of it would sustain strain. Strain is one of the parameters to use to measure the strength of materials so that the design should meet their requirements. The basic formula for force is as follows:

$$\sigma = \frac{F}{A}\frac{N}{m^2} \qquad (1)$$

σ : Force (kPa)
F : force or load on body (N or kg)
A : Cross-sectional area of body (m2)

Stretching is a force of push and pull (P) of an workpiece interacting one another and pushing force on the workpiece’s cross-sectional area (Picture 1). Because of pull forces are resulted in workpiece stretching and are followed by the workpiece length (δ), the comparative between this additional and initial lengthy is called stretching (ε) [8].

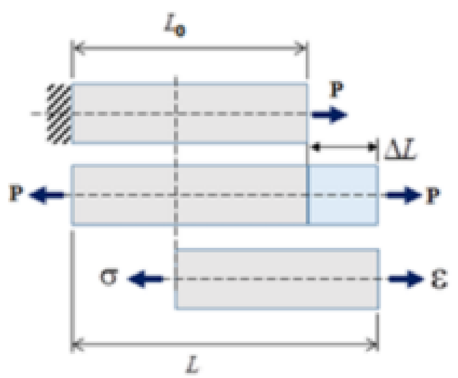

Figure 1. Workpiece with pulling and stretching [8]

The correlation between force and stretching is depicted in the form of force-stretch diagram as seen in Picture 2. Point A is the proportional limit (σp) in which a force and stretching linearity is depicted. At this point, as well, a body would back to its initial position together with the loss of body’s load capacity or as it is known as elasticity limit. Nonetheless, if the body is pulled out of a proportional limit that reaches landing area, this body would endure plasticity deformation that result in the body remaining stable or is not to be back to its initial position though its load capacity is released.

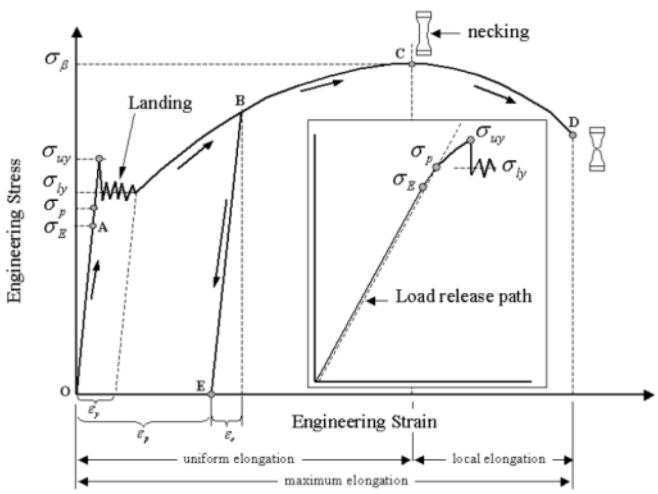

Figure 2. Diagram about the relation between force and stretching [8]

The working of bending pipe is throughout two force components: pulling and pushing. And on the process of bending, there be stretching, neutral, and wrinkling. Induction heating is a heat transfer without a direct contact between its heating source and the body. This happens because of the interaction among electromagnetic complexities.

2. METHODS

This study is based on an experimental research. Arboleda [11] defines experimental research as conducting research by manipulating one or more variables so that is resulted in certain changes in one or more variables examined, of course by applying certain means or methods. In addition, Gay [12] said that experimental is the only method to use to examine truly hypotheses relating causality (cause-and-effect relationship).

In this regard, the step to undergo is to heat the iron specimen of diameter 0,5 inch and thickness 1,4 mm. When this specimen is deployed on the heater induction, the temperature should be set up to 650 ^oC. And as the process reaches this desired temperature, the heater induction is switched off, then specimen is pulled out of bending position. While specimen is on this position, this is the time to wait for temperature reaching a specific level between 410 ^oC – 500 ^oC before having bent. The bending is undertaken by applying eight bending movements in 6 seconds.

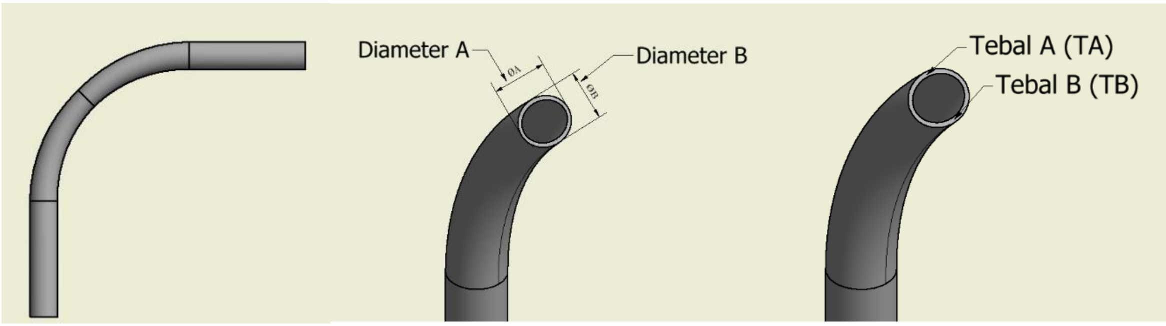

Figure 3. Sketch of experimental specimen pipe

Metal structure given a load through certain mean would remain changes. Slim pipe would wrinkle. It is due to the time allocated for bending is directly resulted in the unstable structure of geometry and it happens only when metal structure loaded with some loads that is equal to the metal critical load [13].

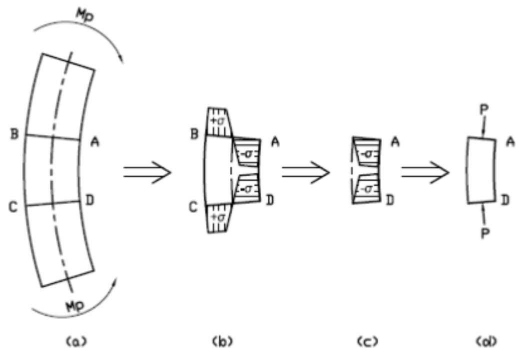

Figure 4. The transformation of pipe bending load toward the column pushed [13]

There are four steps for the load transformation; first, the time needed for bending as been indicated by Picture 4a; second, conducting analysis on strain distribution as in Picture 4b; third, isolating strain on the pipe parts where they are pulled out as seen in Picture 4c; forth, transforming distributed strain on the bent surface to become a pushed load as in Picture 4d [13].

2.1 Parameters to apply in this study

For some differences among the pipe diameters (ovality), there are two kinds of diameters to apply to specify their ovality, namely maximum diameter (right-left) or Dimeter A ($Ø_A$) and minimum diameter (up-buttom) or Dimeter B ($Ø_B$) (Picture 3). The initial diameter for a workpiece is 19mm that is eventually known as nominal diameter.

To determine the level of ovality distortion, it need to be quantified using Equation (2)

$$\text{Ovality (\%)} = \frac{D_{max} - D_{min}}{D_{nom}} \text{ x } 100\ \% \quad (2)$$

Where :

$Ø_A$: Maximum diameter (mm)

$Ø_B$: Minimum diameter (mm)

$Ø_{nom}$: Nominal diameter (mm)

The difference between pipe thickness because of pulling which is then initialed by Thick (T_A) and that thickness because of wrinkling which is now initialed by Thick (T_B) (Picture 3). The pipe initial thickness is 1,4 mm that now it is cited as nominal thickness. Their comparison is quantified by an equation:

$$\text{Thickness (\%)} = \frac{T_B - T_A}{T_{nom}} \text{ x } 100\ \% \quad (3)$$

Where:

T_A : Pipe thickness due to pulling or Thick A (mm)

T_B : Pipe thickness due to pushing or Thick B (mm)

T_{nom} : Nominal thickness (mm)

2.2 Steps to take in this Study

1) Cutting off specimen for 30 cm, in 50 pieces
2) Setting up the hydraulic of bending equipment through induction heating machine
3) Determining the range of temperature (410 °C – 500 °C). Here, the researchers undergo a series of experiments for temperature 100 °C to 540 °C.

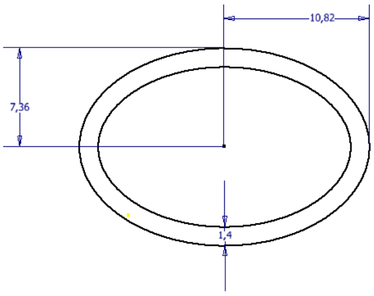

Figure 5. Creating Ovality on Specimen

Table 1. Ovality Percentage on Heating Temperatures

Heating Temperature	Ovality Percentage
100 °C	36.42%
150 °C	34.95%
200 °C	35.47%
250 °C	40%
300 °C	39.53%
350 °C	29.74%
400 °C	25.74%
500 °C	41.26%
540 °C	46.47%

4) Then it is known that for the temperature ranging from 100 °C – 300 °C is distorted over 30 %, for 350 °C – 400 °C temperature is distorted over 20 %, and ranging from 500 °C – 540 °C be distorted its ovality over 40 %. Seen from this background, it is then determined its temperature's range that would be examined, that ranging from 410 °C to 500 °C

5) For the specimen hot working, the pipe is inserted into heating induction (Picture 6). On this process, the hot working is held that specimen parts attained by probe thermocouple reaching temperature 650 °C. After having reached this temperature point, induction heater is not activated and specimen is pulled out of the bending machine of hydraulic pipe.

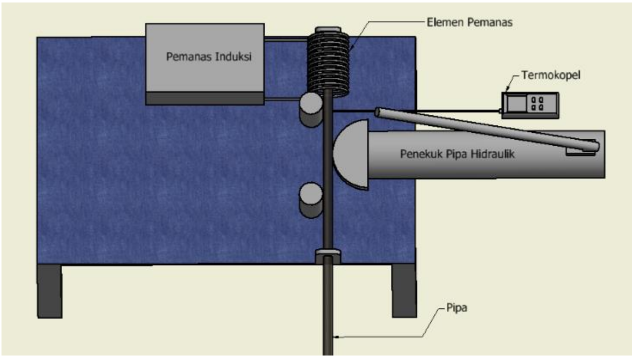

Figure 6. Heating for Steel Pipe

6) Within the process of specimen bending, this specimen is set down to a bending position and held up for the temperature goes down between 410 °C to 500 °C. Soon after the temperature points out a desired level, the bending procedure is undertaken by 8 bending moves in 6 seconds or through a constant speed of moves. This desired temperature, as intended in this study, is when it reaches the level between 410 °C to 500 °C. On every heating temperature would be taken 5 specimen data.
7) The process of collecting data. To gain a valid data, each specimen is examined for its elbows, and the pipe tolerable elbows to apply in this study is 10° of the aviation. If it is found that a specimen has an intersection below 80°, it should be reexamined under the mentioned temperature.

Figure 7. Example of Specimen after having been Bent on a Cross Section of Heating 10 cm

3. RESULTS AND DISCUSSION

Low-carbon steel would be melted in a temperature 1500 °C or when it is upper-recrystallization temperature. In this study, the heating temperature is below recrystallization that metal structural adjustments is unspecified due to the maximum heating to apply in this study is just 650 °C. The embodied metal-carbon is between 0.10 to 0.25 %. Because of its lower embodied carbon, the carbon is lenient, unable to be solidified, able to forge, pour, weld, and to harden its case (case hardening). The metal of 0.15 % has lower machinability and is generally used to build bridges, building, among others [14].

3.1 Ovality of the Pipe Diameter

For some differences among the pipe diameters (ovality), there are two kinds of diameters to apply to specify their ovality, namely maximum diameter (right-left) or Dimeter A and minimum diameter (up-buttom) or Dimeter B. The initial diameter for a workpiece is 19mm that is eventually known as nominal diameter. To count ovality percentage is to apply equation (2).

Table 2. Ovality Percentage

Heating Temperature (ºC)	For Heating Section Length of 10 cm (%)	For Heating Section Length of 14 cm (%)
410º	47.43%	24.01%
420º	48.83%	25.15%
430º	51.54%	22.82%
440º	47.71%	22.04%
450º	53.93%	21.93%
460º	53.31%	23.38%
470º	54.85%	24.83%
480º	59.72%	24.61%
490º	63.44%	27.95%
500º	62.08%	31.23%

The above table shows that on the heater with 10 cm length and on temperature 410 ºC would sustain the lowest adjustment of 47,43 %, of an initial diameter 19 cm. While the highest percentage is undergone on the heating temperature 490 ºC, with adjustment up to 63,44 % of its initial thickness.

For the heating temperature of 14 cm, it is resulted in its lowest ovality on 450 ºC, with adjustment of 21,93 % comparing to its initial diameter 19 cm. While the highest percentage is on 500 ºC that adjust 31,23% of its initial diameter.

Hence, all the data presented above could be compare that between 10cm and 14 cm heating length are found a crucial differences due to their percentage is too distinguished among them. 14 cm heating length followed by ovality percentage of 21,93 % is far better than that of 10 cm that is followed by ovality percentage 47,43 % of its initial diameter.

3.2 Differences of the Pipe Thickness

The difference between pipe thickness because of pulling which is then initialed by Thick A and that thickness because of wrinkling which is now initialed by Thick B. The pipe initial thickness is 1,4 mm that now it is cited as nominal thickness. Their comparison is quantified by an equation(3)

Table 3. Differences of the Pipe Thickness

Heating Temperature (ºC)	For Heating Section Length of 10 cm (%)	For Heating Section Length of 14 cm (%)
410º	12.14%	5.57%
420º	11.29%	6.71%
430º	12.71%	5.00%
440º	11.86%	5.29%
450º	12.71%	4.86%
460º	11.14%	5.57%
470º	11.43%	5.14%
480º	11.14%	5.71%
490º	12.00%	7.57%
500º	13.86%	6.71%

The above table indicates that on the heating length 10 cm, 460 ºC and 480 ºC makes the lowest pipe thickness 11,14 % of its initial thickness 1,4 mm. And the highest percentage is on 500 ºC that makes adjustments up to 13,86 % of the pipe initial thickness. For the heating temperature of 14 cm, it is resulted in its lowest ovality on 450 ºC, with adjustment of 4,86 % comparing to its initial diameter 1.4 mm. While the highest percentage is on 500 ºC that adjust 7,57% of its initial diameter. Hence, all the data presented above could be compare that between 10cm and 14 cm heating length are found a crucial differences due to their percentage is too distinguished among them. 14 cm heating length followed by ovality percentage of 4,86 % is far better than that of 10 cm that is followed by ovality percentage 11,14 % of its initial diameter.

4. CONCLUSION

The data presented and discussed above can be concluded as follows:

1) The finest temperature for the heater cross-section is 10 cm. While the lowest is on temperature 410 ºC that makes the lowest adjustments 47,43 % of its initial diameter 19 cm.
   And, the thickness differences is among a heating level 460 ºC and 480 ºC that make the pipe adjustments 11,14 % of its initial thickness 1,4 mm.
2) The finest temperature for the heater cross-section is 14 cm. Whereas, the lowest ovality is under temperature 450 ºC that makes the lowest ovality adjustments 21,93 % of its initial diameter 19 cm.
   And, the thickness differences is among a heating level and 480 oC that make the pipe adjustments 4,86 % of its initial thickness 1,4 mm.
3) After having conducted research it is found that the more breadth is the more significant impact on the pipe bending, by which heater cross-section 10 cm is resulted in 47 % and for that 14 cm is 22 %. For the thickness comparison on a heater cross section 10 cm is 11 %, and for that of 14 cm is 5 %. Bending a pipe that is preceded by a heating would be resulted in mare orderly micro structure as well as fixing atom structure after the bending.

5. ACKNOWLEDGEMENT
The researchers thank the board of Director of State Polytechnic of Malang that allow us to complete this study on Master Program in Applied Manufacturing Technology Engineering, Department of Mechanical Engineering, State Polytechnic of Malang for two years.

6. REFERENCES
[1] Surdia, T. & Saito, S. 1999. *Pengetahuan Bahan Teknik*. Pradnya Paramita, Jakarta
[2] Samlawi, A.K. & Siswanto, R. 2016. Material Teknik.
[3] Sukarman dkk, (2020). Analisis pengaruh radius dies terhadap springback Logam lembaran stainless-steel pada proses bending Hidrolik v-die. Jurnal Teknologi. Volume 12 No. 2 Juli 2020
[4] Mustaqim, A. 2012. Rancang Alat/Mesin Pengerol Pipa. Tugas Akhir.Yogyakarta: Universitas Negeri Yogyakarta.
[5] Dadang. 2013. *Teknik Dasar Pengerjaan Logam. Semester 1*. Malang. Indonesia. PPPPTK BOE Malang
[6] Troive, Lars et al. 2018. "Springback Compensation for a Vehicle's Steel Body Panel." International Journal of Computer Integrated Manufacturing 31(2): 152–63. https://doi.org/10.1080/0951192X.2017.1379096
[7] Phanitwong, W., Sontamino, A., & Thipprakmas, S. (2013). *Effects of part geometry on spring-back/spring-go feature in U-bending process*. Key Engineering Materials, 549, 100–107. https://doi.org/10.4028/www.scientific.net/KEM.549.100
[8] Paloboran, M. & Yahya, M.2021. *Mekanikan Bahan.Teknik Mesin*. Scopindo Media Pustaka. Surabaya
[9] Ambiyar dkk., 2008. *Teknik Pembentukan Pelat Jilid 3*, Jakarta: Direktorat Pembinaan Sekolah Menengah Kejuruan.
[10] Rudnev, V., Loveless, D., & Cook, R. L. (2017). Handbook of Induction Heating. CRC Press. From https://www.routledgehandbooks.com/doi/10.1201/9781315117485-3
[11] Arboleda, C. R. 1981. Communications Research. Manila: CFA.
[12] Gay, L. R. 1981. Educational Research: Competencies for Anlysis and Application. London: Prentice-Hall International (UK) ltd.
[13] Iswahyudi, S., 2011. Mekanisme pembentukan kerutan pada proses penekukan pipa. *In Prosiding Seminar Nasional Sains dan Teknologi* ke-2. hal. 65– 69.
[14] Ferdiansyah, E 2013. *Ilmu Bahan Teknik*. Jakarta. Indonesia. Direktorat Pembinaan Sekolah Menengah Kejuruan Kementerian Pendidikan dan Kebudayaan Republik Indonesia
[15] Sulaiman, 2010. *Pengaruh Proses Pelengkungan Dan Pemanasan Garis Pelat Baja Kapal Aisi E 2512 Terhadap Nilai Kekerasan Dan Laju Korosi*. Program Studi Magister Teknik Mesinprogram Pascasarjanauniversitas Diponegoro Semarang

LOGIC
Journal of Engineering Design and Technology
Vol. 23 No.2 Julu 2023 ; p. 138 - 146

p-ISSN : 1412-114X
e-ISSN : 2580-5649
http://ojs2.pnb.ac.id/index.php/LOGIC

ANALYSIS OF THE SELECTION AND INSTALLATION OF A PUMP FOR AN OVERFLOW SWIMMING POOL WITH A VOLUME OF 67 CUBIC METERS

1, Department of Mechanical Engineering, Politeknik Negeri Bali, Indonesia

Correponding email [1] :
wibolo@pnb.ac.id

Achamad Wibolo[1], I Ketut Suherman[1], I Dewa Made Pancarana[3], I Ketut Adi[1]

Abstract. In the swimming pool there is a pump system that is useful for circulating water. Pumps in swimming pools can affect water quality. Dirty water will be cleaned by the filter and will be re-circulated to the swimming pool. The calculations that must be known are the volume of the swimming pool, pump power, flow rate, and the curve of the pump. In order for the selection of a swimming pool pump to be appropriate, the correct calculation must be made so that the pump can provide the best performance for a swimming pool with a volume of 67 cubic meters and is able to circulate swimming pool water 4 times during 12 working hours.

Keywords: power, pump, flowrate, swimming pool.

1. INTRODUCTION

The main objective in the analysis of the selection and installation of a pump for an overflow swimming pool with a volume of 67 cubic meters is to ensure water supply adequate at any time, both in terms of the pressure required and the debits for all outlets, equipment, and equipment.

A swimming pool is an artificial construction designed to be filled with water and used for swimming, diving or other water activities. The private swimming pool is a status symbol for the owner, because it requires a lot of space and high maintenance costs. Public swimming pools are usually part of a physical fitness center or recreational park, with other facilities including saunas, swimming sports courts (squash, tennis, etc.) and restaurants. To purify and disinfect water, chlorine is usually used. In swimming pools there is a pump that functions to circulate water so that it continues to flow and the water remains full. The swimming pool circulation systems that are commonly used are skimmer, overflow and semi-overflow systems [1][2], [3].

The Overflow System is a water circulation system that conditions the swimming pool water to overflow to certain sides or overflow to all sides of the swimming pool. The overflowing pool water then spills automatically into the Gutter Overflow (Gutter is a channel made on the edge of the pool which functions as a channel to accommodate the overflow of pool water and simultaneously directs overflow water to the Balancing Tank) [4], [5].

Figure 1. Overflow System

The way the Overflow circulation system works is that the overflow of our swimming pool water will enter the Balancing Tank through the Gutter Overflow pipe, then the water that is already in the Balancing Tank will be sucked into the Pump Then the water enters the Sand Filter After that the water that has been filtered clean will return back into the pool through the Inlet Fitting. That's the working pattern of the Overflow swimming pool water circulation system continuously. By using this circulation system, of course the cost of building a swimming pool will seem more expensive because to support this circulation system, two additional small buildings are needed, namely Gutter Overflow and Balancing Tank.

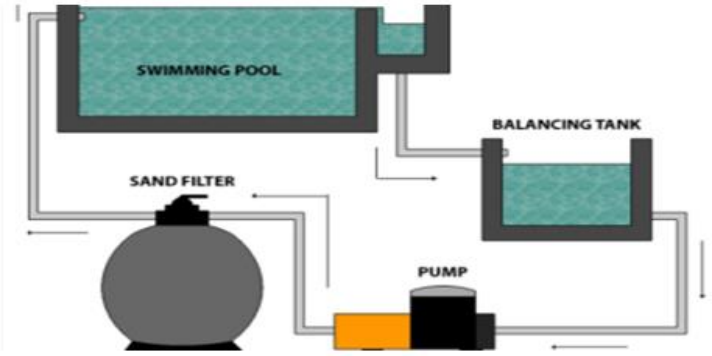

Figure 2. Overflow Swimming Pool Schematic

Centrifugal pumps are included in the type of dynamic pressure pump, where this type of pump has an impeller that functions to lift fluid from a low place to a higher place or from lower pressure to higher pressure. Power from outside is given to the shaft to rotate the impeller into the pump housing, then the fluid around the impeller will also rotate as a result of the impeller blades pushing. Due to the emergence of centrifugal force, the fluid flows from the middle of the impeller out through the channels between the impeller blades. The fluid head will increase because the fluid is accelerating. The fluid coming out of the impeller is accommodated by a volute-shaped channel around the impeller and channeled out of the pump through the nozzle, in the nozzle the fluid flow velocity is converted into pressure head [6]–[8].

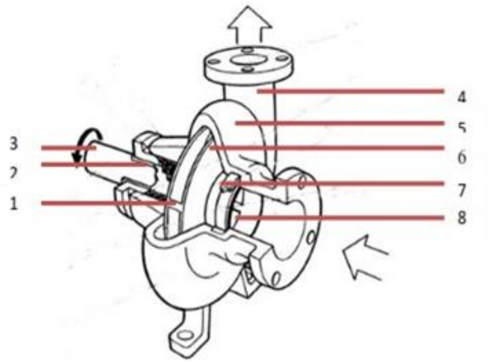

Figure 3. Centrifugal Pump

Centrifugal pump parts are:
1. Impeller blades are impellers that function as a place for liquid to pass through the impeller.
2. Packing is used to prevent and reduce fluid leakage from the pump casing associated with the shaft, usually made of Asbestos or Teflon.
3. The shaft or shaft serves to continue the torque from the drive during operation and the pedestal of the impeller and other rotating parts
4. Discharge nozzle is part of the pump that functions as a place for the pumped fluid to come out.
5. Casing is the outer part of the pump which functions as a protective element inside.
6. The impeller functions to convert the mechanical energy from the pump into velocity energy in the fluid which is pumped continuously, so that the fluid on the suction side will continuously enter to fill the void due to the displacement of the previously entered fluid.
7. Bearings function to support or hold the load from the shaft so that it can rotate. Bearings also function to smooth the rotation of the shaft and hold the shaft to keep it rotating in place, so that frictional losses can be minimized.

8. The input impeller is the part that enters the suction direction of the impeller.

The swimming pool consists of various components that help the pump circulate the water contained in it, the following is an explanation of the main components found in the swimming pool:

a. Balancing tank serves to balance the pool water. If it rains, the overflow of water that enters the pool is accommodated by this tool. If the pool water starts to recede, the water in the balancing tank will flow into the pool.

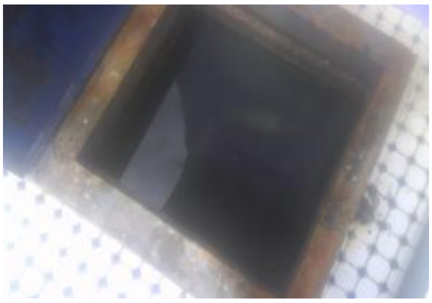

Figure 4. *Balancing Tank*

b. Gutter is located on the edge of the swimming pool. Serves to accommodate pool water spills to be channeled to the balancing tank. Then from the balancing tank it flows to the filter to be filtered

Figure 5. *Gutter*

c. Sand Filter as a filter component of dirt contained in swimming pool water. Apart from being affordable, the Sand Filter operational and maintenance system is also very easy to learn. As a filtering medium, this Sand Filter uses silica sand which has a diameter of 0.4-0.5mm. To get maximum clarity, you can use silica sand with an even smaller diameter. For information, this silica sand can also be replaced with other media such as Green Solid. Because it has better filtering quality, this media is far more expensive than silica sand.

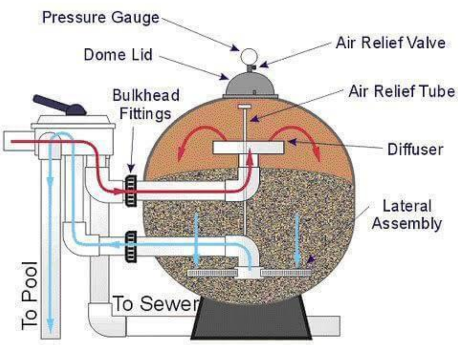

Figure 6. Sand Filter System

2. METHODS

The scheme built in the analysis of the selection and installation of pumps for overflow swimming pools is as shown in Figure 7 in below [9][10].

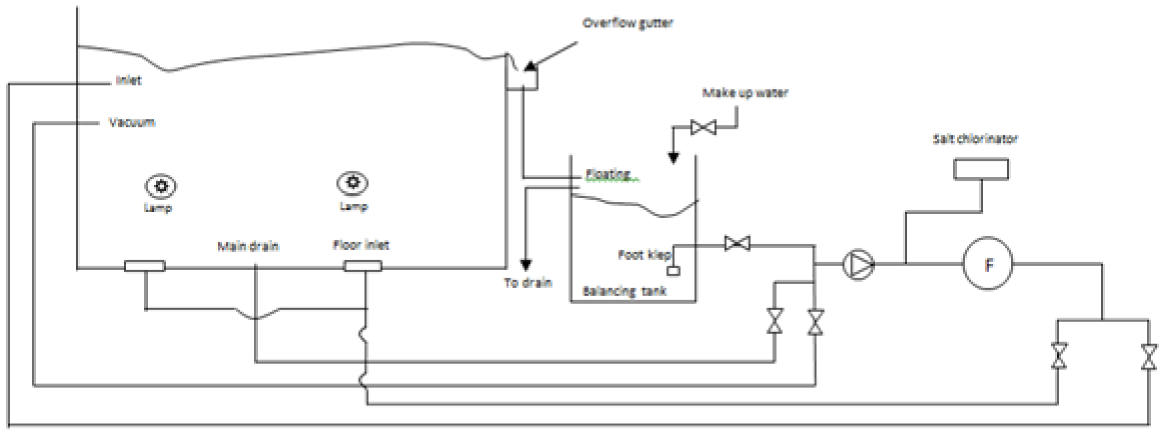

Figure 7. Overflow pool schematic

In the process of selecting a pump for a swimming pool, of course there are processes or stages that must be carried out before installing a pump, the following are things to look for [11][12]:

a. Swimming pool volume

$$V = P \times L \times T \quad (1)$$

In which:
V = Volume (m^3)
P = Swimming pool length (m)
L = Swimming pool width (m)
T = Pool depth (m)

b. Debit

$$Q = \frac{V}{W} \quad (2)$$

In which:
Q = Debit (m^3/s)
V = Flow volume (m^3)
W = Flow time (detik)

c. Input losses

$$V_s = \frac{Q}{A_s} \quad (3)$$

In which:
V = Flow rate average (m/s)
Q = Volumetric flow rate (m^3/s)
A = Cross-sectional area (m^2)

$$h_{L1} = K\frac{v_s^2}{2g} \quad (4)$$

In which:
h_{L1} = Input losses (m)
K = 1 (The discharge from the pipe into the pool)
v = Average speed of flow (m/s)
g = Earth's gravity (9,81 m/s^2)

d. Friction loss in the suction line

$$N_R = \frac{v_s . D_s . \rho}{\mu} \quad (5)$$

In which:
N_R = Reynold's number
v = Average speed of flow (m/s)
D = Inside Diameter (m)
ρ = Density (kg/m^3)
μ = DynamicViscosity ($N.s/m^2$)

$f = \frac{64}{N_R}$ (6)

In which:

f = friction factor

$h_{L2} = f_s \frac{L.v_s^2}{D_s.2g}$ (7)

In which:

h_{L2} = Friction loss in the suction line (m)

L = Channel length (m)

e. Loss of valves

$V_d = \frac{Q}{A_d}$ (8)

In which:

A = Flow area (m^2)

$h_{L3} = f_T \frac{L_e}{D} \frac{v_d^2}{2g}$ (9)

In which :

h_{L3} = Loss of valves (m)

f. ElbowLosses

$h_{L4} = f_T \frac{L_e}{D} \frac{v_d^2}{2g}$ (10)

In which:

h_{L4} = Elbow losses (m)

g. Output losses

$h_{L5} = K \frac{v_d^2}{2g}$ (11)

In which:

h_{L5} = Output losses (m)

h. Total loss due to friction

$h_L = h_{L1} + h_{L2} + h_{L3} + h_{L4} + h_{L5}$ (12)

In which:

h_L = Total loss due to friction (m)

i. Pump head

hA = (Z2 – Z1) + hL (13)

In which:

hA = Pump head (m)

(Z1 – Z2) = Difference in height (Reservoir 1 dan Reservoir 2) (m)

3. RESULT AND DISCUSSION

3.1 Result

The swimming pool used is a type of overflow swimming pool, the reason for choosing this overflow swimming pool is that this type of swimming pool has an artistic element and is pleasing to the eye because all the edges of the wall are immersed in water. This overflow swimming pool also has the advantage that the dirt or leaves that are above the floating swimming pool will fall into the overflow gutter and make the swimming pool always look clean, another advantage is that someone who swims in it will not be sucked in because of the Maindrain. The type of swimming pool filter used is a type of sand filter, the advantage of using this type of sand filter is that the sand used can be cleaned again and can be reused by backwashing. This sand filter has a construction that is durable and strong compared to other filters, the sand used in this sand filter has a service life of 5-8 years. The selection of the pump used in this swimming pool is a pump that has a high discharge or flowrate, because the pump here is used to circulate swimming pool water many times, so the pump needed is a pump with a head that is not too high with a high discharge. The application of a swimming pool water circulation system is based on the clarity of the water itself, if the water is clear then the swimming pool water circulates 4 times in 12 hours for one day.

The selection of swimming pool pumps has previously gone through a valid data collection stage, so that the performance of the pump can be maximized for the swimming pool to be circulated. The following is valid data that has been obtained from the Overflow swimming pool: [13], [14]

Pool length = 12 m

Swimming pool width = 4 m
Pool height = 1.4 m
Water flows at 25^0 C
Density (ρ) = 997 kg/m^3
DynamicViscosity (μ) = 8.91 x 10^{-4} N.s/m^2
Nomonal pipe size $1\frac{1}{2}$ inch, friction factor (f_T) = 0.021
Dimension of PVC Pipe, Schedule 40 :
Nomonal pipe size $1\frac{1}{2}$ inch
Inside diameter (D) = 40.9 mm = 0.0409 m
Flow area (A) = 1.314 x 10^{-3} m^2
Channel length L = 15 m
Difference in height = 2.5 m
Ball valve fully open , Equivalent Length in pipe Diameters (L_e/D) = 0.05
90^0 Standart Elbow, Equivalent Length in pipe Diameters (L_e/D) = 30
The input from the balancing tank is sguare – edget inlet type (K) = 0,5
The discharge from the pipe into the pool (K) = 1

The next process is to perform pump calculations, namely to find pump head (h_A)

a. Swimming pool volume

$$V = P \times L \times T$$
$$= 12\ m \times 4\ m \times 1.4\ m$$
$$= 67\ m^3$$

b. Debit

$$Q = \frac{V}{W}$$
$$= \frac{67\ m^3}{10800/\text{detik}}$$
$$= 0{,}00620\ m^3/s$$

c. Input losses

$$V_s = \frac{Q}{A_s} = \frac{0{,}00620\ m^3/s}{1314\ x\ 10^{-3}\ m^2} = \frac{0{,}00620\ m^3/s}{1{,}314\ m^2} = 0{,}0047\ m/s$$
K = 0,5 (sguare-edget inlet type)
$$h_{L1} = K\frac{v_s^2}{2g}$$
$$= 0{,}5\ \frac{(0{,}0047\ m/s)^2}{2.9{,}81\ m/S^2} = 0{,}5\ \frac{0{,}000022\ m^2/S^2}{19{,}62\ m/S^2} = \frac{0{,}000011\ m^2/S^2}{19{,}62\ m/S^2} = 0{,}00000056\ m$$

d. Friction loss in the suction line

$$N_R = \frac{v_s.D_s.\rho}{\mu}$$
$$= \frac{(0{,}0047\ m/s)\ (0{,}0409\ m)(997\ kg/m^3)}{8{,}91\ x\ 10^{-4}\ Pa.s} = \frac{0{,}192}{0{,}000891}$$
= 215,48 (Laminer)
$$f = \frac{64}{N_R} = \frac{64}{215{,}48} = 0{,}297$$
$$H_{L2} = f_s\frac{L.v_s^2}{D_s.2g}$$
$$= 0{,}297\ \frac{\mathbf{15m}.(0{,}0047\ m/s)^2}{0{,}0409m.2.9{,}81\ m/s^2} = \frac{9{,}84\ x\ 10^{-5}\ m^2/S^2}{0{,}80\ m/s^2} = 0{,}00012\ m$$

e. Valve losses

$$V_d = \frac{Q}{A_d} = \frac{0{,}00620\ m^3/s}{0{,}00131\ m^2} = 4{,}73\ m/s$$
$$h_{L3} = f_T\frac{L_e}{D}\frac{v_d^2}{2g}$$
$$= 0{,}021.0.05\ \frac{(4{,}73\ m/s)^2}{2.9{,}81\ m/s^2} = 0{,}021.0.05\ \frac{22{,}372\ m^2/S^2}{19{,}62\ m/s^2}$$
$$= \frac{0.0234\ m^2/S^2}{19{,}62\ m/s^2} = 0{,}001\ m$$

f. Elbow losses

$$h_{L4} = f_T\frac{L_e}{D}\frac{v_d^2}{2g}$$
$$= 0{,}021.30\ \frac{(4{,}73\ m/s)^2}{2.9{,}81\ m/s^2} = 0{,}021.30\ \frac{22{,}372\ m^2/S^2}{19{,}62\ m/s^2}$$
$$= \frac{14{,}094\ m^2/S^2}{19{,}62\ m/s^2} = 0{,}71\ m$$

There are 3 Elbow then 3 x 0,71 m = 2,13 m

g. Output losses

$$h_{L5} = K\frac{v_d^2}{2g}$$

$$= 1\ \frac{(4{,}73\ m/s)^2}{2.9{,}81\ m/s^2} = 1\ \frac{22{,}372\ m^2/s^2}{19{,}62\ m/s^2}$$

$$= \frac{22{,}372\ m^2/s^2}{19{,}62\ m/s^2} = 1{,}14\ \text{m}$$

h. Total loss due to friction

$$h_L = h_{L1} + h_{L2} + h_{L3} + h_{L4} + h_{L5}$$

$$= (0{,}00000056 + 0{,}00012 + 0{,}001 + 2{,}13 + 1{,}14)$$

$$= 3{,}27\ \text{m}$$

i. Pump Head

$$h_A = (Z_2 - Z_1) + h_L$$

$$= 2{,}5\ \text{m} + 3{,}27\ \text{m}$$

$$= 5{,}77\ \text{m} \approx 6\ \text{m}$$

The required pump head is 6 m

3.2 Discussion

The selection of a swimming pool pump is carried out using a graph of the pump, by plotting the results of the calculations that have been carried out as shown in figure 7.[13]

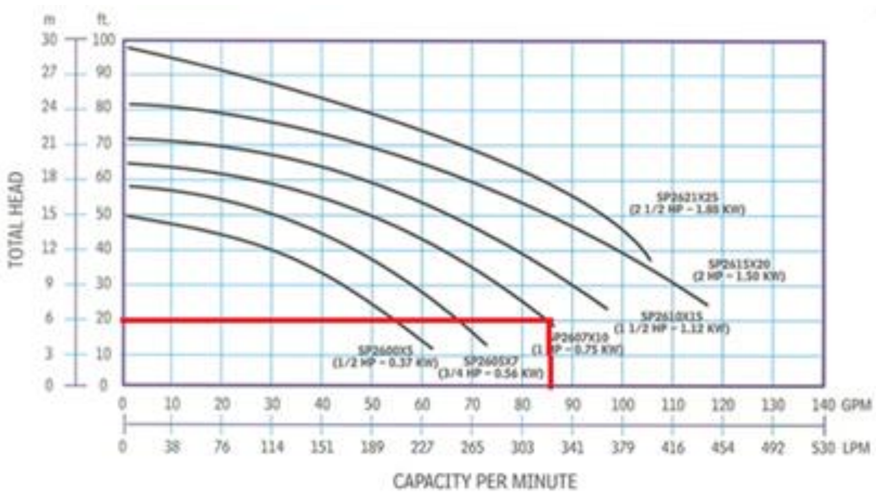

Figure 8. Pump chart

In the graph above, it can be seen that the pump head is 6 m, so a discharge of 325 liters/minute is obtained with a pump power of 1 HP. The following is a specification of a centrifugal pump that will be installed in an overflow type swimming pool.

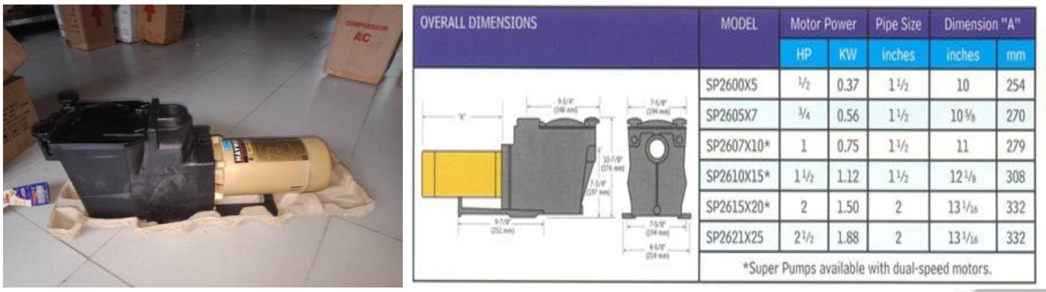
OVERALL DIMENSIONS

MODEL	Motor Power		Pipe Size	Dimension "A"	
	HP	KW	inches	inches	mm
SP2600X5	½	0.37	1½	10	254
SP2605X7	¾	0.56	1½	10⅝	270
SP2607X10*	1	0.75	1½	11	279
SP2610X15*	1½	1.12	1½	12⅛	308
SP2615X20*	2	1.50	2	13 1/16	332
SP2621X25	2½	1.88	2	13 1/16	332

*Super Pumps available with dual-speed motors.

Figure 9. Centrifugal Pump

The pump room is located underground, the goal is to save space and does not require special soil for this part of the pump room. Before installing the pump, it is ensured that it complies with predetermined procedures, namely, has sufficient air ventilation, has special channels used to dispose of water in the event of a flood and has sufficient light to make work easier [15].

Figure 10. Pump room

The centrifugal pump used has a foundation that functions to support the pump and withstand vibrations from the pump. This foundation is longer and wider than the size of the pump holder. The pump foundation that has been made has been calculated and follows the agreed procedures. The pump foundation must be higher than the floor, which aims to avoid a short circuit from the pump in the event of a flood in the pump room.

Figure 11. Pump foundation

There are several standards for pump protection used in centrifugal pumps, namely protection against backflow. The output flow of the pump is equipped with a check valve which allows the flow to only go in one direction, in the same direction as the pump output flow. Protection against overload. Several devices such as low pressure switch, high flow switch, and overload relay on the pump motor are installed in the pump system to avoid overloading the pump. Protection for the water level switch, if there is no load, the pump will be turned off automatically. ELCB (Earth Leakage Circuit Breaker) protection aims to avoid short circuit effects that occur in swimming pools. The pump protection used is in accordance with applicable standards.

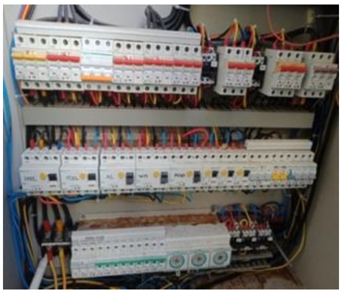

Figure 12. Pump protection

Swimming pool pump testing is carried out with the help of a measuring instrument, namely a measuring cup. Measurement of swimming pool discharge is done by calculating the flow rate using the help of a stopwatch, then the discharge flowing through the inlet of the swimming pool will be known.The test results from each inlet in the swimming pool are:
Inlet 1 swimming pool: 0.9 liter/second
Inlet 2 swimming pool: 0.9 liter/second
Inlet 3 swimming pool: 0.9 liter/second
Inlet 4 swimming pool: 1.0 liter/second
Inlet 5 swimming pool: 0.9 liter/second
Inlet 6 (waterfall) swimming pool: 0.8 liter/second

The total circulation of swimming pool water as a result of the test is 5.4 liters/second or 324 liters/minute. The time needed for 1 circulation, which is 180 minutes x 0.324 m^3/minute, is 58.32 m^3, so the pump has succeeded in circulating the swimming pool water 4 times in 12 hours.

4. CONCLUSION

Based on the test result and the discussion, it can be concluded that:

a. The pump chosen to circulate the overflow swimming pool at the hotel is a centrifugal pump with a head of 6 meters and a discharge of 325 liters/minute and a pump power of 1HP. Then the pump that has been installed is able to circulate pool water with a volume of 58.32 m3 within 3 hours.
b. In installing a swimming pool pump, it is adjusted according to the order and does not violate existing procedures.

Based on the results and conclusions of the research, some recommendations that can be submitted are as follows:

a. Maintenance carried out on swimming pool pumps must be carried out routinely or scheduled, because the operating time for swimming pool pumps is very long and is always in the on position every day to maintain water quality so that it remains clear.
b. The main components in the pump are in good condition and ready to operate. If there is noise at the pump, the pump must be turned off immediately and immediately check the cause of the noise that occurs at the pump.

5. REFERENCES

[1] Y. Li, Z. Ding, and Y. Du, "Techno-economic optimization of open-air swimming pool heating system with PCM storage tank for winter applications," *Renew. Energy*, vol. 150, pp. 878–890, 2020.
[2] E. Diniardi and A. Ali, "PERENCANAAN DAYA POMPA UNTUK KOLAM RENANG KONVENSIONAL DENGAN KAPASITAS 2000M," *SINTEK J. J. Ilm. Tek. Mesin; Vol 7, No 1 SINTEK J.*, Jun. 2013.
[3] L.-T. Wong, C.-S. Chan, K.-W. Mui, and D. Zhang, "Optimizing the Pump Storage System for Hot Water Showering at Swimming Pools," *Water*, vol. 15, no. 11. 2023.
[4] A. ur Rehman, A. R. Paul, and A. Jain, "Performance Analysis and Cavitation Prediction of Centrifugal Pump Using Various Working Fluids," *Recent Patents Mech. Eng.*, 2019.
[5] M. Stewart, "3 - Centrifugal pumps," M. B. T.-S. P. O. Stewart, Ed. Boston: Gulf Professional Publishing, 2019, pp. 61–309.
[6] M. Sreekanth, R. Sivakumar, M. Sai Santosh Pavan Kumar, K. Karunamurthy, M. B. Shyam Kumar, and R. Harish, "Regenerative flow pumps, blowers and compressors – A review," *Proc. Inst. Mech. Eng. Part A J. Power Energy*, vol. 235, no. 8, pp. 1992–2013, May 2021.
[7] M. Szreder and M. Miara, "Impact of Compressor Drive System Efficiency on Air Source Heat Pump Performance for Heating Hot Water," *Sustainability*, vol. 12, no. 24. 2020.
[8] G. Jinke, Z. Xianlei, L. Guanlin, H. Shouhui, and Y. Di, "Analysis of Aerodynamic Noise on Small Centrifugal Compressor," *J. Hunan Univ. Nat. Sci.*, vol. 44, no. 8, 2017.
[9] Y. MINAMI, M. OTSUKA, M. NANYO, and S. KOJIMA, "PLUMBING DESIGN LOAD AND MAINTENANCE OF A DISPORSER DRAINAGE SYSTEM(Environmental Engineering)," *J. Technol. Des.*, vol. 11, no. 22, pp. 329–333, 2015.
[10] S. G. Kamble, "Problems Associated With Plumbing and its Maintenance," *Int. J. Eng. Res. Technol.*, vol. 4, no. 04, pp. 324–329, 2015.
[11] J. Larminie and A. Dicks, "Compressors, Turbines, Ejectors, Fans, Blowers, and Pumps," in *Fuel Cell Systems Explained*, 2003, pp. 309–330.
[12] R. S. R. Gorla and A. A. Khan, *Turbomachinery Design and Theory*. Basel,Switzerland: MarcelDekker,Inc., 2013.
[13] I. J.Karassik, *Pump Handbook*, Fourth Edi. United State of America: The McGraw-Hill Companies, 2008.
[14] M. Stewart, *Pumps and Compressors*. USA: Gulf Professional Publishing, 2018.
[15] A. Carravetta, G. Del Giudice, O. Fecarotta, M. C. Morani, and H. M. Ramos, "A New Low-Cost Technology Based on Pump as Turbines for Energy Recovery in Peripheral Water Networks Branches," *Water*, vol. 14, no. 10, 2022.

LOGIC
Journal of Engineering Design and Technology
Vol. 23 No.2 July 2023; p. 147 - 154

p-ISSN : 1412-114X
e-ISSN : 2580-5649
http://ojs2.pnb.ac.id/index.php/LOGIC

THE EFFECT OF HOLDING PRESSURE AND INJECTING PRESSURE TO SHORT SHOT DEFECT IN INJECTION MOLDING COVER POT

Muhammad Sambodo Aribowo [1], Agus Dani [1]

1) Mechanical Engineering Production and Maintenance, Politeknik Negeri Malang, Jawa Timur, Indonesia.

Correponding email [1] :
sambodoari8@gmail.com

Abstract. Inappropriate injection molding parameters often result in product defects, one of which is the short shot, which is a condition where the plastic to be injected into the cavity does not reach the ideal capacity. The purpose of this research is to understand and be able to explain the parameters of holding pressure, inject pressure, and the interaction of these two parameters on short-shot defects in cover pot products with the injection molding process. This research uses independent variables, namely holding pressure with variations of 20 bar, 30 bar, and 40 bar, and injecting pressure with variations of 15 bar, 30 bar, and 45 bar, and dependent variables in the form of short-shot defects. The method used in this research is a factorial experiment with replication of 10 (ten) times and data processing analysis using ANOVA with the help of statistical software. The result of this research is that there is a significant influence of holding pressure, inject pressure and the combination of these two parameters on short shot defects in cover pot products with injection molding process. The average weight of the product produced at the combination of the parameters holding pressure 40 bar and injecting pressure 45 bar is 8.8 grams (normal) so as to minimize product defects to improve the quality and quantity of cosmetic packaging production cover pot.

Keywords : Holding Pressure, Inject Pressure, Injection Molding, Polystyrene, Short Shot.

1. INTRODUCTION

The need for plastic consumption in Indonesia is quite large, based on data from the Ministry of Environment and Forestry in 2022 the amount of plastic packaging consumption in Indonesia reaches 18 million tons [1]. With high public interest and purchasing power, companies in the field of plastic packaging make various innovations to their products. The most commonly used plastic processing method is injection molding [2]. Injection molding is the process of processing a part or product made from plastic that is heated and injected into a tool in the form of a mold. Common product defects in injection molding methods include voids, surface blemishes, short shots, flashing, flow marks, weld lines, burning, and warpage [4].

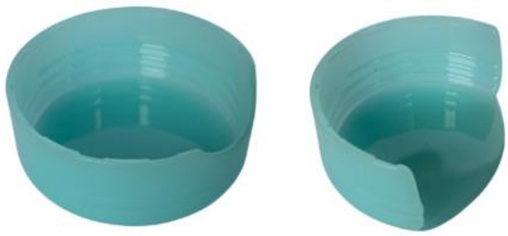

Figure 1. Short shot defect in injection molding cover pot

Based on these various defects, short shots are types of product defects that are not intact, so that the plastic hardens first before filling the cavity.

Plastic is a material that is in great demand by consumers as a substitute for other materials, because plastic materials are easy to find and easy to process. The formation of this thermoplastic material through a heating process then melts in the cylinder, which then the melt is injected into the mold [3].

This research was conducted because there were problems at PT Albea Rigid Packaging Surabaya with the 2019 mold cover pot production by polystyrene materials with a stable number of orders but declining performance. In 2019-2022, the average order reached 5,254,124 but mold performance is declining every year. The root of the problem of defects in plastic products is divided into 4 categories, namely material, injection machine, parameters, and mold [4]. The purpose of this research is to understand and be able to explain the effect of the independent variable holding pessure and inject pressure on the dependent variable, namely short shot.

2. RESEARCH METHODS

2.1 Types of Research

The type of research used is quantitative with experimental methods. This method is used to find out what factors can affect the results of the research. Data analysis was carried out with the aim of testing the research hypothesis with the ANOVA method.

2.2 Time and Place of Research

This research was conducted from February 2023 to April 2023, located at PT Albea Rigid Packaging Surabaya with the address Jl. Rungkut Industri IV No.23, Rungkut Tengah, Gunung Anyar District, Surabaya City, East Java 60293.

2.3 Research Tools and Materials

The tools and materials used in this research include:

1. Injection Molding Machine

Injection molding machines are used to melt plastic pellets and then inject molten plastic into mold, as in this Figure 2.

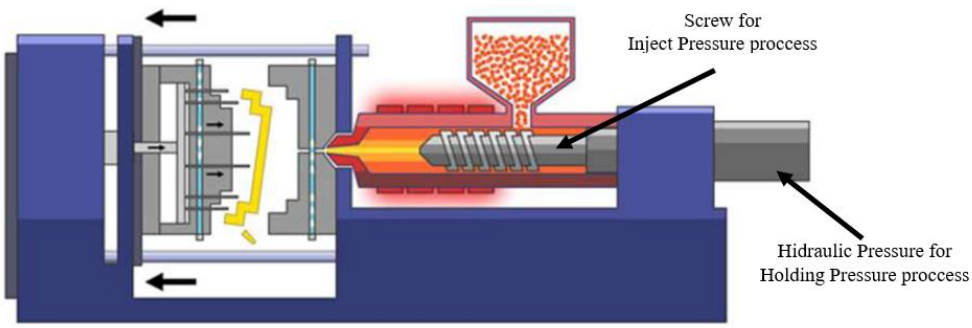

Figure 2. Injection molding machine [5] (waykenrm.com)

2. Mold Cover Pot

Mold is useful as a container for forming products/parts with plastic material that has been injected by an injection molding machine.

Figure 3. Mold cover pot

3. Polystyrene Plastic Material
The material used in making cover pot is polystyrene (PS). Polystyrene material is a rigid and hard material. This material is suitable for use as the basic material for cover/casing products.

4. Digital Scales
Digital scales function to weigh the materials to be used and the results of finished products, as in Figure 5. Next:

2.4 Research Variables
In this research, there are variables that play an important role in taking data during research, as in Table 1. Next:

Table 1. Research variables

Independent Variable		
1.	Holding Pressure (bar)	: 20, 30, & 40
2.	Inject Pressure (bar)	: 15, 30, & 45
Dependent Variables		
1.	Weight of cover pot product	: $8,8^{\pm 0,1}$ grams
Controlled Variables		
1.	Materials	: Polystyrene (PS)
2.	Nozzle Temperature	: 220°C
3.	Shoot Materials	: 93 grams
4.	Runner Gate	: Submarine Gate
5.	Inject Time	: 3,5 s

2.5 Research Hypothesis
The hypotheses in this research are:

^{Nul} Hypothesis (H_0) : There is no effect of Holding pressure, Inject pressure and combination of both variables on product defects Short shot

^{Alternative} Hypothesis (H_1) : There is an influence of Holding pressure, Inject pressure and the combination of both variables on Short shot product defects.

3. RESULTS AND DISCUSSION
3.1 Result
The results of product identification and weight measurement obtained from the data collection process were 90 cover pot products. Products with short shot defects weigh less than $8.8^{\pm 0.1}$ grams, as shown in Table 2:

Table 2. Product weight data retrieval

NO	Holding Pressure	Inject Pressure	Replication (grams)										Avarage (grams)
			1	2	3	4	5	6	7	8	9	10	

	(bar)	(bar)											
1	20	15	6,6	6,6	6,6	6,3	6,3	6,9	6,3	6,6	6,6	6,9	6,6
2	20	30	7,6	7,6	7,6	7,7	7,7	8,0	8,0	8,7	8,7	8,0	8,0
3	20	45	8,0	8,8	8,7	8,0	8,7	8,8	8,0	8,9	8,8	8,8	8,6
4	30	15	6,9	6,9	6,9	7,3	7,4	6,9	6,6	6,9	7,3	7,3	7,0
5	30	30	8,0	8,0	8,7	8,7	8,0	8,0	8,0	8,7	8,8	8,0	8,3
6	30	45	8,7	8,7	8,0	8,0	8,8	8,8	8,9	8,9	8,8	8,7	8,6
7	40	15	7,4	7,4	7,4	7,3	7,3	7,6	8,0	7,6	7,6	7,4	7,5
8	40	30	8,0	8,0	8,7	8,7	8,0	8,0	8,0	8,7	8,8	8,8	8,4
9	40	45	8,7	8,7	8,8	8,8	8,7	8,8	8,8	8,9	8,8	8,8	8,8

From the data collection of 90 products, product documentation was obtained with short shot (a) and normal (b) conditions as in Figure 4. the following:

(a) (b)

Figure 4. (a) Product weight 6.6 grams (short shot) and (b) Product weight 8.8 grams (normal)

Cover pot product weight under $8{,}8^{\pm 0{,}1}$ grams is defect (short shot) as show arrow in Figure 5:

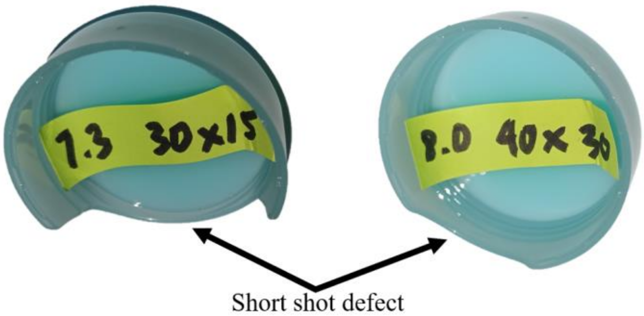

Figure 5. Product weight is 7,3 g and 8,0 g are short shot defect

3.2 Discussion

The normality test is an important part of regression analysis. Normal probability plots are an effective alternative method in determining the model to be analyzed whether the research is normally distributed or not.

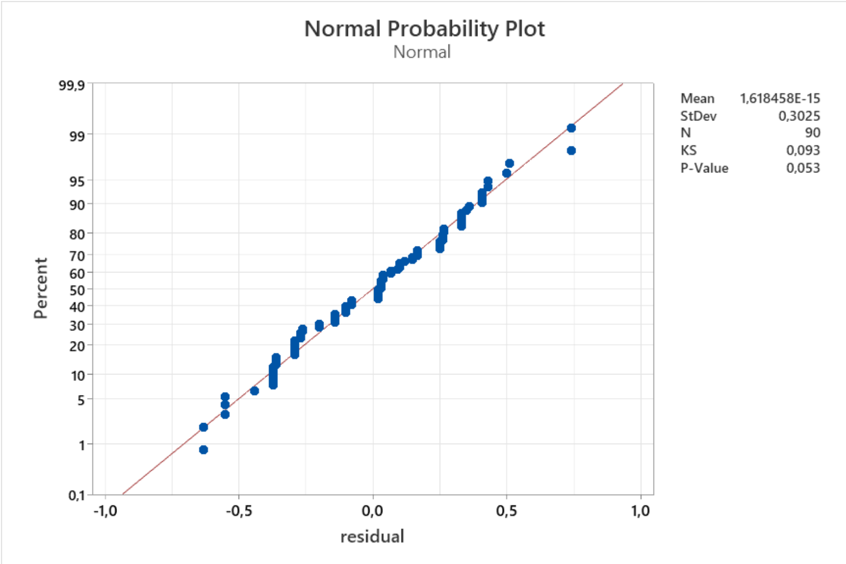

Figure 5. Graphic normal probability plot

The normality method uses the Kolmogorov smirnov method, where the data is said to be normally distributed if the p-value is greater than the alpha value. it can be seen in Figure 6. that the P-value is 0.053 > 0.050 so that it can be concluded that the data of this research are normally distributed and the data points spread around the normal line or not far from the normal line. Thus it can be known that the data in this research meet normal assumptions.

Next is an ANOVA (analysis of variance) table image and a summary model from the analysis results using statistical software.

Analysis of Variance

Source	DF	Adj SS	Adj MS	F-Value	P-Value
Model	8	47,399	5,9249	58,92	0,000
Linear	4	45,988	11,4970	114,33	0,000
holding pressure	2	4,129	2,0647	20,53	0,000
inject pressure	2	41,858	20,9292	208,12	0,000
2-Way Interactions	4	1,411	0,3528	3,51	0,011
holding pressure*inject pressure	4	1,411	0,3528	3,51	0,011
Error	81	8,146	0,1006		
Total	89	55,545			

Figure 6. Analysys of variance

In this study, the confidence level or alpha value (α) was determined to be 5% or 0.050 in decimal form it can see in Figure 8. The alpha value (α) is the limit value of acceptable hypothesis error. From Figure 4.8 above shows that the P-value of the variable holding pressure (0.000), injecting pressure (0.000), and the interaction of both variables (0.011) are smaller than the alpha value (α). This resulted in the decision that the null hypothesis (H0) which includes no there is no influence of the holding pressure factor on short shot product defects, there is no effect of the inject pressure factor on short shot product defects, and there is no interaction effect of the holding pressure and inject pressure factors on short shot product defects is rejected, which means that there is an influence of the holding pressure factor on short shot product defects. holding pressure on short shot product defects, there is an effect of the factor inject pressure on short shot product defects, and there is an interaction effect of holding pressure and inject pressure on short shot product defects. factors of holding pressure and inject pressure on short shot product defects.

Model Summary

S	R-sq	R-sq(adj)	R-sq(pred)
0,317116	85,34%	83,89%	81,90%

Figure 7. Model summary

Like Figure 8. there is a model summary image, which is a collection of observations as a percentage of each category. R-sq is the correlation number of independent variables, as in Figure 4.9 above, the R squared (R-sq) value is indicated value of 85.34% the following figure means that the two independent variables holding pressure and inject pressure have an effect on the dependent variable, namely short shot by 85.34% for the remaining 14.66% explained by other variables outside the independent variables.

Next is a linear regression graph, which is a data analysis technique that is useful for predicting product weight values from unstudied parameters using known and related product weight values. From the results of research on holding pressure analysis of short shot defects based on product weight, a linear regression graph as shown in Figure 9 was obtained.

In the graph above there is a simple regression picture of the analysis results holding pressure on short shot defects, like this $Y = 6{,}909 + 0{,}0457x - 0{,}000326x^2$ holding pressure increases by 1 unit (bar), the weight of the product will increase by 0,0457 units (grams). Then if the holding pressure value is 0, the resulting weight is 6,909 units (grams). Next is a linear regression graph from the results of inject pressure analysis of short shot defects that refer to the weight of the product obtained by the graph as in Figure 11.

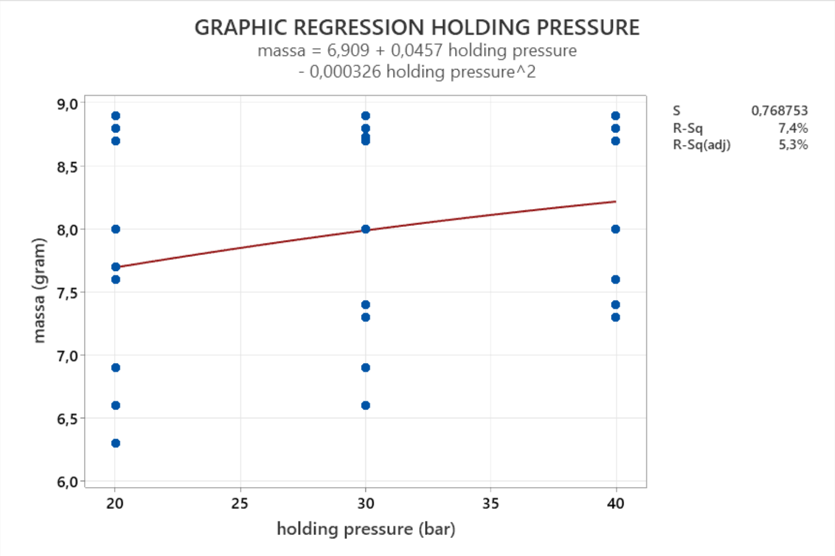

Figure 8. Graphic regression holding pressure

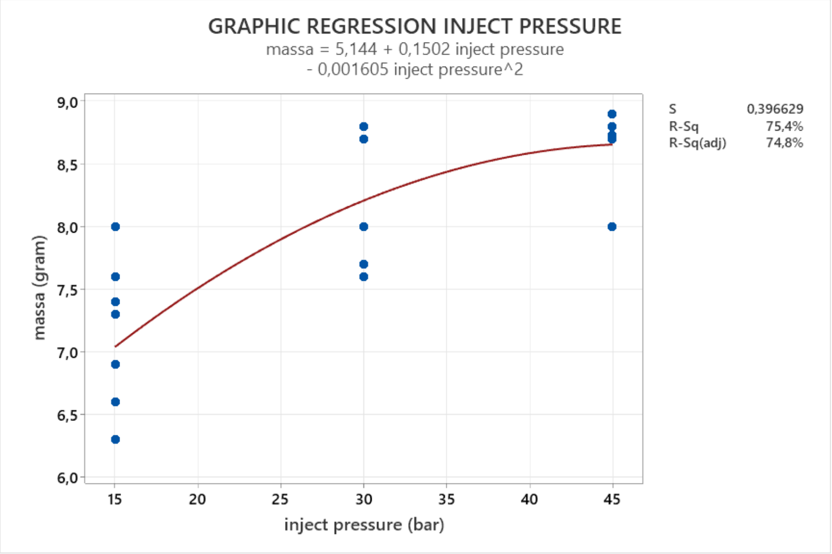

Figure 9. Graphic regression inject pressure

In the graphic image above, linear regression from the results of inject pressure analysis of short shot product defects , namely. This means that if the $Y = 5{,}144 + 0{,}1502x - 0{,}001605x^2$ inject pressure increases by 1 unit (bar) then the weight of the product will increase by 0,1502 units (grams). Then if the inject pressure value is 0 then the resulting weight is 5,144 units (grams).

The left side there is a graph of the effect of holding pressure and the right side is the graph of the effect of inject pressure. At the horizontal axis shows the variation of the independent variables when the the holding pressure and inject pressure, the vertical axis shows the the dependent variable of the study is short shot with reference to product weight. The graph the left side shows that at a holding pressure variation of 20 bar the average weight of the of cover pot products produced is 7.7 grams, at a holding pressure variation of 30 bar the average weight of the cover pot product produced is 8.0 grams, and at a variation of holding pressure 40 bar the average weight of the cover pot product produced is 8.2 gram. Furthermore, the right side graph shows that in the variation of inject pressure 15 bar the average weight of the cover pot product produced is 7.0 grams, in the 30 bar inject pressure variation the average weight of the cover pot product produced is 8.2 grams. 8.2 grams, and in the 45 bar inject pressure variation the average weight of the cover product is 8.7 grams. pot produced is 8.7 grams. From Figure 4.11 it can be concluded that the higher the level of holding pressure and inject pressure, the lower the potential short shot defects with the weight of the cover pot product produced approaching the normal standard of 8.8 grams. normal standard of 8.8 grams.

Next there is an interaction graph or interaction plot, which is a graph to display a level of one factor at the level of another factor (interaction level of two factors).

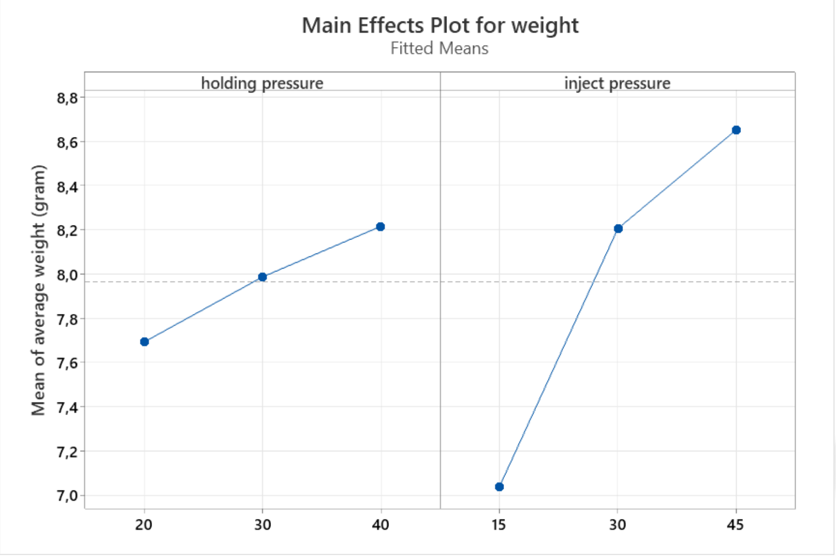

Figure 10. Main effect plot

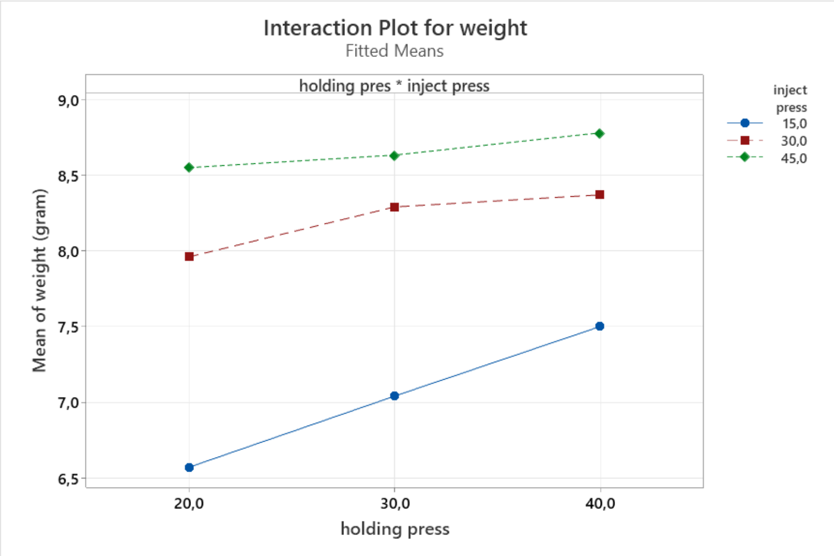

Figure 11. Graphic interaction plot

There are three types of lines with different colors, the three lines represent 15 bar inject pressure (blue line), 30 bar inject pressure (red line), and 45 bar inject pressure (green line). The horizontal axis shows the levels of 20 bar, 30 bar, and 40 bar of holding pressure, the vertical axis shows the bound variable, namely short shot with reference to the weight of the cover pot product.

From the plot, it is known that the smallest possibility of short shot product defects is found in the holding pressure of 40 bar interacting with the inject pressure of 45 bar (green line) with an average weight of 8.8 grams of cover pot product. Then the greatest possibility of short shot product defects is found in the holding pressure of 20 bar interacting with the inject pressure of 15 bar (blue line) with an average weight of 6.6 grams of cover pot product. It can be concluded that the higher the holding pressure and inject pressure levels, the less likely the short shot product defect.

4. CONCLUSION

From the results of the holding pressure and inject pressure research on the weight of the cover pot product (short shot product defects), the conclusions that can be drawn are:

1. Independent variable holding pressure has a significant influence on short shot product defects based on the weight of the cover pot product. This is because the holding pressure serves to hold the product after the filling process so that the cavity remains fully filled and the material does not return to the barrel. From the results of the main effects plot graph, it can be concluded that the higher the level of holding pressure, the heavier the resulting cover pot product, which is 8.2 grams

2. Independent variable inject pressure has a significant influence on short shot product defects based on the weight of the cover pot product. This is because the inject pressure is in charge of transferring material into the cavity cavity. From the results of the main effects plot graph, it can be concluded that the higher the level of inject pressure, the heavier the resulting cover pot product, which is 8.6 grams

3. The interaction of the two variables independent holding pressure and inject pressure has a significant influence on the defects of short shot products based on the weight of the cover pot product. On average, the weight of the product interaction holding pressure 40 bar and inject pressure 45 bar is in accordance with the normal cover pot product weight guidelines, which is $8.8^{\pm 0.1}$ grams. From this it can be concluded that the higher the level of interaction of holding pressure and inject pressure, the heavier the resulting cover pot product, this affects the reduction of short shot product defects.

5. REFERENCES

[1] SIPSN. (2022). Komposisi sampah menurut jenis sampah. Access Maret, 2023. https://sipsn.menlhk.go.id/sipsn/

[2] Yulianto, I. *et.al.*, 2014. Rancangan Desain *Mold* Produk Knob Regulator Gas pada Proses *Injection Molding*. Reka Integra. Vol. 2 (3). Page : 141.
[3] Han, J.H. and Kim, Y.C. 2017. *Research on Effect of Mold Temperature on The Injection Molded Article*. Arch. Metall. Mater. Vol. 62 (2B). Page : 1271.
[4] Yusoff, S.M.M. *et.al.*, 2004. *A Plastic Injection Molding Process Characterisation Using Experimental Design Technique : A Case Research*. Jurnal Teknologi. Vol. 41 (A). Page : 2-4.
[5] Wayken Rapid Manufacturing. (2022). What Is Injection Molding: A Detailed Guide On Plastic Injection Molding Access date July, 2023. https://waykenrm.com/
[6] Wahyudi, U. 2015. Pengaruh *Injection Time* dan *Back pressure* Terhadap Cacat Penyusutan Pada Produk Kemasan Toples dengan Injection Molding menggunakan Material *Polystyrene*. Jurnal Teknik Mesin (JTM). Vol. 04 (3). Page : 81-82.
[7] Langga, EHM, Sya'bani, MW, & Wulung, RS. 2017. Pengaruh Suhu Dan Tekanan Injeksi Terhadap Cacat *Short Shot* Produk Polikarbonat Pada Mesin *Injection Moulding*. Berkala Penelitian Teknologi Kulit, Sepatu, dan Produk Kulit , 16 (2), 1-13.

LOGIC
Jurnal Rancang Bangun dan Teknologi
(Journal of Engineering Design and Technology)
Address : Gedung P3M, lt.1 Politeknik Negeri Bali, Bukit Jimbaran
PO BOX 1064 Kuta Selatan, Badung, Bali - Indonesia
Telp. (+62)361 701981 Fax. (+62)361 701128
Email: logic@pnb.ac.id

1412-114X